RELATIONSHIP OF ERK1/2 PHOSPHORYLATION TO D_1 DOPAMINE RECEPTOR
ACTIVATION, BEHAVIORAL SENSITIZATION, AND STRUCTURAL PLASTICITY
IN THE NEONATE 6-HYDROXYDOPAMINE-LESIONED RAT

by
Sophia T. Papadeas

A dissertation submitted to the faculty of the University of North Carolina at Chapel Hill in
partial fulfillment of the requirements for the degree of Doctor of Philosophy in the
Curriculum in Neurobiology, School of Medicine.

Chapel Hill
2005

Approved by

Chair: Robert A. Mueller

Advisor: George R. Breese

Reader: Hugh E. Criswell

Reader: Lee M. Graves

Reader: A. Chistina Grobin

Reader: Franck Polleux

ABSTRACT

SOPHIA T. PAPADEAS: Relationship of ERK1/2 Phosphorylation to D_1 Dopamine Receptor Activation, Behavioral Sensitization, and Structural Plasticity in the Neonate 6-Hydroxydopamine-Lesioned Rat

(Under the direction of George R. Breese, Ph.D.)

Repeated administration of the D_1-dopamine receptor agonist SKF-38393 to adult rats lesioned with 6-hydroxydopamine (6-OHDA) as neonates results in increasingly greater behavioral responsiveness with each dose, a phenomenon known as "priming of D_1 receptor sensitivity." This dissertation examines the role of the extracellular signal-regulated kinase 1/2 (ERK), an intracellular mediator of signal transduction, in D_1-dopamine receptor activation, priming of behavioral sensitivity, and structural plasticity in the neonate-lesioned rat. Using immunohistochemistry, I found that repeated administration of SKF-38393 produced a prolonged increase in phosphorylated (phospho-) ERK in the medial prefrontal cortex (mPFC) of neonate-lesioned rats. A corresponding increase in the phosphorylation of CREB (cyclic AMP-response element binding protein), a downstream target of ERK signaling, implied a functional consequence for the prolonged ERK activation in mPFC. Pretreatment with the D_1 antagonist SCH-23390, but not the $5\text{-}HT_2$ antagonist ketanserin, prior to each dose of SKF-38393 blocked the persistently increased phospho-ERK. The competitive and non-competitive NMDA receptor antagonists MK-801 and CGS-19755, which inhibit the induction of behavioral sensitization in neonate-lesioned rats, also blocked the increased

phospho-ERK. In addition, intracerebroventricular (ICV) and systemic administration of SL327 or PD98059, inhibitors of the upstream ERK activator MEK (mitogen-activated protein kinase/extracellular signal-regulated kinase kinase 1/2), prior to each SKF-38393 treatment eliminated mPFC phospho-ERK. Computer-monitored activity chambers and visual observation both revealed that the global MEK inhibition increased horizontal behavior and decreased certain stereotyped behaviors after an additional sensitizing dose of SKF-38393. In addition, intra-mPFC infusions with PD98059 only decreased stereotyped behaviors in primed animals. Finally, using immunohistochemistry for MAP2 combined with recombinant adenovirus (AAV) transduction of green fluorescent protein (GFP) in mPFC neurons, I found that repeated administration of SKF-38393 produces robust, long-lasting changes in the morphology of dendrites in mPFC of neonate-lesioned rats. Pretreatment with SL327 and PD98059 prevented these changes, suggesting that the alterations in dendritic morphology require ERK pathway activation. Collectively, these results demonstrate that D_1 and NMDA receptors cooperatively produce prolonged ERK pathway activation in mPFC of primed neonate-lesioned rats, and suggest that persistent ERK phosphorylation in mPFC plays a pivotal role in long-lasting behavioral and structural adaptations in these animals.

The work in this dissertation is dedicated to my parents, Ted and Poly, whose patience,

love, and understanding have been invaluable.

ACKNOWLEDGEMENTS

I would also like to thank my family for their never ending love and support. My brother, Paul, for his inspirational talks and continuous interest in my work and progress, and most of all my parents, for their love and encouragement through the really tough times.

Lastly, I thank my husband and best friend Bill, whose continuing support and loving presence has helped me succeed.

PREFACE

I have prepared my dissertation in accordance with the guidelines set forth by the University of North Carolina Department of Graduate Studies. This dissertation consists of a general introduction, three chapters of original data, and a conclusions chapter. Each data chapter includes an introduction, materials and methods, results, and discussion section. A complete list of literature cited throughout the dissertation has been appended to the end of the dissertation. References are listed in alphabetical order and follow the format of The Journal of Neuroscience.

Abstracts representative of this work:

Papadeas ST, Blake BL, Knapp DJ, and Breese GR (2004) Sustained ERK phosphorylation following repeated D_1-dopamine receptor agonist treatment to neonate 6-OHDA-lesioned rats: potential regulation by phosphatases. *Society for Neuroscience Annual Meeting, New Orleans LA. Program # 632.4, 2004.*

Papadeas ST, Knapp DJ, Fernandes A., and Breese GR (2002) Increased cortical MAP kinase with dopamine receptor mediated priming. *Society for Neuroscience Annual Meeting, New Orleans LA. Program # 832.17, 2002.*

Manuscripts representative of this work:

Papadeas ST, Blake BL, Knapp DJ, and Breese GR (2004) Sustained ERK1/2 phosphorylation in neonate 6-OHDA-lesioned rats following repeated D_1-dopamine receptor agonist administration: implications for NMDA receptor involvement. J Neurosci 24: 5863-76.

TABLE OF CONTENTS

Chapter

LIST OF TABLES

LIST OF FIGURES

LIST OF ABBREVIATIONS

$5\text{-}HT_2$	serotonin receptor type 2
$5\text{-}HT_{2A}$	serotonin receptor subtype 2A
$5\text{-}HT_{2A/2C}$	serotonin receptor subtypes 2A and 2C
$5\text{-}HT_{2C}$	serotonin receptor subtype 2C
6-OHDA	6-hydroxydopamine
AAV	recombinant adeno-associated virus
AC	adenylyl cyclase
ANOVA	analysis of variance
BLA	basolateral amygdala
B_{max}	maximum number of binding sites
CaM	calmodulin
CaMKII	calcium/calmodulin-dependent protein kinase II
cAMP	cyclic adenosine monophosphate
CC	corpus callosum
CgC	cingulate cortex
CGS	CGS-19755
CGS R-Saline	CGS pretreatment before each R-Saline injection
CGS R-SKF	CGS pretreatment before each R-SKF injection
CGS-19755	4-phosphonomethulpiperidine-2-carboxylic acid
CNS	central nervous system
CPu	caudate-putamen
CRE	calcium response element

CREB	cyclic AMP-response element binding protein
D_1	dopamine receptor type D_1
DA	dopamine
DAB	3,3'-diaminobenzidine tetrahydrochloride
DAG	diacylglycerol
DMSO	dimethylsulfoxide
EP	entopeduncular nucleus
ERK (ERK1/2)	extracellular-signal related kinase 1 and 2
ERK5	extracellular-signal related kinase 5
FITC	fluorescein isothiocyanate
GABA	γ-amino-butyric acid
GFAP	glial fibrillary acidic protein
GFP	green fluorescent protein
GP	globus pallidus
Hipp	hippocampus
i.c.	intracisternal
i.p.	intraperitoneal
ICV	intracerebroventricular
IEG	immediate early gene
IL	infralimbic cortex
KA	kainic acid
K_d	dissociation coefficient
Ketanserin R-SKF	Ketanserin pretreatment before each R-SKF injection

Ketanserin	3-[2-[4-(4-fluorobenzoyl)-1-piperidinyl]ethyl]-2,4(1H,3H)-quinazolinedione tartrate
L-DOPA	*L*-dihydroxyphenylalanine
Lesioned (Lesion)	neonate-lesioned
Lesion-SKF	neonate-lesioned rats given repeated SKF injections
LGP	lateral globus pallidus
LNS	Lesch-Nyhan Syndrome
LTP	long-term potentiation
M1	primary motor cortex
M100907	(*R*)-(+)- α-(2,3-dimethoxyphenyl)-1-[2-(4-fluoro-phenyl)ethyl]-4-piperidine methanol
M2	secondary motor cortex
MAP2	microtubule-associated protein 2
MAPK	mitogen activated protein kinase
MAPKK	MAPK kinase
MC	motor cortex
MD	medial dorsal thalamus
MEK (MEK1/2)	MAPK/ERK kinase 1 and 2
MK-801 R-Saline	MK-801 pretreatment before each R-Saline injection
MK-801 R-SKF	MK-801 pretreatment before each R-SKF injection
MK-801	1-methyl-4-phenyl-1,2,3,6-tetrahydropyridine
MKP	mitogen-activated protein kinase phosphatase
mPFC	medial prefrontal cortex

mRNA	messenger ribonucleic acid
NA (NAc)	nucleus accumbens
Neonate-lesioned	rats treated with 6-OHDA (i.c.) at PND3-4
NMDA	n-methyl-d-aspartate receptor
PBS	0.1 M phosphate-buffered saline, pH 7.40
PBS-T	PBS with 0.1% Tween-20
PD	PD98059
PD98059	2-(2'-amino-3'-methoxyphenyl)-oxanaphthalen-4-one
PDSKF	PD pretreatment before 3 of 4 SKF treatments
PFC	prefrontal cortex
Phospho-CREB	CREB phosphorylated at Ser133
Phospho-ERK	ERK1/2 phosphorylated at Thr202/Tyr204
Phospho-JNK	phospho-SAPK/JNK
Phospho-SAPK/JNK	SAPK/JNK phosphorylated at Thr183 and Tyr185
PirC	piriform cortex
PKA	cyclic AMP-dependent protein kinase A, protein kinase A
PKC	Ca^{2+}/phospholipid-dependent kinase C, protein kinase C
PLC	phospholipase C
PLSD	protected least significant difference
PND	postnatal day
R-PDSKF	PD pretreatment before each R-SKF injection
RS102221	8-[5-(5-amino-2,4-dimethoxyphenyl) 5-oxopentyl]-1,3,8-triazaspiro[4.5]decane-2,4-dione

R-Saline (Saline, R-Sal)	repeated saline (i.p.) treatment
R-Sal, PDSaline Challenge	R-Saline treatment for Doses 1-3, and PD pretreatment before final saline injection
RSK2	ribosomal S6 kinase 2
R-SKF	repeated SKF (i.p.) treatment
R-SKF, PDSKF Challenge	R-SKF treatment for Doses 1-3, and PD pretreatment before final SKF injection
R-SKF, SLSKF Challenge	R-SKF treatment for Doses 1-3, and SL pretreatment before final SKF injection
R-SLSKF	SL pretreatment before each R-SKF injection
S1	primary somatosensory cortex
SAPK/JNK	stress-activated protein kinase/c-Jun amino-terminal kinase
SCH R-Saline	SCH-23390 pretreatment before each R-Saline injection
SCH R-SKF	SCH-23390 pretreatment before each R-SKF injection
SCH	SCH-23390
SCH-23390	7-chlor-2,3,4,5-tetrahydro-3-methul-5-phenyl-1H-3-benzazepine-7-ol
SDS	sodium dodecyl sulfate
SEM	standard error measurement
Sham	sham-lesioned
Sham-lesioned	rats treated with saline (i.c.) at PND3-4
Sham-SKF	sham-lesioned rats given repeated SKF injections
SIB	self-injurious behavior
SKF	SKF-38393
SKF-38393	2,3,4,5-tetrahydro-7,8-dihydroxy-1-phenyl-1H-3-

benzazepine

SL	SL327
SL R-SKF	SL pretreatment before each R-SKF injection
SL327	α-[amino[(4-aminophenyl)thio]methylene]-2-(trifluoromethyl)benzeneacetonitrole
SLSKF	SL pretreatment before 3 of 4 SKF treatments
SNc	substantia nigra pars compacta
SNr	substantia nigra pars reticularis
SSC	somatosensory cortex
sSLSKF	systemic SLSKF treatment
STN	subthalamic nucleus
STR	striatum
TEY	threonine-glutamic acid-tyrosine
Th	thalamus
TH	tyrosine hydroxylase
U0126	1,4-diamino-2,3-dicyano-1,4-bis(aminophenylthio)butadiene
VC	visual cortex
Veh	Vehicle
VLOC	ventrolateral orbital cortex, orbitofrontal cortex
VO	ventral orbital cortex
VP	ventral pallidum
VTA	ventral tegmental area

CHAPTER I.   BACKGROUND AND SIGNIFICANCE

The Neonate 6-Hydroxydopamine (6-OHDA)-Lesioned Rat Model

Administration of the neurotoxicant 6-hydroxydopamine (6-OHDA), with desmethylimipramine pretreatment, to adult and neonate rats results in the selective destruction of dopamine-containing neurons (Smith et al., 1973), and enhances the behavioral effects of dopamine agonists (Ungerstedt, 1971a,b; Uretsky and Schoenfeld, 1971; Hollister et al.,1974, 1979; Creese and Iversen, 1973). Rats lesioned with 6-OHDA as neonates (neonate-lesioned) have increased susceptibility for aggression, hyperexcitability, and self-injurious behavior in response to mixed D_1/D_2 receptor agonists L-DOPA and apomorphine (Breese et al., 1984a,b). These behaviors are similar to those observed clinically with Lesch-Nyhan syndrome (LNS), a developmental disorder characterized by reduced brain DA, choreoathetoid movements, and compulsive self-injurious behavior (Lesch and Nyhan, 1964). The susceptibility for self-injurious behavior observed in neonate-lesioned rats is not present in rats lesioned with 6-OHDA as adults, the latter of which mimic Parkinson's disease (Breese et al., 1984a,b; Marsden, 1984). Thus, the neonatal rat brain must retain sufficient plasticity to allow for the development of compensatory mechanisms that attenuate, to some degree, the debilitating effects of dopamine depletion.

D$_1$ Receptor-Mediated Priming of Neonate 6-OHDA-Lesioned Rats

The administration of the partial D$_1$ receptor agonist SKF-38393 to neonate-lesioned rats leads to a profound increase in locomotor activity at doses which have no effect in unlesioned animals. Breese and colleagues (1984a) made the initial observation that multiple treatments with SKF-38393 leads to progressively greater locomotor responses in neonate-lesioned rats (a priming effect). Criswell et al. (1989) further investigated the enhanced sensitivity of D$_1$ receptors following repeated agonist administration to these animals. These researchers found that the priming effect could still be seen as a drug-induced locomotor increase 6 months after the final dose in the repeated SKF-38393 treatment. Additionally, the progressive increase in sensitivity to repeated SKF-38393 treatments occurred not only with respect to increased locomotor activation, but also increased the incidence of stereotyped behaviors. These included sniffing, licking, grooming, digging, rearing, head nodding, paw-treading, and taffy pulling (coordinated movement of front paws toward the mouth and then away from the body). From studies involving intraaccumbens and intrastriatal antagonist-induced suppression of behaviors, enhanced locomotor effects could be attributed mainly to activation of D$_1$ receptors in the accumbens, and stereotypies to activation of D$_1$ receptors in either the accumbens or the striatum (Breese et al., 1987). Further experiments found that a classical conditioning phenomenon, whereby drug effects are conditioned to a particular environment, was not responsible for the priming phenomenon. Rats that received initial SKF-38393 treatments in either the same or a different environment from the one used for testing locomotor activity displayed the same degree of sensitization (Criswell et al., 1989).

Administration of a D_2 agonist to neonate-lesioned rats produced little or no reflection of a priming mechanism, in that repeated systemic administration of the D_2 agonist quinpirole had no notable effects on locomotor and stereotyped activities in neonate-lesioned animals (Criswell et al., 1989; Brus et al., 2003). Repeated D_2 agonist treatment, however, did result in slightly higher behavioral responses on a subsequent administration of SKF-38393 (Criswell et al., 1989; Brus et al., 2003). In addition, Criswell et al., (1989) showed that co-administration of the D_2 receptor antagonist, haloperidol, with repeated doses of SKF-38393 did not alter the priming response, while co-administration of the D_1 receptor antagonist SCH-23390 fully prevented the priming of D_1 receptor-mediated behavioral responses. These results led to the conclusion that the abnormal behaviors observed in this animal model were exclusively due to the actions of the D_1 receptor. Moreover, it was concluded from these data that D_1 receptors are essential for the action of D_2 receptors, a phenomenon called "coupling" of receptor function.

N-methyl-D-aspartate (NMDA) Receptor Involvement in D_1 Receptor-Mediated Priming of Neonate-Lesioned Rats

The long-lasting nature of D_1 receptor-mediated priming of neonate-lesioned rats led to the hypothesis that this form of sensitization involves neural and behavioral adaptive mechanisms similar to other forms of plasticity (i.e. memory and drug addiction) in the central nervous system (CNS) (Criswell et al., 1989). It has been known for some time that several forms of learning and behavioral plasticity depend on glutamatergic mechanisms, which are in large part mediated by the NMDA receptor-subtype of

glutamate receptors (Kelley, 2004). For instance, NMDA receptor antagonists interfere with classical long-term potentiation (LTP), an *in vitro* model of learning and memory formation (Lynch et al., 1983; Davis et al., 1992, for review, see Riedel et al., 2003), and NMDA receptor activation is critical for development of psychomotor stimulant-induced behavioral sensitization (Karler et al., 1989; Wolf and Jeziorski, 1993; Stewart and Druhan, 1993). Criswell et al. (1990) demonstrated that co-administration of the non-competitive NMDA receptor antagonist MK-801 along with priming doses of SKF-38393 blocked sensitization of neonate-lesioned rats to repeated D_1 agonist administration. Subsequently, it was found that the competitive NMDA receptor antagonist CGS-19755 produced a similar effect. Since previous work demonstrated that the D_1 antagonist SCH-23390 blocked priming (Criswell et al., 1989), the concomitant activation of D_1 and NMDA receptors appear necessary for priming to occur. The indication that NMDA receptor activation is also a necessary prerequisite for other responses that convey long-term neural message suggest that these phenomena and D_1 receptor-mediated priming may share a common biochemical mechanism.

5-HT$_2$ Receptor Involvement in D$_1$ Receptor-Mediated Priming of Neonate-Lesioned Rats

Proliferative sprouting of serotonin (5-HT) fibers occurs in the striatum of rats lesioned with 6-OHDA as neonates, resulting in 5-HT fiber hyperinnervation (Breese et al., 1984a; Stachowiak et al., 1984; Berger et al., 1985; Luthman et al., 1987; Towle et al., 1989). In a study by Towle et al., (1989), 5-HT neurons did not appear to have a major influence on D_1 agonist-induced locomotor activity and stereotyped behaviors in

these animals. More recent studies, however, suggested otherwise by demonstrating changes in striatal 5-HT$_2$ receptor function after neonatal dopamine depletion (el Mansari et al., 1994; Basura and Walker, 1999; Gresch and Walker, 1999), including increased striatal 5-HT$_{2A}$ mRNA levels (Numan et al., 1995; Laprade et al., 1996; Basura and Walker, 1999). Laprade and colleagues (1996) showed that 5-HT$_{2A}$ upregulation in the striatum of neonate-lesioned rats was abolished after chronic treatment with the dopamine agonists apomorphine or SKF-38393, suggesting that D$_1$ receptor activation participates in the regulation of the expression of the 5-HT$_{2A}$ receptor. Moreover, behavioral hyperactivity accompanying neonatal dopamine loss and elevated oral dyskinesia induced by ventral striatal infusions of SKF-38393 was blocked by 5-HT$_{2A/2C}$ receptor antagonists (Luthman et al., 1991; Gong et al., 1992; Plech et al., 1995). More recently, it has been demonstrated that hyperlocomotor activity induced by systemic or intrastriatal infusion of D$_1$ agonist can be suppressed by co-administration with the 5-HT$_2$ receptor antagonist ketanserin (Breese et al., 2005; Walker et al., 2004) or the 5-HT$_{2A}$ receptor antagonist M100907 (Walker et al., 2004), but not by the 5-HT$_{2C}$ antagonist RS102221 (Walker et al., 2004). Collectively, these studies suggest that 5-HT$_2$ receptors, particularly of the 5-HT$_{2A}$ subtype, may play a critical role in mediating striatal dopamine signaling and contribute to the mechanism of D$_1$ sensitization that develops in response to neonatal dopamine depletion.

Neurobiological Mechanisms Previously Thought to Underlie D_1 Receptor-Mediated Priming of Neonate 6-OHDA-Lesioned Rats

Several mechanisms potentially responsible for the priming phenomenon in neonate-lesioned rats have been explored (Breese et al., 1994). Results from these studies, however, have mostly proven to be negative. Initial efforts focused on whether an increase in dopamine receptor number could explain the functional supersensitivity of D_1 agonists in neonate-lesioned rats. Early investigations of [^{3}H] spiperone binding to striatal tissue from neonate-lesioned rats failed to demonstrate an increase in receptor number (Mailman et al., 1981). Subsequent studies showed that binding characteristics (Kd or B_{max}) for [^{3}H] spiperone and [^{3}H] SCH-23390 were not altered in primed neonate-lesioned rats compared with controls (Breese et al., 1987; Duncan et al., 1987; Luthman et al., 1991; Dewar et al., 1990). Additional studies revealed that levels of D_1 receptors in striatum and nucleus accumbens measured autoradiographically (Simson et al., 1992), as well as D_1 receptor mRNA levels, measured by *in situ* hybridization, were unaltered by neonatal lesioning (Duncan et al., 1993). Thus, alterations in D_1 and D_2 receptors are not responsible for the sensitization seen in neonate-lesioned rats repeatedly dosed with D_1 agonist.

The lack of any change in receptor number or agonist affinity led to speculation that perhaps enhanced intraneuronal second messenger levels or efficiency likewise accompanied D_1 receptor-mediated priming of neonate-lesioned rats. It is well-known that D_1 receptors are linked to activation of adenylyl cyclase (Kebabian and Calne, 1979). Adenylyl cyclase activity is stimulated by aluminum tetrafluoride $(AlF_4)^-$ and forskolin, which specifically act on the stimulatory guanine nucleotide regulatory protein and

catalytic subunit of the enzyme, respectively (Rodbell et al., 1980; Seamon et al., 1981). Gong et al. (1994) demonstrated that dopamine-stimulated enzyme activity was not altered in the striatum of neonate-lesioned rats. Repeated SKF-38393 treatment failed to affect basal and dopamine-stimulated adenylyl cyclase activity in the striatum of both unlesioned and neonate-lesioned rats. Simson et al. (1992) also reported that SKF-38393 stimulated adenylyl cyclase activity was not altered in the striatum of D_1 agonist-primed, neonate-lesioned rats. Thus, D_1 receptor-linked adenylyl cyclase is not a major determinant of the enhanced behavioral responses of neonate-lesioned rats to repeated D_1 agonist administration.

Finally, because earlier studies had linked the protooncogene *c-fos* to behavioral supersensitivity to L-DOPA or D_1 agonists in rats either unilaterally or bilaterally lesioned with 6-OHDA as adults, *c-fos* expression was examined in neonate-lesioned rats after D_1 agonist treatment. Expression of *c-fos* occurred only after a dose of D_1 agonist that was much higher than the behaviorally active dose, and was not increased to a greater extent following repeated D_1 agonist treatments (Johnson et al., 1992). In addition, NMDA receptor antagonists did not block *c-fos* expression in these animals (Johnson et al., 1992). Thus, it was concluded that *c-fos* was not a critical component in the priming phenomenon. Accordingly, the exact neurobiological mechanisms underlying D_1 receptor-mediated priming of neonate-lesioned rats remain uncertain.

Extracellular Signal-Regulated Kinase 1/2

Mitogen-activated protein kinases (MAPKs) are intracellular mediators of signal transduction that are activated in response to a variety of extracelluar stimuli (Johnson

and Lapadat, 2002; Pearson et al., 2001). There are three major classes of MAPKs: extracellular signal-regulated kinases (ERKs) (Sweatt JD, 2001), p38 (Johnson and Lapadat, 2002), and stress-activated protein kinase/c-Jun amino-terminal kinase (SAPK/JNK) (Davis, 2000). Among these, the most well-studied are the closely related extracellular signal regulated kinases 1 and 2 (ERK1/2). Biological processes involving ERK1/2 include stimulation of cell proliferation and survival, neoplastic transformation, neuronal differentiation and plasticity (Seger and Krebs 1995; Paul et al., 1997). Thus, ERK1/2 is a likely candidate for a specific neurobiological substrate of adaptive change(s) that might accompany the enduring behavioral responsiveness of neonate-lesioned rats to repeated D_1 receptor stimulation.

D_1 Receptor Activation of Extracellular Signal-Regulated Kinase 1/2

Activation of ERK1/2 by D_1 receptors is a complex process that may involve multiple mechanisms (Brami-Cherrier et al., 2002; Liu et al., 2002; Gerfen et al., 2002; Zhen et al., 2001). Fig. 1-1 demonstrates how ERK1/2 is potentially linked to D_1 receptors with priming of D_1 receptor function. Recent studies show that D_1 receptor activation of ERK1/2 occurs via a Gs/adenylyl cyclase/protein kinase A (PKA)-dependent pathway that causes activation of the small GTPase, Rap1 (Vossler et al., 1987; Schmitt and Stork; 2002), and the subsequent activation of B-Raf isoform (Vossler et al., 1997; Yao et al., 1998; York et al., 1998). B-Raf then activates MAPK-kinase (MAPKK), or MEK1/2, by dual Ser/Thr phosphorylation, which then activates ERK1/2 by dual phosphorylation within a conserved Thr-Glu-Tyr (TEY) motif in its activation loop (Grewal et al., 1999). A further alternative path (not shown in Fig. 1-1) is provided

by D_1 receptor coupling to $G_{q/11}$ protein which is linked to phosphoinositide (PI) hydrolysis (Wang et al., 1995b; Jin et al., 2001).

Another possible intermediate between D_1 receptors and ERK1/2 activation could be calcyon, a D_1 receptor-interacting protein that stimulates intracellular calcium (Ca^{2+}) release, a process which is known to activate the ERK1/2 signaling pathway (Lev et al., 1995). Lev et al. (1995) showed that D_1 receptors and calcyon localize to pyramidal cell dendritic spines, the site of excitatory amino acid input. Therefore, other neurotransmitters could facilitate the D_1 receptor-stimulated intracellular Ca^{2+} release (Lev et al, 1995). Several electrophysiological as well as molecular models of plasticity require both D_1 receptor activation and NMDA receptor-mediated glutamate transmission (Cepeda et al., 1992; Konradi et al., 1996). In fact, activation of NMDA receptors on their own phosphorylate ERK1/2 (Sgambato et al., 1998; Mao et al., 2004), probably via a signaling mechanism involving several Ca^{2+}-sensitive kinases (Fig. 1-1) (Perkinton et al., 1999, 2002). Therefore, the necessary activation of NMDA receptors during D_1 receptor-mediated priming of neonate-lesioned rats (Criswell et al., 1990) might provide a strong contribution to ERK1/2 activation in these animals.

As mentioned previously, 5-HT$_2$ receptors, particularly of the 5-HT$_{2A}$ receptor subtype, appear to play a critical role in the hyperlocomotor responsiveness of neonate-lesioned rats to D_1 receptor stimulation. Although 5-HT$_{2A}$ receptors seem to couple to signaling pathways that exert long term neuronal changes (Denton and Tavare, 1995), very little is known about the pathway for receptor coupling to ERK1/2 in neurons. Quinn et al. (2002) recently demonstrated 5-HT$_{2A}$ receptor activation of ERK1/2 in a neuronal cell line through a PKA- and protein kinase C (PKC)-independent pathway

requiring activation of Ca^{2+}/calmodulin/tyrosine kinases. Cross-talk between 5-HT_{2A}, D_1, and presumably NMDA receptors could converge upon ERK1/2 to facilitate long-term adaptative change(s) with priming of neonate-lesioned rats (see Fig. 1-1).

Downstream Targets of Extracellular Signal-Regulated Kinase 1/2 Activation Potentially Involved in D_1 Receptor-Mediated Priming

ERK1/2 targets include several cytosolic and membrane-bound proteins (Schaeffer and Weber 1999). Upon translocation from the cytoplasm into the nucleus, ERK1/2 can phosphorylate different transcription factors and thus regulate gene transcription (Schaeffer and Weber 1999). Both *in vitro* and *in vivo* studies have demonstrated that ERK1/2 has both a transient (< 60 min) and a sustained activation (> 60 min), and that the difference in the kinetics of ERK1/2 activation corresponds to the distinct regulatory functions of this kinase (for review, see Marshall, 1995). The best-studied example of this is demonstrated in PC12 cells, in which prolonged NGF-induced activation of ERK1/2 causes its long-lasting nuclear translocation and neuronal differentiation, whereas short, EGF-induced activation of ERK1/2 is unable to trigger an efficient nuclear translocation and instead, causes cell proliferation. A major goal of this dissertation was to define the time course of ERK1/2 activation in the major dopamine-terminal regions of forebrain after repeated D_1 agonist administration to neonate-lesioned rats.

The most well-characterized nuclear target of ERK1/2 is the transcription factor cyclic AMP-Response Element Binding protein (CREB; for review, see Lonze and Ginty, 2002). CREB can be activated by phosphorylation at Ser-133 in an ERK1/2-dependent

10

manner via stimulation of the CREB kinase Ribosomal S6 Kinase-2 (RSK2; Xing et al., 1996) (see Fig. 1-1). The phosphorylation of CREB controls transcriptional expression via the cAMP and calcium response element (CRE) present in the promoter regions of various immediate early genes (IEGs), i.e. c-fos, junB, zif268, and Arc (for review, see Herdegen and Leah, 1998). CREB is thought to play a key role in regulating the induction of gene expression-dependent LTP (Impey et al., 1998; Roberson et al., 1999; Sweatt, 2001), and is involved in initiating downstream molecular events that underlie psychostimulant-induced behavioral sensitization (Berke and Hyman, 2000). In this dissertation, CREB phosphorylation was measured as a functional 'readout' for ERK1/2 activation following D_1 receptor-mediated priming of neonate-lesioned rats. The examination of ERK1/2-dependent changes in CREB after priming provided further evidence that ERK translocated to the nucleus to cause long-term gene transcription and subsequent enhancement of enduring plasticity-associated changes in these animals.

It is also worth noting that typical transcriptional targets of ERK1/2 are genes encoding MAP kinase phosphatases (MKPs) (Farooq and Zhou, 2004). MKPs are dual-specificity phosphatases, which include MKP-1 and MKP-2, localized in the nucleus, and MKP-3, localized in the cytoplasm. The binding of active ERK1/2 to MKPs activates their phosphatase catalytic domain, thus causing the dephosphorylation, or inactivation, of ERK1/2. This direct coupling of inactivation of ERK1/2 to activation of MKPs provides a tightly controlled regulation that enables these two enzymes to keep each other in check, thus guaranteeing fidelity and temporal control of ERK1/2 signaling.

Active ERK1/2 that does not translocate to the nucleus can be retained in the cytoplasm by association with the microtubule cytoskeleton (Reszka et al., 1995).

11

Microtubule-associated protein-2 (MAP2) is mainly found in soma and dendrites and plays a key role in maintaining neuronal architecture (Sanchez et al., 2000). MAP2 is also involved in cellular differentiation and in structural and functional plasticity (Sanchez et al., 2000). It is postulated that the association of ERK1/2 with microtubules is mediated through MAP2, and modulated by phosphorylation of MAP2 by ERK1/2 (Morishima-Kawashima and Kosik, 1996; Reszka et al., 1997). By destabilizing MAP2-microtubule interactions, ERK1/2 can regulate the dynamics and organization of the neuronal cytoskeleton.

Extracellular Signal-Regulated Kinase 1/2 and Behavioral Sensitization

As with priming of neonate-lesioned rats, psychostimulant-induced behavioral sensitization in normal rats is thought to involve alterations in the sensitivity of postsynaptic D_1 receptors (Pierce and Kalivas, 1997a). Recent evidence suggests that ERK1/2 signaling plays a major role in behavioral responses related to psychostimulant-induced behavioral sensitization (Valjent et al., 2000), and D_1 receptors participate in ERK1/2 activation in this model (Valjent et al., 2004). For instance, blockade of ERK1/2 signaling with SL327, a systemic inhibitor of MEK1/2, inhibits cocaine-induced hyperlocomotor activity in rats (Valjent et al., 2000). Likewise, ERK1/2 activation elicited by cocaine administration can be blocked by SCH-23390 in dorsal striatum, nucleus accumbens, and cingulate or prefrontal cortex. These regions are particularly relevant in processes involving long-term behavioral alterations (see below) (Pierce and Kalivas, 1997b). With respect to this data, ERK1/2 signaling in these regions could play

an important role in the behavioral sensitization of neonate-lesioned rats to repeated D_1 agonist treatment.

Neuronal Circuitry Potentially Involved in Behavioral Sensitization of Neonate 6-OHDA-Lesioned Rats to D_1 Receptor Agonist

Particular neuronal circuitry involved in the priming phenomenon has yet to be elucidated. The mapping of ERK1/2 activation following priming of neonate-lesioned rats will likely reveal clues as to which neuronal circuits are involved in this phenomenon. The following sections highlight the major circuits potentially altered by neonatal 6-OHDA lesioning and involved in sensitization of neonate-lesioned rats to repeated D_1 agonist treatment.

The Basal Ganglia Circuit

The 'classic' model of the basal ganglia circuit proposes that basal ganglia input neurons in the striatum project to basal ganglia output neurons in the globus pallidus (GP) and substantia nigra pars reticularis (SNr) by way of direct and indirect pathways (Albin et al., 1989; DeLong, 1990) (Fig. 1-2*A*). Neurons in direct and indirect pathways exert inhibitory and excitatory influences, respectively, on GP/SNr neurons and regulate their inhibitory effect on thalamo-cortical and brainstem neurons involved in motor circuitry. The substantia nigra pars compacta (SNc) dopamine neurons differentially influence the basal ganglia system by activating D_1 and inhibiting D_2 receptors on striatal neurons that give rise to the direct and indirect pathways (Gerfen, 2000).

According to this model, neonatal dopamine depletion would result in a net increase in the firing rate of GP/SNr neurons, in turn leading to excessive inhibition of thalamo-cortical projection neurons (Fig. 1-2*B*). Ordinarily, this would produce parkinsonian like motor features, as exhibited by rats with 6-OHDA-induced dopamine lesions in adulthood (Olanow, 2004). However, neonate-lesioned rats exhibit normal if not hyperactive behavior, indicating that some compensatory mechanism overcomes the loss of nigrostriatal dopamine in development. It is possible that this mechanism lies within the hyperinnervation of 5-HT fibers in dorsal striatum (Breese et al., 1984a; Stachowiak et al., 1984; Berger et al., 1985; Luthman et al., 1987; Towle et al., 1989), along with the overexpression of 5-HT$_{2A}$ receptors at this site (Numan et al., 1995; Laprade et al., 1996; Basura and Walker, 1999).

Exactly how the microcircuitry of the basal ganglia act in concert after repeated D$_1$ agonist treatment to neonate-lesioned rats has yet to be determined. We hypothesize that excessive activation of direct pathway neurons, induced by repeated D$_1$ receptor stimulation, amplifies the firing rate of GP/SNr neurons to an extent such that "dis-inhibition" of inhibition of thalamo-cortical projection neurons occurs (Fig. 1-2*C*). Accordingly, an over-excitation of cortical motor regions in neonate-lesioned rats administered repeated doses of D$_1$ agonist could lead to potentiated behavioral responses in these animals.

The 'Motive Circuit'

We speculate that in neonate-lesioned rats, various neuronal circuits become activated in response to repeated D$_1$ agonist treatment as a result of chronic exposure to

14

the drug. The 'motive circuit' is likely one of these, since it has a consequential role in translating biologically relevant stimuli into adaptive behavioral responses (Pierce and Kalivas, 1997b). The motive circuit is regarded as a 'gain control' mechanism, whereby it can regulate both the threshold and intensity of behavioral responses to a given stimulus. Importantly, the motive circuit is thought to play a critical role sensitization processes that underlie drug abuse and schizophrenia.

The main nuclei of the motor circuit include the prefrontal cortex (PFC), medial dorsal thalamus (MD), ventral pallidum (VP), nucleus accumbens (NA), and ventral tegmental area (VTA) (see Fig. 1-3A & B). Reciprocal connections between these nuclei allow the flow of information from limbic nuclei to both pyramidal and extrapyramidal motor systems (Pierce and Kalivas, 1997b). Dopamine arises solely from the VTA and innervates nuclei within the motive circuit. Glutamate inputs emanate from the thalamus and limbic nuclei (i.e., amygdala, hippocampus, and PFC) and widely innervate the motive circuit. There are reciprocal γ-amino-butyric acid (GABA) projections between the NA and VP. In addition, the VP is a source of GABAergic innervation to the VTA and MD.

Following neonatal dopamine lesions with 6-OHDA, there is sparing of dopaminergic neurons within the VTA (Snyder-Keller, 1991). These dopaminergic neurons may somehow overcompensate for the loss of nigrostriatal dopamine during development of these animals (van Oosten and Cools, 2002; van Oosten et al., 2005). In this respect, sensitization in neonate-lesioned rats to repeated D_1 agonist treatment might occur because of a distributed change in neurotransmission resulting from overactive VTA dopaminergic neurons, which could alter the gain of the motive circuit such that a

15

greater behavioral response would be elicited by subsequent agonist treatments (see Fig. 1-3B).

Research Goals

Dysfunction of the dopamine system has been implicated in a number of developmental and other disorders including LNS (Lesch and Nyhan, 1964), schizophrenia (Goldman-Rakic et al., 2004), and drug abuse (Hummel and Unterwald, 2002). Sensitization processes that are thought to underlie these disorders appear to be dependent upon D_1 receptor function (Breese et al., 1985a; Goldman-Rakic et al., 2004; Hummel and Unterwald, 2002). The neonate-lesioned rat provides an excellent model to study D_1 receptor function, given that these rats, unlike normal rats, demonstrate a functional "uncoupling" of D_1 and D_2 receptors throughout development (Breese et al., 1994). If ERK1/2 proves to be a key mediator of adaptive change in these animals, this system could provide regionally specific molecular targets for the development of novel treatments for symptoms involved in disorders related to dopamine dysregulation and altered D_1 receptor signaling.

The studies presented in this dissertation will explore the activation of ERK1/2 along with its molecular and behavioral consequences in neonate-lesioned rats primed with repeated doses of D_1 agonist. Chapter II describes the time course of ERK1/2 phosphorylation in selected cortical and subcortical regions of the mesolimbic and nigrostriatal dopamine systems at acute and extended time points after repeated D_1 agonist treatment. This chapter also examines phosphorylation of transcription factor CREB as a functional output for ERK1/2 phosphorylation. Furthermore, this chapter

explores the role of neurotransmitter receptors previously established as critical for priming (i.e., D_1, NMDA, and 5-HT_2) in the phospho-ERK1/2 response. Chapter III determines the role of phosphorylated ERK in the behavioral sensitivity of neonate-lesioned rats to repeated D_1 agonist treatment. Chapter IV examines dendritic structure in these animals, and explores whether any changes in dendrites produced by repeated D_1 agonist treatment are dependent on ERK1/2 phosphorylation. Chapter V presents a summary of the major findings and suggestions for future research.
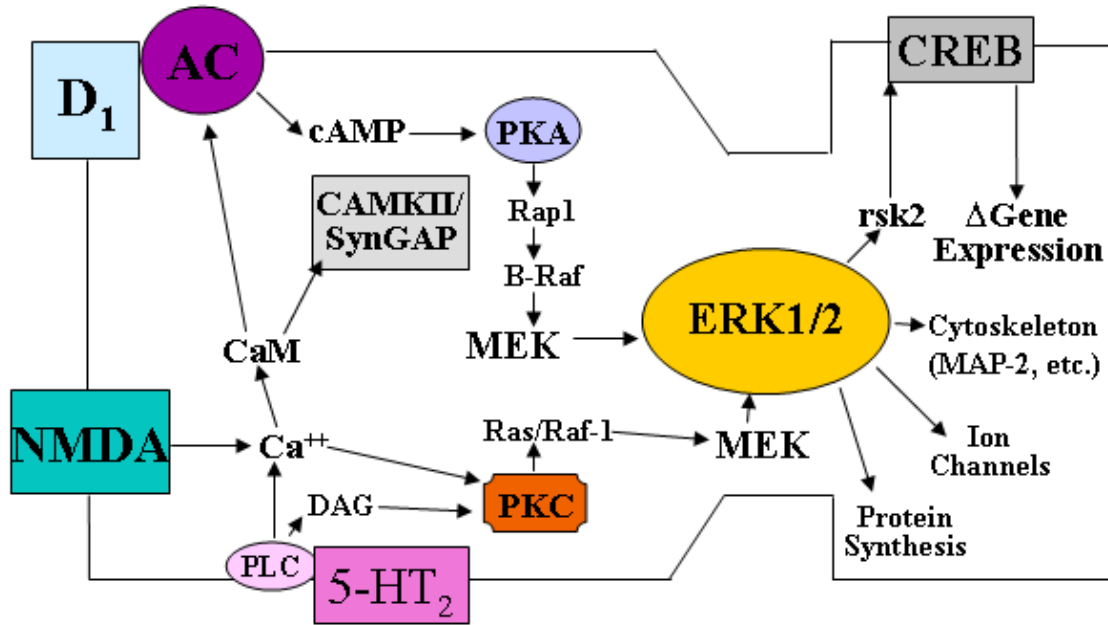
Figure 1-1: ERK1/2 integration of diverse cell-surface signaling mechanisms. *AC*, adenylyl cyclase; *PLC*, phospholypase C; *DAG*, diacylglycerol; *CaM*, calmodulin; *CaMKII*, calcium/calmodulin-dependent protein kinase II (*Adapted from Sweatt, 2001*)
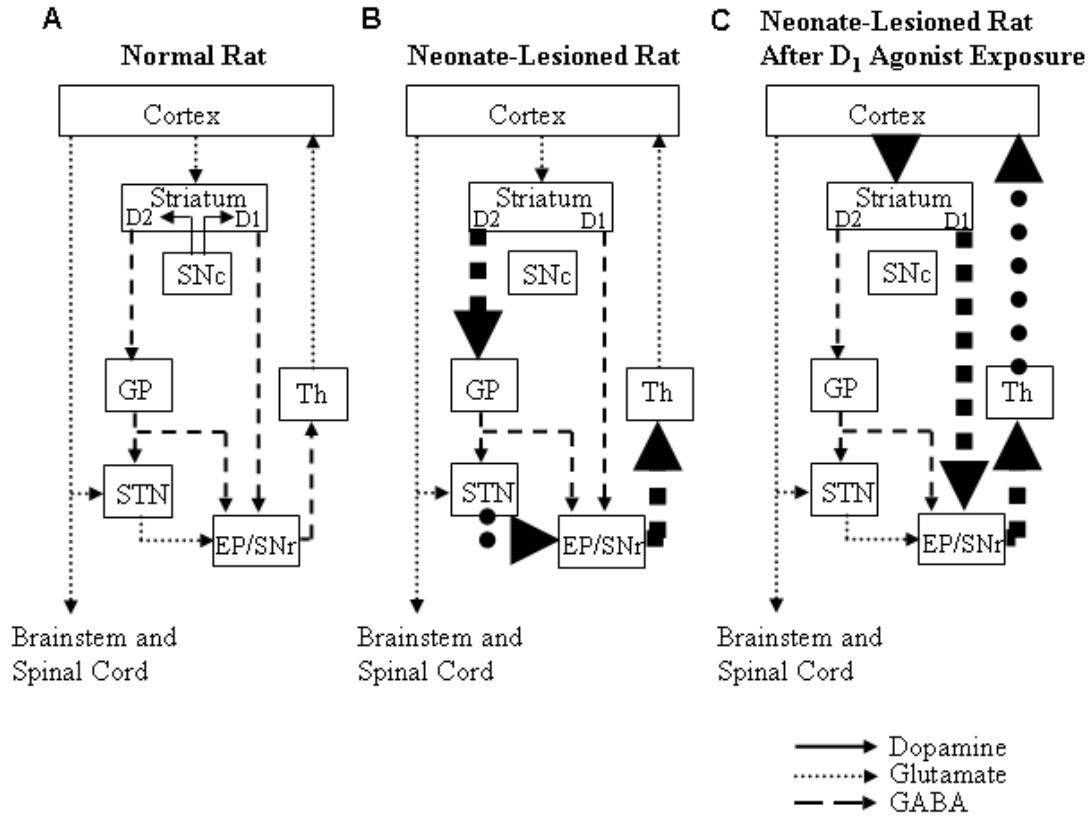
Figure 1-2: Classic model of the basal ganglia circuit in (*A*) normal rats, (*B*) neonate-lesioned rats, and (*C*) D$_1$ agonist-treated neonate-lesioned rats. Thickened lines indicate increases in neurotransmission. *SNc*, substantia nigra pars compacta; *GP*, globus pallidus; *STN*, subthalamic nucleus; *EP/SNr*, entopeduncular nucleus/substantia nigra pars reticularis; *Th*, Thalamus. (*Adapted from Olanow et al., 2004*)
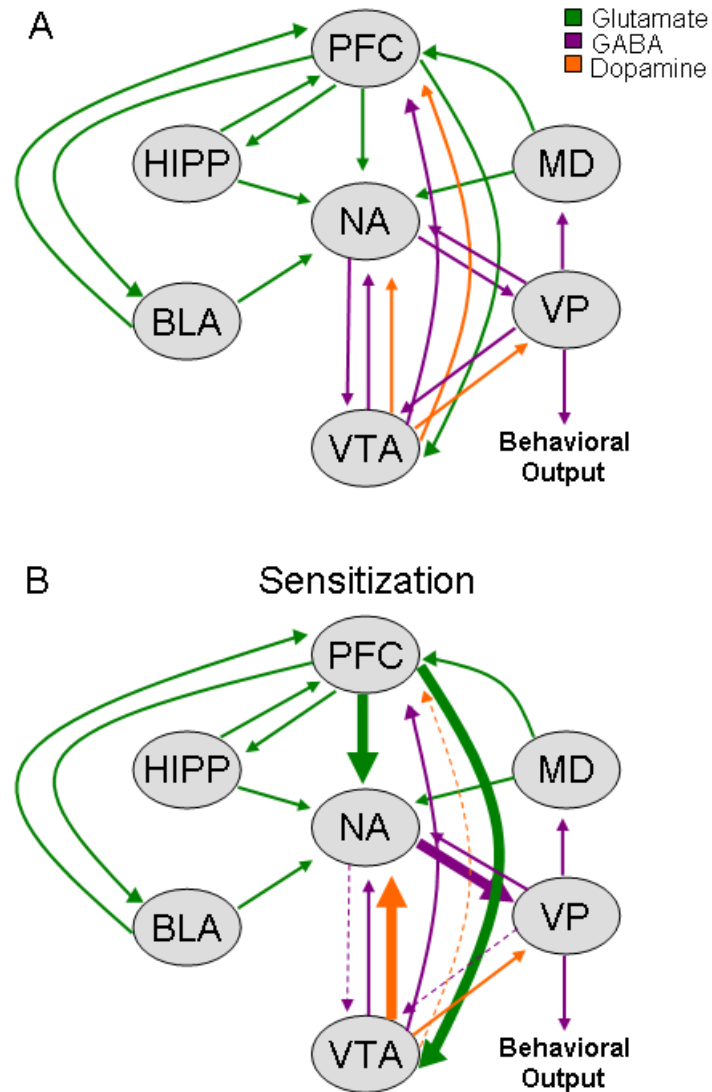
Figure 1-3: Simplified model of the 'motive' circuit in (*A*) normal rats and (*B*) D₁ agonist-sensitized (primed) rats. Thick lines indicate increases, while dotted lines represent decreases in neurotransmission. *PFC*, prefrontal cortex; *MD*, medial dorsal thalamus; *VP*, ventral pallidum; *NA*, nucleus accumbens; *VTA*, ventral tegmental area; *Hipp*, hippocampus; *BLA*, basolateral amygdala. (*Adapted from Pierce and Kalivas, 1997b and Wolf, 2002*)

CHAPTER II. SUSTAINED EXTRACELLULAR SIGNAL-REGULATED KINASE 1/2 PHOSPHORYLATION IN NEONATE 6-HYDROXYDOPAMINE-LESIONED RATS AFTER REPEATED D_1-DOPAMINE RECEPTOR AGONIST ADMINISTRATION: IMPLICATIONS FOR NMDA RECEPTOR INVOLVEMENT.

A.   Introduction

Administration of the neurotoxicant 6-hydroxydopamine (6-OHDA), with desmethylimipramine pretreatment, results in the selective destruction of dopamine-containing neurons (Smith et al., 1973). Rats bilaterally lesioned with 6-OHDA as neonates have increased susceptibility for aggression, hyperexcitability, and self-injurious behavior in response to dopamine (DA) receptor agonists (Breese et al., 1984a). These behaviors are similar to those observed clinically with Lesch-Nyhan syndrome (LNS), a developmental disorder characterized by reduced brain DA, choreoathetoid movements, and compulsive self-injurious behavior (Lesch and Nyhan, 1964). The susceptibility for self-injurious behavior observed in neonate-lesioned rats is not present in rats lesioned with 6-OHDA as adults, the latter of which mimic Parkinson's disease (Breese et al., 1984a; Marsden, 1984). Thus, the neonatal rat brain must retain sufficient plasticity to allow for the development of compensatory mechanisms that attenuate, to some degree, the debilitating effects of DA depletion.

Repeated dosing with the D_1-dopamine receptor agonist SKF-38393 (2,3,4,5-tetrahydro-7,8-dihydroxy-1-phenyl-1H-3-benazepine HCl) to neonate-lesioned rats results in long-lasting behavioral sensitization, which is seen as an agonist-induced

increase in locomotor activity for at least 6 months after the sensitization (Breese et al., 1984a; Criswell et al., 1989). Treatment with D_1 receptor antagonists blocks the increasing motor responsiveness (Breese et al., 1985a,b; Criswell et al., 1989, 1990), a finding that demonstrates a requirement for D_1 receptor activation in SKF-38393-mediated sensitization of these animals. Studies have shown that the sensitization is not dependent on contextual cues associated with SKF-38393 administration (Criswell et al., 1989), nor is it related to changes in density or binding affinity of D_1 receptors in striatum (Breese et al., 1987).

Central to the notion that SKF-38393-mediated sensitization of neonate-lesioned rats relates to behavioral and neural plasticity is the discovery that pretreatment with the noncompetitive NMDA receptor antagonist MK-801 ((+)-5-methyl-10,11-dihydroxy-5H-dibenzo(a,d)cyclohepten-5,10-imine) abolishes this sensitization (Criswell et al., 1990). It is well established that NMDA receptor activation is critical for development of psychomotor stimulant-induced behavioral sensitization (Karler et al., 1989; Stewart and Druhan, 1993; Wolf and Jeziorski, 1993) and that NMDA receptor antagonists interfere with long-term potentiation, a model of learning and memory formation (Lynch et al., 1983; Davis et al., 1992; for review, see Riedel et al., 2003). These findings have established a critical role for NMDA receptor-dependent mechanisms that can lead to persistent cellular and behavioral adaptive changes. Thus, the finding that MK-801 antagonizes SKF-38393-mediated sensitization in neonate-lesioned rats supports consideration of this model as a type of "neuronal learning" (Criswell et al., 1989).

The discovery of specific neurobiological substrates of adaptive change(s) that accompany the enduring hyper-responsiveness of neonate-lesioned rats to repeated D_1

22

receptor stimulation might provide insight into developmental and other disorders involving permanent DA-mediated sensitization, such as schizophrenia and psychostimulant abuse. A likely candidate, extracellular signal-regulated kinase (ERK) 1/2, is a cell-signaling molecule thought to be critical for various forms of neuroplasticity. Stimulation of D_1 and NMDA receptors can recruit several second messenger systems to activate ERK (Xia et al., 1996; Sweatt, 2001). In this respect, Gerfen et al. (2002) demonstrated enhanced striatal ERK phosphorylation after acute SKF-38393 administration in unilateral adult 6-OHDA-lesioned rats. Furthermore, immediate-early gene transcription in DA-depleted striatum was ERK dependent, a finding that suggests ERK pathway involvement in adaptive changes occurring in these animals (Gerfen et al., 2002). Neuronal ERK phosphorylation has been linked to a number of other cellular signaling processes (for review, see Adams and Sweatt, 2002). Among these, activation of the transcription factor cAMP response element-binding protein (CREB) has emerged as a major regulatory mechanism for activity-dependent neuroplasticity (Lonze and Ginty, 2002).

The aim of the present study was to investigate whether repeated SKF-38393 administration to neonate-lesioned rats would result in enhanced ERK activation in the primary DA-terminal fields of the forebrain. Immunostaining for phosphorylated (phospho)-ERK revealed distinct temporal patterns in dorsal striatum (striatum), nucleus accumbens (accumbens), and cortex. The medial prefrontal cortex (mPFC) was unique in that it demonstrated remarkably sustained phospho-ERK that was accompanied by increased phospho-CREB immunostaining. Moreover, the prolonged mPFC phospho-ERK immunostaining was dependent on D_1 and NMDA receptor coactivation. Our data

strongly suggest that the sustained ERK phosphorylation observed in mPFC reflects a neuroadaptive change that occurs with D_1 agonist-induced sensitization of neonate-lesioned rats.

B.   Materials and Methods

Preparation of neonate 6-OHDA-lesioned rats

Pregnant Sprague Dawley rats obtained from Charles River Laboratories were individually housed, with Wayne Lab Blox laboratory chow and water available *ad libitum*. On day 3 after delivery, male and female rat pups were anesthetized with ether and then administered 100 μg (free base) of 6-OHDA intracisternally (i.c.), 60 min after desipramine (20 mg/kg, i.p.), to protect noradrenergic neurons (Breese et al., 1984a). The bilateral lesion causes >90% loss of dopamine innervation into the striatum and disrupts basal ganglia-cortical system circuits (Smith et al., 1973). Some rats received desipramine (20 mg/kg, i.p.) and saline (i.c.) and served as unlesioned (sham-lesioned) controls. Rats treated with 6-OHDA or saline neonatally were weaned at day 30 and testing began at 40-60 d of age. All animal use procedures were in strict accordance with the Institutional Animal Care and Use Committee (2003), and all efforts were made to minimize the number of animals used.

Although several lines of evidence implicate gender differences in the activation of ERK and CREB (Cardona-Gomez et al., 2002; Bi et al., 2003; Wade and Dorsa, 2003), no significant SKF-38393-dependent differences in phospho-ERK or phospho-CREB immunoreactivity were found between male and female rats, regardless of neonatal lesioning (data not shown). Thus, SKF-38393-induced phospho-ERK, ERK, phospho-

CREB, or CREB immunoreactivity was examined in the striatum, accumbens, mPFC, and other selected cortical regions of both male and female rats.

The following sections describe all adult drug treatments, dosing regimens, and times of killing for animals used in this study. Data in supplemental Figure 2-1S are provided as an additional guide for the experimental paradigm.

Single SKF-38393 treatment to neonate-lesioned adult rats

To assess the acute effects of a single dose of SKF-38393, naive neonate-lesioned and sham-lesioned rats were injected with 3 mg/kg SKF-38393 at 40-60 d of age and killed at 15 min ($n = 4$ per treatment group), 30 min ($n = 4$), 60 min ($n = 4$-5), 120 min ($n = 5$-12), and 360 min ($n = 2$) after agonist treatment. A separate group of adult neonate-lesioned or sham-lesioned rats were administered saline, rather than agonist, and killed at 15, 60, and 120 min to serve as controls ($n = 2$). Neonate-lesioned and sham-lesioned rats were also killed at 3 d ($n = 4$) and 7 d ($n = 4$-6) after this treatment regimen to examine the long-term effects of a single dose of agonist to these animals.

Repeated SKF-38393 treatment to neonate-lesioned adult rats

Neonate-lesioned rats do not show maximal sensitivity to D_1 agonists unless exposed repeatedly to such agonists (Breese et al., 1985b; Criswell et al., 1989). Therefore, beginning at 40-50 d of age, neonate-lesioned rats in this treatment group received repeated treatments with SKF-38393 sufficient to allow the animals to reach a plateau of maximal behavioral supersensitivity (Criswell et al., 1989, 1990). To accomplish this sensitization process, lesioned animals were administered a total of 12

mg/kg SKF-38393, divided into three doses as follows: 6, 3, and 3 mg/kg, each spaced 1 week apart as described previously (Breese et al., 1985a,b; Criswell et al., 1989). A separate group of sham-lesioned rats received the same agonist-dosing regimen. To assess acute effects of repeated SKF-38393 administration, animals were killed at 15 min ($n = 4$-5 per treatment group), 60 min ($n = 4$-5), 120 min ($n = 4$), and 360 min ($n = 2$) after agonist treatment. To serve as controls, groups of neonate-lesioned and sham-lesioned rats were administered three consecutive injections of saline at weekly intervals and killed at 15 min ($n = 2$-4), 60 min ($n = 2$), 120 min (2-3), and 360 min ($n = 2$) after the final saline administration. To examine the chronic effects of repeated SKF-38393 administration, animals were killed at 3 d ($n = 4$-6), 7 d ($n = 10$-15), 14 d ($n = 5$-8), 21 d ($n = 6$-7), or 36 d ($n = 5$-6) after the final agonist or saline treatment. At 36 d, a separate group of previously treated neonate-lesioned and sham-lesioned rats were administered an additional dose of SKF-38393 (3 mg/kg) or saline and killed 7 d later ($n = 5$-6).

Immediately after the final dose of SKF-38393 or saline to neonate-lesioned or sham-lesioned rats, behavioral activity was assessed to assure maximal responsiveness of neonate-lesioned rats to the agonist. Rats were placed in clear 17 x 17 inch computer-monitored activity chambers (Med Associates, St. Albans, VT), and horizontal, vertical, and stereotypical activity was recorded in 5 min bins over a 3 hr testing period. ANOVA F test of model fit for motor activity between treatment groups yielded $F_{(3,206)} = 54.90$, $p < 0.0001$ for horizontal activity, $F_{(3,206)} = 17.68$, $p < 0.0001$ for vertical activity, and $F_{(3,206)} = 11.94$, $p < 0.0001$ for stereotypical activity. As determined by *post hoc* analysis using Fisher's PLSD test (mean ± SEM), neonate-lesioned rats receiving multiple SKF-38393 treatments demonstrated 120,486.24 ± 10,641.87 total horizontal counts, 2348.51

± 263.30 total vertical counts, and 15,167.80 ± 535.27 total stereotypical counts compared with 20,681.32 ± 2357.34 total horizontal counts ($p < 0.0001$), 799.09 ± 77.84 total vertical counts ($p < 0.0001$), and 11,646.37 ± 476.32 total stereotypical counts ($p < 0.0001$) observed for neonate-lesioned rats injected with saline, 20,389.82 ± 2751.24 total horizontal counts ($p < 0.0001$), 1040.34 ± 118.37 total vertical counts ($p < 0.0001$), and 12,371.19 ± 772.15 total stereotypical counts ($p = 0.0026$) observed for sham-lesioned rats dosed repeatedly with SKF-38393, and 20,579.15 ± 1648.53 total horizontal counts ($p < 0.0001$), 965.13 ± 71.12 total vertical counts ($p < 0.0001$), and 10,864.39 ± 579.04 total stereotypical counts ($p < 0.0001$) observed for sham-lesioned rats injected with saline. The novelty of the testing environment unlikely affected our results, because no significant differences were found in motor activity between the SKF-38393-sensitized neonate-lesioned animals and a separate group of neonate-lesioned animals (not used in this study) that were placed in activity chambers after each of four weekly treatments with SKF-38393 (supplemental Table 2-1S) ($p = 0.4229$, horizontal activity; $p = 0.3034$, vertical activity; $p = 0.5824$, stereotypical activity indicating no difference with Fisher's PLSD test). This finding is consistent with previous data accumulated in neonate-lesioned rats showing that behavioral sensitization results in comparable levels of activity in response to SKF-38393 when the rats are repeatedly dosed in the same or a different environment from that in which the rats are finally tested (Criswell et al., 1989).

Pretreatment with the MEK inhibitor SL327 before repeated SKF-38393 administration to neonate-lesioned rats

For this experimental series, SL327 (α-[amino[(4-aminophenyl)thio]methylene]-2-(trifluoromethyl) benzeneacetonitrile) (100 mg/kg), a selective inhibitor of the upstream ERK activator MEK, was administered to neonate-lesioned rats 30 min before each of three weekly doses of SKF-38393 (3 mg/kg), with the fourth weekly treatment consisting of only dimethylsulfoxide (DMSO) vehicle followed by SKF-38393 ($n = 5$). Control treatment groups included (1) four weekly treatments of DMSO followed by SKF-38393 ($n = 4$) and (2) four weekly treatments of DMSO followed by saline ($n = 4$). All rats thus received DMSO before the fourth and final dose of SKF or saline and were killed 7 d later.

Pretreatment with the D_1 antagonist SCH-23390 or the 5-HT$_2$ receptor antagonist ketanserin before repeated SKF-38393 administration

Groups of neonate-lesioned and sham-lesioned rats each received four doses of SCH-23390 ((R)-(+)-8-chloro-2,3,4,5-tetrahydro-3-methyl-5-phenyl-1H-3-benzazepine-7-OL maleate; 0.3 mg/kg), ketanserin (3-[2-[4-(4-fluorobenzoyl)-1-piperidinyl]ethyl]-2,4(1H,3H)-quinazolinedione tartrate; 2 mg/kg), or saline 15 min before each of four weekly doses of SKF-38393 or saline. The primary treatment groups were as follows: (1) SCH-23390 followed by SKF-38393 ($n = 6\text{-}10$) and (2) ketanserin followed by SKF-38393 ($n = 4$). Control treatment groups included (1) saline followed by SKF-38393 ($n = 2\text{-}10$), (2) SCH-23390 followed by saline ($n = 2\text{-}10$), and (3) saline followed by saline ($n = 4\text{-}5$). Rats were killed 7 d after the final drug treatment.

28

Pretreatment with NMDA receptor antagonist MK-801 or CGS-19755 before repeated SKF-38393 administration

For the noncompetitive NMDA receptor antagonist MK-801, male rats were dosed with 0.3 mg/kg, whereas females received 0.14 mg/kg because female rats have much greater responsiveness to the motor effects of MK-801 (Fleischmann et al., 1991; Blanchard et al., 1992; Honack and Loscher, 1993; Haggerty and Brown, 1996; Frantz and Van Hartesveldt, 1999). MK-801, the competitive NMDA receptor antagonist CGS-19755 (*cis*-4-(phosphonomethyl)-2-piperidinecarboxylic acid; 10 mg/kg), or saline was administered 15 min before four weekly doses of SKF-38393 (3 mg/kg) or saline. The two primary treatments were (1) MK-801 followed by SKF-38393 ($n = 13$ per treatment group) and (2) CGS-19755 followed by SKF-38393 ($n = 6$-18 per treatment group). Control treatments included (1) saline followed by SKF-38393 ($n = 5$), (2) MK-801 followed by saline ($n = 6$-8), (3) CGS-19755 followed by saline ($n = 6$-15), and (4) saline followed by saline ($n = 7$-10). Rats were killed 7 d after the final drug treatment.

Drugs

6-OHDA hydrobromide (ICN Biochemicals, Irvine, CA) was dissolved in saline containing 0.5% ascorbic acid and administered intracisternally. Desipramine hydrochloride (Sigma, St. Louis, MO), SKF-38393 (Sigma), SCH-23390 (Schering Corporation, Bloomfield, NJ), ketanserin (Sigma), MK-801 (a gift from Merck, Rahway, NJ), and CGS-19755 (a gift from CIBA-GEIGY Corporation, Summit, NJ) were dissolved in saline and administered intraperitoneally. The MEK inhibitor SL327 (kindly provided by DuPont Pharmaceuticals Company, Boston, MA) was dissolved in 100%

DMSO and administered intraperitoneally (2 ml/kg) (Atkins et al., 1998; Selcher et al., 1999; Yamagata et al., 2002).

Immunohistochemistry: tissue preparation and immunostaining

Rats were deeply anesthetized with an overdose of sodium pentobarbital (100 mg/kg), perfused transcardially for 4 min with PBS (150 m$_M$ NaCl, 100 m$_M$ sodium phosphate, pH 7.4) followed by 7 min of 4% phosphate-buffered paraformaldehyde (100 m$_M$ sodium phosphate), and their brains were collected and postfixed for 24 hr at 4°C. Forty-micrometer-thick sections were then cut with a vibrating microtome for the immunohistochemistry. Standard avidin-biotin-horseradish peroxidase methods were used as described previously (Knapp et al., 1998, 2001). After rinsing in fresh PBS three times (10 min each), free-floating tissue sections were blocked in 10% normal goat serum and 0.2% Triton X-100 in PBS for 1 hr. Affinity-purified polyclonal tyrosine hydroxylase (TH) (1:4000; Calbiochem, La Jolla, CA), phospho-ERK [phospho-p44/42 MAP kinase (thr202/tyr204); 1:500; Cell Signaling Technology, Beverly, MA], phospho-CREB, and CREB (both 1:500; Cell Signaling Technology) were used to detect protein expression. All sections were incubated in 3% normal serum, 0.2% Triton X-100, and antisera for 48-72 hr at 4°C with agitation. An antibody-blocking peptide to phospho-ERK containing phosphorylated amino acid residues threonine 202 and tyrosine 204 (Santa Cruz Biotechnology, Santa Cruz, CA) was used to verify specificity of the antibody. A 10-fold higher concentration of the blocking peptide was incubated with phospho-ERK primary antibody at room temperature for 30 min and then incubated with selected brain tissue as described above. Tissue sections were further processed using Vectastain Elite ABC kits

(Vector Laboratories, Burlingame, CA) per the manufacturer's instructions with immunochemical detection using nickel-cobalt intensification of the diaminobenzidine reaction product. For analysis, great care was taken to match sections through the same region of brain at the same level. All visible positive nuclei or cell bodies within a 10 x 10 eyepiece reticule field were counted and expressed as number of cells per square millimeter of tissue for each brain site. For a single brain site, counts were averaged from three sections from each animal.

Western blot analysis: tissue preparation and immunoblotting

For Western blotting, rats were killed by decapitation, their brains were rapidly removed from the skulls, and the mPFC and striatum were dissected on ice and stored at -80°C until use. Tissues were homogenized by sonication in solubilization buffer (10 mM Tris-Cl, 50 mM NaCl, 1% Triton X-100, 30 mM sodium pyrophosphate, 50 mM NaF, 5 nM $ZnCl_2$, 100 μM Na_3VO_4, 1mM DTT, 5 nM okadaic acid, 2.5 μg aprotinin, 2.5 μg pepstatin, and 2.5 μg leupeptin). Insoluble material was removed by centrifugation (13,000 rpm for 20 min at 4°C), and protein concentration was determined using a BCA protein assay kit (Pierce, Rockford, IL). Samples were mixed with Novex 2x Tris-glycine SDS sample buffer (San Diego, CA) containing 5% 2-mercaptoethanol and heated to 90°C for 3 min. Aliquots of 20 μg of protein per lane were separated on 8-16% gradient Tris-glycine gels (Novex) under reducing conditions using the Novex Xcell II minicell apparatus. Proteins were transferred to polyvinylidene difluoride membranes (Immobilon-P, Millipore, Bedford, MA). Membranes were incubated in PBS with 0.05% Tween 20 (PBS-T), containing 1% milk powder for 2 hr at room temperature to block non-specific

binding. Blots were probed with an antibody corresponding to the inactive form of ERK (p44/42 MAPK; 1:1000; Cell Signaling Technology) or to phospho-ERK (1:1000; Cell Signaling Technology), followed by goat anti-rabbit IgG conjugated with horseradish peroxidase (Chemicon, Temecula, CA) at a 1:20,000 dilution in blocking solution for 60 min. Membranes were then washed three times with PBS-T. Bands were detected using enhanced chemiluminescence (Pierce) apposed to x-ray film under nonsaturating conditions and analyzed by densitometric measurements using NIH Image 1.57 (public domain software developed by the National Institutes of Health and available at http://rsb.info.nih.gov/nih-image). Data are representative of four animals per treatment group and normalized on the basis of estimates obtained in the samples from sham-lesioned, saline-treated controls.

Quantification and statistical analysis

Details of brain region identification and cell counting strategy have been reported previously in our laboratory (Knapp et al., 1998). Average counts for a specific brain region for each animal were grouped by treatment and averaged for each time point to obtain the mean counts per square millimeter ± SEM for that brain site. Average cell counts for each defined brain region were compared within and between treatment groups using ANOVA. Statistical comparisons between control groups versus lesioned groups administered either SKF-38393 or saline were followed by *post hoc* tests. A more conservative significance level was set at $p = 0.01$ for all time-course experiments to correct for multiple comparisons, whereas the significance level for all other experiments

was set at the traditional 0.05 level. The Fisher's PLSD test was performed when comparing combinations of means.

C.   Results

Assessment of dopamine-containing neuronal destruction in neonate-lesioned adult rats

Previous studies (Smith et al., 1973; Breese et al., 1985a,b) documented that DA content within the striatum, accumbens, and cortex is drastically reduced in adult rats lesioned as neonates with 6-OHDA. Such loss of DA-containing terminals in the striatum of neonate-lesioned rats is illustrated in Fig. 2-1 by the >90% reduction in TH immunoreactivity compared with the TH level in a sham-lesioned control animal. Because TH is the rate-limiting enzyme in the biosynthesis of dopamine (Nagatsu et al., 1964), TH immunoreactivity was determined for all lesioned and control animals in this investigation to establish that the neonate 6-OHDA lesioning induced an adequate loss of DA-containing neurons.

Acute effects of single and repeated D_1 agonist SKF-38393 administration on phospho-ERK immunoreactivity in neonate-lesioned rats

Phospho-ERK was evaluated in the primary forebrain DA-terminal regions (i.e., striatum, accumbens, and mPFC) of neonate-lesioned rats at various time points after D_1 agonist administration. The initial 15 min time point was chosen on the basis of Gerfen et al. (2002), who demonstrated maximum phospho-ERK immunoreactivity in striatum of unilateral adult-lesioned rats 15 min after a single SKF-38393 administration. In the

present study, distinctive patterns of time-dependent ERK phosphorylation were observed across these brain regions in response to SKF-38393.

Striatum and nucleus accumbens

In the striatum, both single and repeated SKF-38393 treatments to neonate-lesioned rats produced acute, transient increases in phospho-ERK that peaked at 15 min after drug administration (Fig. 2-2*A,D,E*). Although slightly more phospho-ERK-positive cells were observed at 15 min in naive neonate-lesioned rats compared with rats sensitized with the agonist, the difference was not significant ($p = 0.2096$). ERK activation was absent in the striatum by 60 min in neonate-lesioned rats administered a single dose of SKF-38393; however, phospho-ERK immunoreactivity remained significantly elevated at this time point in rats administered repeated doses of SKF-38393 ($p < 0.0001$). This prolongation of ERK phosphorylation appeared to occur most prominently in the dorsomedial and dorsolateral quadrants of the striatum, with lighter staining occurring ventrally (Fig. 2-2*B*). Phospho-ERK was no longer detected at 120 min in striatum of SKF-38393-treated neonate-lesioned rats. No phospho-ERK immunoreactivity was detected in striatum of neonate-lesioned rats treated with saline or in sham-lesioned rats treated with single or repeated doses of SKF-38393 or saline at any of the time points examined (Fig. 2-2*A,C,F*).

In accumbens, a single dose of SKF-38393 to drug-naive neonate-lesioned animals or controls failed to produce significant change in phospho-ERK at any time point (Fig. 2-3*A,C,E,F*). Neonate-lesioned rats administered repeated doses of SKF-38393, however, exhibited significant phospho-ERK immunoreactivity at acute time

points before 120 min (Fig. 2-3*A,B,D*) compared with neonate-lesioned animals administered saline ($p < 0.0001$, 15 min; $p < 0.0001$, 60 min). This enhanced ERK phosphorylation was observed specifically in the rostral pole of the accumbens and was not present in the caudal shell or core of neonate-lesioned rats receiving repeated doses. Although the time course of accumbens phospho-ERK immunoreactivity was similar to that of striatum, total phospho-ERK-positive cell counts in the accumbens were ~20-40% of striatum, and the intensity of phospho-ERK immunostaining in the accumbens was much lower. It is unlikely that these effects were artifacts of tissue processing, because representative sections of the striatum and accumbens were always stained concurrently.

Medial prefrontal cortex

A baseline of ~18-25 phospho-ERK-positive cells per square millimeter was observed consistently in mPFC and did not significantly differ among the sham or saline-treated lesioned groups (Fig. 2-4*A*). Neonate-lesioned rats that received a single dose of SKF-38393 demonstrated a transient (0-60 min) increase in ERK phosphorylation over baseline in mPFC, which was similar in profile and duration to the striatum of these animals (compare Figs. 2-2*A*, 2-4*A*). Phospho-ERK immunoreactivity in this treatment group was significantly elevated over control groups only at 15 min after agonist administration ($p < 0.0001$ for Lesioned SKF vs control groups).

Among the dopamine-rich regions, mPFC displayed a unique, highly prolonged increase in phospho-ERK in neonate-lesioned rats previously administered repeated doses of SKF-38393. In these animals, phospho-ERK-immunoreactive cell counts were increased four- to sixfold, primarily within layers II-III of the mPFC. These phospho-

ERK-positive counts remained elevated over the course of the examination (up to 360 min) (Fig. 2-4*A-H*) ($p = 0.0085$ at 15 min, $p = 0.0015$ at 60 min, $p < 0.0001$ at 120 min for Lesioned R-SKF vs Lesioned SKF groups; $p < 0.01$ at 15, 60, and 120 min, and $p < 0.02$ at 360 min for Lesioned R-SKF vs other control groups). The conspicuous persistence of ERK hyperphosphorylation in mPFC, but not in striatum or accumbens, suggests that different processes of neuroadaptation occur among these brain regions and, furthermore, that the adaptive changes occurring in the mPFC are more enduring.

Sustained duration of ERK phosphorylation in mPFC of neonate-lesioned rats after repeated SKF-38393 administration

Because the persistent increase in ERK phosphorylation was observed for up to 360 min in mPFC of neonate-lesioned rats sensitized with SKF-38393, an additional evaluation of the time course of the sustained ERK response in this region was performed. As shown in Table 2-1, control groups did not significantly differ from each other across time points, with phospho-ERK-positive cell counts remaining at the baseline level of ~18-25 cells per square millimeter. Neonate-lesioned rats sensitized with repeated doses of SKF-38393 demonstrated a sustained increase in phospho-ERK immunoreactivity in mPFC that was significantly elevated over neonate-lesioned rats injected with saline (as well as sham-lesioned control groups) across all extended time points ($p < 0.0001$ at 3, 7, and 14 d; $p = 0.0109$ at 21 d; $p = 0.0025$ at 36 d comparing R-Saline and R-SKF groups). Prominent phospho-ERK in mPFC of these animals persisted for >7 d after the final agonist treatment (Table 2-1). Beyond 7 d, sensitized phospho-ERK immunoreactivity began to diminish, yet remained significantly elevated from that

observed in saline-treated neonate-lesioned and sham-lesioned rats for up to 36 d ($p <$ 0.01 for all comparisons).

As shown in Table 2-1, an additional dose of SKF-38393 administered at 36 d to previously sensitized neonate-lesioned rats resulted in significantly elevated levels of phospho-ERK immunoreactivity 7 d later (i.e., at 42 d) compared with levels observed at 36 d ($p = 0.0001$). Phospho-ERK-positive cell counts in these animals were nearly identical to those found in neonate-lesioned rats killed 3 and 7 d after the initial SKF-38393 dosing regimen ($p \geq 0.1110$, indicating no significant difference). In neonate-lesioned rats injected repeatedly with saline, an additional dose of saline at 36 d did not result in elevated phospho-ERK immunoreactivity at 7 d after injection (data not shown), nor did a single dose of SKF-38393 to neonate-lesioned or sham-lesioned rats (Table 2-1). Sham-lesioned rats that received saline treatment at 36 d also did not exhibit a significant increase in phospho-ERK immunoreactivity at 7 d after injection (data not shown).

To ascertain that the observed immunohistochemical staining was phospho-ERK and not another phosphoprotein or nonspecific reaction, immunoblotting was performed with protein isolated from mPFC of lesioned rats administered repeated doses of SKF-38393 or injected with saline (data not shown). Blots probed with the same concentration of phospho-ERK antibody used for immunohistochemistry revealed the typical doublet of bands near 42 and 44 kDa related to phospho-ERK1 and phospho-ERK2, respectively. No other bands were visualized, a finding that provides strong evidence that the elevated immunohistochemical staining observed in mPFC of rats dosed repeatedly with SKF-38393 was specific for phospho-ERK.

A plausible explanation for our findings with sustained phospho-ERK would be that total ERK protein levels were elevated chronically in the neonate-lesioned animals after repeated exposure to SKF-38393. Therefore, we examined whether sensitization of neonate-lesioned rats to SKF-38393 would produce long-lasting changes in total ERK protein in mPFC. Because immunohistochemistry for unphosphorylated ERK failed to produce a consistent signal, total ERK protein was analyzed by SDS-PAGE and immunoblotting of equally loaded total proteins from mPFC and striatum (blot not shown). No significant differences were found for optical density measurements (mean ± SEM) of total ERK levels among neonate-lesioned rats repeatedly dosed with SKF-38393 (mPFC, 101.86 ± 5.42; striatum, 91.0 ± 5.59), sham-lesioned rats repeatedly dosed with SKF-38393 (mPFC, 95.60 ± 4.75; striatum, 91.56 ± 1.96), saline-treated neonate-lesioned rats (mPFC, 105.30 ± 3.30; striatum, 94.00 ± 1.12), or saline-treated sham-lesioned rats (mPFC and striatum standardized to 100%) at day 7 after the final injection of agonist (ANOVA F test of model fit: $F_{(3,12)} = 1.040$, $p = 0.4102$ for mPFC; $F_{(3,12)} = 1.865$, $p = 0.1893$ for striatum). Because total ERK levels were not changed by the repeated D_1 agonist treatments in neonate-lesioned rats, the sustained increase in phospho-ERK immunoreactivity in mPFC could not be attributed to a sustained increase in total ERK protein.

Sustained duration of ERK phosphorylation in other cortical regions of neonate-lesioned rats after repeated SKF-38393 administration

Because of the extraordinarily sustained phospho-ERK response observed in mPFC, we examined other cortical areas of neonate-lesioned rats dosed repeatedly with

agonist to determine whether ERK phosphorylation was prolonged in these regions. (Fig. 2-5, Table 2-2). Phospho-ERK immunostaining was elevated in ventrolateral orbital cortex (VLOC) and in layer II-III cells of cingulate (CgC), motor (MC), somatosensory (SSC) and piriform (PirC) cortices when examined at day 7 after the final agonist treatment. As shown in Table 2-2, levels of phospho-ERK immunoreactivity for each cortical region were significantly higher at day 7 than levels observed at days 14-21 and 36 after the agonist treatment ($p < 0.01$ for all comparisons). Levels at day 7 after agonist treatment were also significantly higher than levels observed at all time points in saline-treated neonate-lesioned rats and sham-lesioned controls for each cortical region examined (Fig. 2-5) ($p < 0.01$ for all comparisons). Although apparent phospho-ERK-positive cell counts were still elevated (although not statistically significant) at 14-21 d after repeated agonist treatment, phospho-ERK in these cortical regions was clearly reduced by day 36. An additional dose of SKF-38393 at day 36 restored some phospho-ERK immunoreactivity in these cortical regions when examined 7 d later, but these levels were not significantly different from levels observed at day 36 before the additional dose (Table 2-2). Likewise, these levels were not different from those observed in saline-treated neonate-lesioned rats killed at day 36 or in saline-treated neonate- or sham-lesioned rat groups administered a single dose of SKF-38393 at day 36 and killed 7 d after injection (data not shown). In contrast to cortex, neither the striatum nor the accumbens of SKF-38393-sensitized rats exhibited phospho-ERK immunoreactivity at 7 d after the final sensitizing dose of agonist (Fig. 2-5).

Together, these data demonstrate that sustained phospho-ERK immunoreactivity occurs in multiple areas of the cortex, but not in the striatum or accumbens, of D_1 agonist-

sensitized neonate-lesioned rats. These changes are most remarkable in mPFC, where ERK phosphorylation lingers longest and remains most sensitive to full reinstatement with an additional dose of agonist. That the ERK pathway could respond to repeated D_1 agonist stimulation in such a prolonged and regionally selective manner suggests that specific neuroadaptive changes accompany D_1 sensitization in the neonate-lesioned rat. With respect to the mPFC, neuroadaptive changes in this region are thought to play a role in diseases related to dopaminergic dysfunction such as schizophrenia, attention-deficit-hyperactivity disorder, and drug abuse (Laruelle, 2000; Vanderschuren and Kalivas, 2000; Steketee, 2003; Sullivan and Brake, 2003). Because behavioral alterations in the neonate-lesioned rat have been suggested to model each of these diseases (Schwarzkopf et al. 1992; Stevens et al., 1996; Fahlke and Hansen 1999; Moy and Breese 2002; Davids et al., 2003), we chose to focus most of the remainder of our study on exploring this phenomenon in the mPFC.

Sustained CREB phosphorylation in mPFC associated with prolonged phospho-ERK in neonate-lesioned rats after repeated SKF-38393 administration

Phosphorylation of ERK can activate the transcription factor CREB to affect long-term gene expression (Lonze and Ginty, 2002). Thus, phosphorylated CREB potentially represents a functional product of the sustained ERK response after repeated dosing with SKF-38393 to neonate-lesioned rats. When sections from the same animals were immunostained concurrently, we observed a robust increase in phospho-CREB immunoreactivity accompanying phospho-ERK in mPFC at day 7 after repeated SKF-38393 administration (Fig. 2-6*A*). To our surprise, however, increased phospho-CREB

immunoreactivity was observed not only in layers II-III, but throughout all mPFC layers (Fig 2-6*B,F*). When quantified across all mPFC layers, neonate-lesioned animals repeatedly dosed with SKF-38393 demonstrated approximately a four- to fivefold increase in phospho-CREB-positive cell counts (mean ± SEM; 795.07 ± 137.81) compared with neonate-lesioned rats injected repeatedly with saline (146.50 ± 40.28; $p < 0.0001$) and sham-lesioned rats treated repeatedly with SKF-38393 (127.13 ± 12.21; $p = 0.0002$) or saline (226.42 ± 78.00; $p < 0.0003$). Cell counts specifically in layers II-III in the agonist-sensitized rats exhibited nearly a ninefold increase in phospho-CREB-positive cell counts compared with control animals (Fig. 2-6*A*)($p < 0.0001$ for Lesioned R-SKF vs Lesioned R-Saline, Sham R-SKF, or Sham R-Saline). The elevation in number of phospho-CREB-positive cells was not reflective of increased total CREB protein expression (mean values ± SEM were 343.75 ± 8.68 for Lesioned R-SKF, 319.67 ± 8.56 for Lesioned R-Saline, and 329.38 ± 16.55 for Sham R-Saline; ANOVA F test of model fit: $F_{(2,13)} = 1.475$; $p = 0.265$). Notably, only scattered phospho-CREB-positive cells were noted throughout the striatum and accumbens at day 7, regardless of drug treatment (Fig. 2-6*H,I*). Sustained CREB phosphorylation was not observed in any other cortical regions examined (ANOVA F test of model fit: $F_{(3,19)} = 1.181$, $p = 0.345$ for VLOC; $F_{(3,19)} = 0.575$, $p = 0.639$ for CgC; $F_{(3,19)} = 1.086$, $p = 0.380$ for MC; $F_{(3,19)} = 1.051$, $p = 0.394$ for SSC; and $F_{(3,19)} = 0.506$, $p = 0.683$ for PirC). Thus phospho-CREB immunolabeling, unlike phospho-ERK, was restricted to mPFC. Furthermore, the multilamellar expression of phospho-CREB did not mirror the predominant appearance of phospho-ERK in layers II-III, suggesting that some, although perhaps not all, of the phospho-CREB immunolabeling was caused by mechanisms other than activation of ERK.

41

Effect of MEK-inhibitor (SL327) pretreatment on sustained ERK and CREB phosphorylation in mPFC of neonate-lesioned rats after repeated administration of SKF-38393

The involvement of MEK in sustained ERK phosphorylation was demonstrated using systemic injections of SL327, a MEK inhibitor that crosses the blood-brain barrier (Atkins et al., 1998; Selcher et al., 1999; Yamagata et al., 2002). Phospho-ERK immunoreactivity was suppressed in neonate-lesioned rats pretreated with SL327 before each SKF-38393 administration, compared with those pretreated with vehicle (Fig. 2-7*A-C*)($p < 0.0001$). The number of phospho-ERK-positive cells in SL327-pretreated rats did not differ significantly from rats treated with vehicle alone. These data provide further evidence that the elevated immunostaining of mPFC cells observed in SKF-38393-sensitized neonate-lesioned rats is indeed represented by MEK-dependent ERK phosphorylation.

We also examined the effects of SL327 pretreatment on phospho-CREB immunolabeling in mPFC. Phospho-CREB immunoreactivity was reduced to some extent throughout all layers of mPFC by pretreatment with SL327 (Fig. 2-7*D,F*)($p = 0.0238$ for SL R-SKF vs R-SKF). The most dramatic suppression of phospho-CREB immunoreactivity by the MEK inhibitor, however, was produced in layers II-III (Fig. 2-7*D-F*)($p < 0.0001$ for SL R-SKF vs R-SKF), in which cell counts did not significantly differ from rats that were not given the agonist-sensitizing regimen. These findings are consistent with direct involvement of both MEK and ERK activation in sustained CREB phosphorylation in layers II-III, but perhaps indirect, if any, involvement in CREB phosphorylation in deeper layers.

Inhibition of sustained SKF-38393-induced ERK phosphorylation in mPFC of neonate-lesioned rats after pretreatment with the D_1 antagonist SCH-23390

To determine whether the sustained phospho-ERK observed in mPFC of neonate-lesioned rats sensitized with SKF-38393 was dependent on D_1 receptors, rats were pretreated with the D_1 antagonist SCH-23390. As shown in Fig. 2-8*A* and *C*, SCH-23390 pretreatment to neonate-lesioned rats abrogated phospho-ERK immunoreactivity at this brain site ($p < 0.0001$ compared with Lesioned R-SKF group). The number of phospho-ERK-positive cells for this treatment group did not differ significantly from neonate-lesioned rats administered repeated saline injections or from sham-lesioned control groups. Moreover, repeated SCH-23390 treatment on its own did not enhance phospho-ERK immunoreactivity in either neonate-lesioned or sham-lesioned rats.

Rats were also pretreated with the $5\text{-}HT_2$ receptor antagonist ketanserin to control for the antagonist binding properties of SCH-23390 at $5\text{-}HT_2$ receptors (Fig. 2-8*A*) (Bischoff et al., 1988; McQuade et al., 1988). Ketanserin was ineffective at reducing the persistently increased levels of phospho-ERK ($p = 0.578$ compared with Lesioned R-SKF group), indicating that the prolonged phospho-ERK observed in mPFC of SKF-38393-sensitized neonate-lesioned rats is dependent on activation of D_1 receptors.

NMDA receptor blockade prevents the sustained ERK phosphorylation in mPFC induced by repeated doses of SKF-38393 to neonate-lesioned rats

Previous work in our laboratory has demonstrated that MK-801 inhibits SKF-38393-induced behavioral sensitization of neonate-lesioned rats, a finding that implicates NMDA receptor function in adaptive processes underlying repeated SKF-38393 treatment

to these animals (Criswell et al., 1990). In the present study, administration of MK-801 or CGS-19755 to neonate-lesioned and sham-lesioned animals before repeated injections of saline had no effect on basal phospho-ERK immunoreactivity (Fig. 2-9*E*). On the other hand, pretreatment with MK-801 or CGS-19755 before repeated doses of SKF-38393 to neonate-lesioned rats resulted in marked inhibition of sustained phospho-ERK immunoreactivity in mPFC (Fig. 2-9*A,C*) ($p < 0.0001$ for Lesioned MK-801 R-SKF group vs Lesioned R-SKF group, and for Lesioned CGS R-SKF group vs Lesioned R-SKF group). Consequently, these data point to an involvement of NMDA receptors in the sustained phospho-ERK response in mPFC of neonate-lesioned animals.

D.   Discussion

This study demonstrates the remarkably protracted course of ERK phosphorylation in mPFC and other cortical regions of neonate 6-OHDA-lesioned rats behaviorally sensitized to the effects of a D_1 agonist in adulthood. Our observations suggest that prolonged mPFC phospho-ERK is a neurobiological substrate of long-lasting adaptive change in these animals, as indicated by several key findings. First, mPFC is unique among cortical and striatal regions, in that sustained ERK phosphorylation observed primarily in layers II-III declined gradually, yet remained significantly above control levels for at least 36 d. Second, maximal levels of phospho-ERK were restored fully in mPFC, but not significantly in other cortical areas, on day 42 after an additional dose of agonist on day 36. Furthermore, an analogous increase in phospho-CREB in layers II-III of mPFC, but not other cortical regions, at 7 d after the initial sensitizing regimen was MEK dependent. This finding suggests that a functional effect of sustained mPFC ERK phosphorylation is activation of CREB-dependent gene transcription. Finally,

the development of sustained phospho-ERK in mPFC requires both NMDA and D_1 receptor stimulation, a pattern of dependence resembling that identified in several cellular and behavioral neuroadaptive paradigms that have been described in cortical and striatal systems (for review, see Kelley and Berridge, 2002). These findings, together with the proposed contribution of the mPFC in the progressive and enduring behavioral effects of drugs of abuse (Castner and Goldman-Rakic, 2003; Steketee 2003), schizophrenia (Laruelle, 2000; Tzschentke, 2001), and learning and memory (Castner et al., 2000; Elzinga and Bremner, 2002), suggest that the D_1 agonist-sensitized neonate-lesioned rat presents an excellent model for the study of dopamine-dependent neuroadaptations and their functional consequences.

Several studies have demonstrated that activation of D_1 receptors, via a protein kinase A (PKA)-dependent mechanism, can phosphorylate ERK to produce adaptive changes in brain (Vossler et al., 1997; Yao et al., 1998; York et al., 1998; Valjent et al., 2000). In unilateral adult 6-OHDA-lesioned rats, Gerfen et al. (2002) demonstrated transient ERK activation in striatum after acute D_1 agonist administration, an effect attributed to sensitized D_1 receptor-dependent responses. Consistent with this finding, the present study demonstrates a transient phosphorylation (<60 min) of ERK induced by a single dose of SKF-38393 in drug-naive neonate-lesioned rat striatum and mPFC. Notably, the pattern and duration of ERK phosphorylation in striatum of naive neonate-lesioned rats administered a single dose of SKF-38393 were similar to that published by Gerfen et al. (2002) in unilateral adult 6-OHDA-lesioned rats. In agreement with the transient ERK phosphorylation, previous work has shown that a single dose of SKF-38393 can induce Fos expression in striatum of neonate-lesioned rats (Johnson et al.,

1992). Together with the findings of Sgambato et al. (1998) and Gerfen et al (2002), it appears that transient ERK activation can drive immediate-early gene induction in striatum. It remains a question whether transient phospho-ERK observed in the striatum and mPFC of neonate-lesioned rats after a single dose of SKF-38393 is sufficient to drive long-term gene regulation.

Several lines of evidence suggest that prolonged ERK activation (>60 min) is necessary to allow sufficient time for translocation of ERK to the nucleus, long-term gene transcription, and subsequent enhancement of enduring plasticity-associated changes in brain (for review, see Marshall, 1995). Repeated D_1 agonist administration prolonged striatal phospho-ERK immunoreactivity nearly twofold. Conversely, in accumbens, ERK activation was absent with a single dose of agonist and was observed only after repeated treatment with SKF-38393. These findings, together with the prolonged presence of ERK phosphorylation in the mPFC and various other regions of cortex (VLOC, CgC, MC, SSC, and PirC), point to differing mechanisms of adaptation among these regions. Furthermore, the reinstatement of ERK phosphorylation that occurs only in mPFC supports a unique mechanism of adaptation in this region that can trigger rapidly the previous level of ERK activation on reexposure to the agonist.

A well characterized nuclear target for ERK action is the transcription factor CREB (Bourtchuladze et al., 1994; Yin et al., 1994), which is thought to play a central role in long-term plastic changes in brain by controlling the transcriptional expression of several genes (for review, see Curtis and Finkbeiner, 1999). In the present study, immunostaining for phospho-CREB was measured initially as a functional endpoint for sustained ERK activation in mPFC. Surprisingly, although phospho-CREB emerged in

parallel with ERK phosphorylation in layers II-III, the population of immunolabeled cells was more dense and widespread than those labeled with anti-phospho-ERK. In fact, phospho-CREB immunoreactivity appeared throughout all layers of mPFC. At this time, we can only speculate as to the reasons for this seeming incongruence. One obvious possibility is that mechanisms independent of ERK drive CREB phosphorylation. Although phospho-CREB in layers II-III was sensitive to the MEK (and thus ERK) activation state, labeling in the deeper layers of mPFC was less responsive to MEK inhibition. Because CREB is a common substrate of multiple kinase pathways in cell model systems (for review, see Herdegen and Leah, 1998; Curtis and Finkbeiner, 1999), other pathways, such as the PKA, CaM kinase, and stress-activated protein kinase cascades, might be responsible for the phospho-CREB effect. Another possibility could be related to functional integration of phospho-ERK-expressing neurons with nonexpressing cells, whereupon ERK-dependent activity in a small population of mPFC layer II-III neurons could influence activation, signaling, and appearance of phospho-CREB in cortical and subcortical cells beyond simply those that contain phospho-ERK. The mild reduction in phospho-CREB immunoreactivity observed throughout all mPFC layers after MEK inhibition would seem to support a mechanism involving intercellular integration. Nevertheless, additional studies are necessary to resolve these complex issues.

Several lines of evidence suggest that sustained ERK activation may be indicative of neuronal insult, possibly leading to cell death (Stanciu et al., 2000; Kulich and Chu, 2001). Prolonged ERK activation in neurodegenerative processes has been linked to decreased CREB activation (Lee et al., 2002; Trentani et al., 2002). In the present study,

sustained ERK phosphorylation in mPFC was accompanied by increased, rather than decreased, CREB phosphorylation. On the opposite end of the spectrum, prolonged ERK activation accompanied by an increase in CREB has been linked to a continuum of processes that include cell survival and plasticity (Shen et al., 2001; Sweatt, 2001; Dawson and Ginty, 2002). Thus, it appears that the precise kinetics of ERK and CREB phosphorylation can ultimately determine the fate of a cell within a given region. Although neurodegenerative processes cannot be ruled out, we speculate that the sustained increases in ERK and CREB phosphorylation observed herein are likely to be indicative of cell survival and plasticity in mPFC.

The sustained increase in phospho-ERK was dependent on D_1 receptor function, because SCH-23390 antagonist pretreatment blocked the prolonged response to repeated administration of the D_1-selective partial agonist SKF-38393. It is unlikely that SCH-23390 inhibited prolonged ERK phosphorylation through its interaction with 5-HT$_2$ binding sites (Bischoff et al., 1988; McQuade et al., 1988), because systemic injections of the nonselective 5-HT$_2$ antagonist ketanserin, before repeated doses of SKF-38393, had no effect on the sustained phospho-ERK response in mPFC. In addition, the results with ketanserin further support the notion that long-lasting ERK phosphorylation does not drive expression of locomotor responsiveness to D_1 agonists in SKF-38393-sensitized animals. The spontaneous hyperactive behavior of neonate-lesioned animals has been linked to serotonergic mechanisms (Bishop et al., 2004), and ketanserin blocks the locomotor sensitization observed in these animals (our unpublished data), without affecting the sustained activation of ERK in mPFC.

Studies have demonstrated that pharmacological stimulation of NMDA receptors leads to activation of ERK in cortical neurons (Bading and Greenberg, 1991; Xia et al., 1996; Arvanov et al., 1997; Vanhoutte et al., 1999; Wang and O'Donnell, 2001). In this investigation, both the competitive NMDA antagonist MK-801 and the noncompetitive antagonist CGS-19755 eliminated sustained ERK phosphorylation in mPFC, a finding suggestive of NMDA dependence for the ERK phosphorylation. Thus, mPFC of neonate-lesioned rats sensitized with repeated doses of SKF-38393 might undergo persistent biochemical adaptations similar to other biological substrates of neuroplasticity such as long-term potentiation (Impey et al., 1998) and memory processing (Adams and Sweatt, 2002). In addition, accumulated evidence demonstrates an interaction of D_1 and NMDA receptor functions (Konradi et al.; 1996, Pei et al., 2004) (for review, see Adriani et al., 1998; Salter, 2003) and dopamine modulation of glutamate neurotransmission within the prefrontal cortex (Goldman-Rakic and Selemon, 1997; Gonzalez-Islas and Hablitz, 2003; Otani et al., 2003; Sesack et al., 2003). The present findings further illustrate the presence of a dopamine-glutamate interaction in the mPFC, whereby repeated D_1 agonist administration maintains NMDA receptor-mediated responses in cells as reflected in ERK phosphorylation.

The neuromolecular mechanisms underlying sustained ERK hyperphosphorylation remain to be determined. Recent studies have established a critical role for protein phosphatases in coordinating neurotransmitter signaling (for review, see Greengard, 2001). Because phosphatases are presumed to rapidly deactivate phosphorylated proteins in brain, the measured increase in cells exhibiting phospho-ERK after SKF-38393 treatment could be related to altered phosphatase activity. Mitogen-

activated protein kinase phosphatases (MKPs) 1-3 can directly control nuclear accumulation and persistent activation of ERK (for review, see Pouyssegur et al., 2002). Interestingly, MKP1 and MKP3 expression in frontal cortex and other brain regions is differentially altered by acute and chronic methamphetamine administration to rats (Takaki et al., 2001). Thus, a reduction in MKP1-3 or a related phosphatase might be a means by which ERK phosphorylation could be sustained for an extended period. The answer to this puzzle will have to be resolved in future experiments that examine sustained ERK phosphorylation after SKF-38393-mediated sensitization of neonate-lesioned animals.
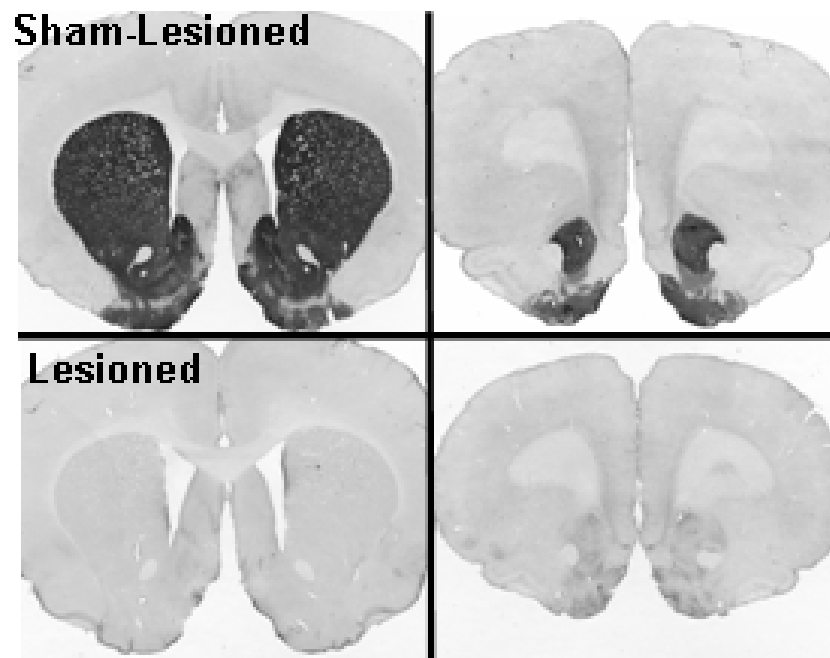
Fig. 2-1: Immunohistochemistry for tyrosine hydroxylase. Immunohistochemistry for tyrosine hydroxylase (1:5000; Calbiochem) in coronal sections representing the striatum, accumbens, and mPFC in sham-lesioned and neonate 6-OHDA-lesioned (Lesioned) adult rats.
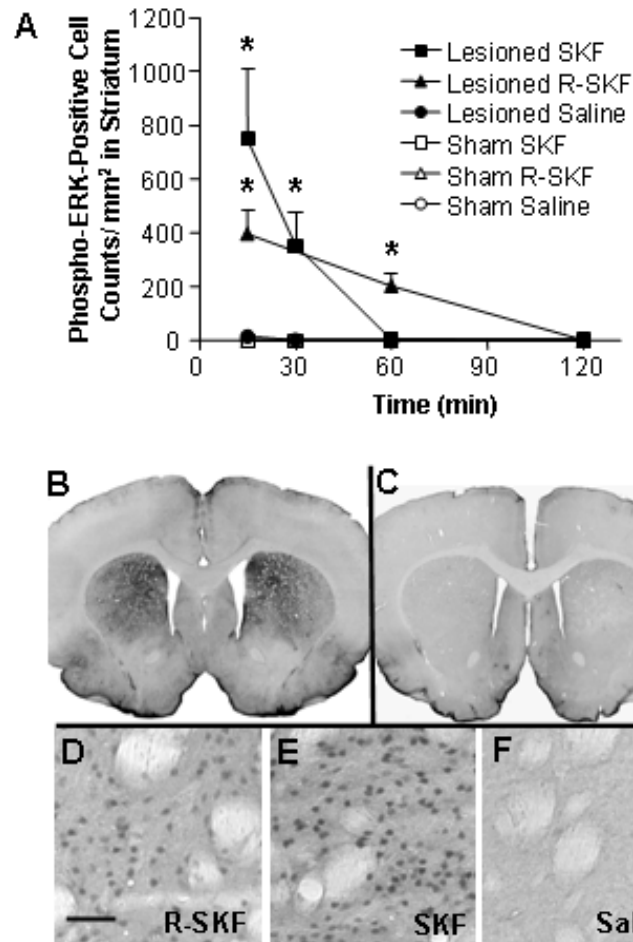
Fig. 2-2: Administration of the partial D$_1$ agonist SKF-38393 to neonate 6-OHDA-lesioned rats transiently activates ERK in striatum. *A*, Time-dependent ERK phosphorylation in striatum (0-120 min). Treatment groups are represented by (■) Lesioned SKF = single dose of SKF-38393 to neonate-lesioned rats; (▲) Lesioned R-SKF = repeated doses of SKF-38393 to neonate-lesioned rats; (●) Lesioned Saline = saline treatment to neonate-lesioned rats; (□) Sham SKF = single dose of SKF-38393 to sham-lesioned rats; (△) Sham R-SKF = repeated doses of SKF-38393 to sham-lesioned rats; (○) Sham Saline = saline treatment to sham-lesioned rats. Phospho-ERK-positive cell counts did not significantly differ between rats receiving single or multiple injections of

saline; thus these data were collapsed for each time point examined. Symbols remain consistent throughout this paper to represent each treatment group. ANOVA *F* test of model fit: $F_{(19,74)} = 9.890$; $p < 0.0001$. *B, C*, At 15 min after SKF-38393 treatment to neonate-lesioned rats, abundant phospho-ERK immunoreactivity is observed in striatum (*B*) but is not present in striatum of neonate-lesioned rats administered saline treatments (*C*). *D*, Representative low-magnification (100x) image of phospho-ERK-expressing cells at 15 min in neonate-lesioned rats administered repeated doses of SKF-38393. *E*, Neonate-lesioned rats administered a single dose of SKF-38393. *F*, Neonate-lesioned rats injected with saline.
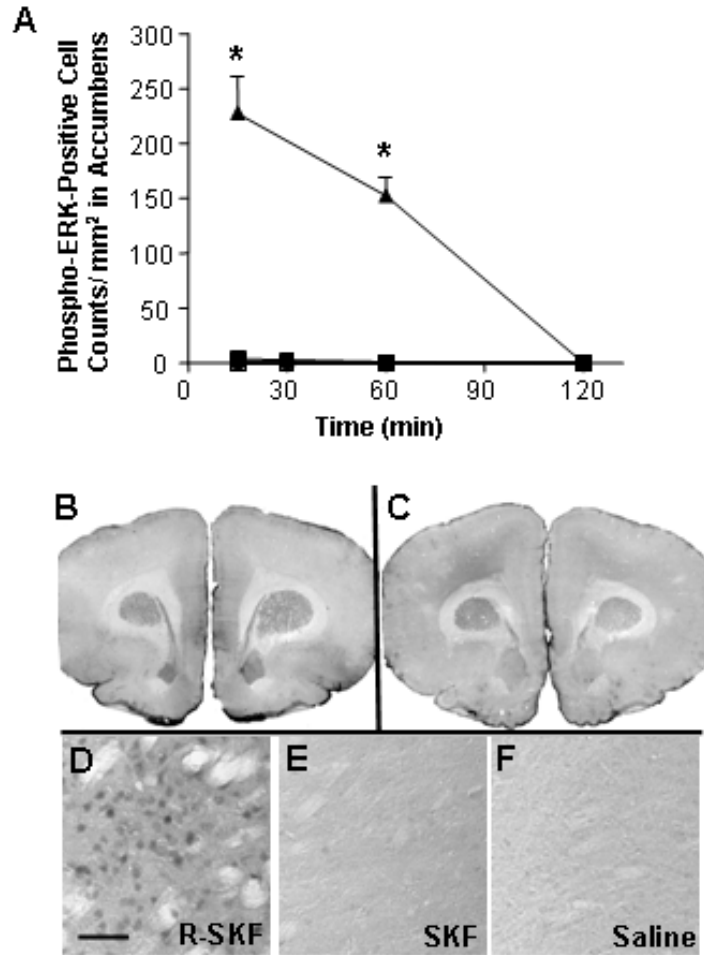
Fig. 2-3: Repeated administration of the partial D$_1$ agonist SKF-38393 to neonate 6-OHDA-lesioned rats transiently increases phospho-ERK in accumbens. *A*, Time-dependent phospho-ERK immunoreactivity in accumbens (0-120 min). ANOVA *F* test of model fit: $F_{(19,74)} = 27.335$; $p < 0.0001$. *B, C*, At 15 min, phospho-ERK immunostaining is observed in accumbens of neonate-lesioned rats administered repeated doses of SKF-38393 (*B*) but is not present in accumbens of neonate-lesioned rats administered only a single dose of SKF-38393 (*C*). *D*, Representative low-magnification (100x) image of phospho-ERK-expressing cells at 15 min in neonate-lesioned animals administered repeated doses of SKF-38393. *E*, Neonate-lesioned rats administered a single dose of

SKF-38393. *F*, Neonate-lesioned rats injected with saline. $^{*}p < 0.01$ with Fisher's PLSD test. Scale bar, 250 μm.
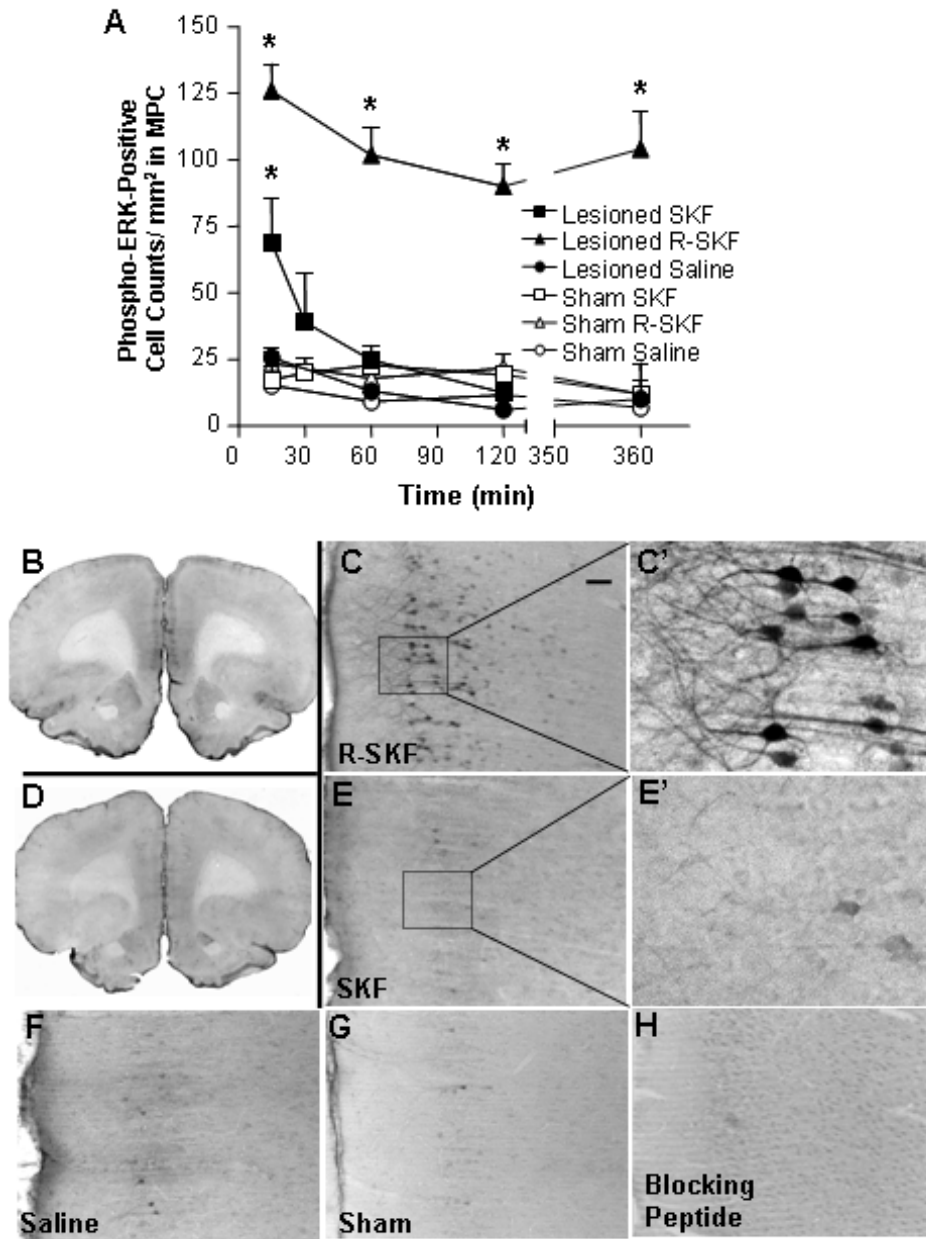
Fig. 2-4: Repeated administration of the partial D$_1$ agonist SKF-38393 to neonate-lesioned rats produces a sustained increase in ERK phosphorylation in mPFC. *A*, Time-dependent phospho-ERK immunoreactivity (0-360 min). ANOVA *F* test of model fit: $F_{(23,79)} = 12.943$; $p < 0.0001$. *B*, Neonate-lesioned rats administered repeated doses of SKF-38393 demonstrated robust phospho-ERK immunostaining at 120 min. *C, C'*,

Representative low-magnification (100x)(*C*) and high-magnification (400x) (*C'*) images of phospho-ERK-expressing cells (120 min) in neonate-lesioned rats administered repeated doses of SKF-38393. *D*, Increased phospho-ERK immunostaining was not present at 120 min in mPFC of neonate-lesioned rats administered a single dose of SKF-38393. *E, E'*, Representative low-magnification (100x)(*E*) and high-magnification (400x)(*E'*) images of phospho-ERK-expressing cells (120 min) in neonate-lesioned rats administered a single dose of SKF-38393. *F*, Neonate-lesioned rats administered repeated saline injections. *G*, Sham-lesioned rats administered repeated doses of SKF-38393. *H*, Corresponding blocking peptide inhibited sustained phospho-ERK immunoreactivity in neonate-lesioned rats repeatedly dosed with SKF-38393. $^{*}p < 0.01$ with Fisher's PLSD test. Scale bar, 250 μm.
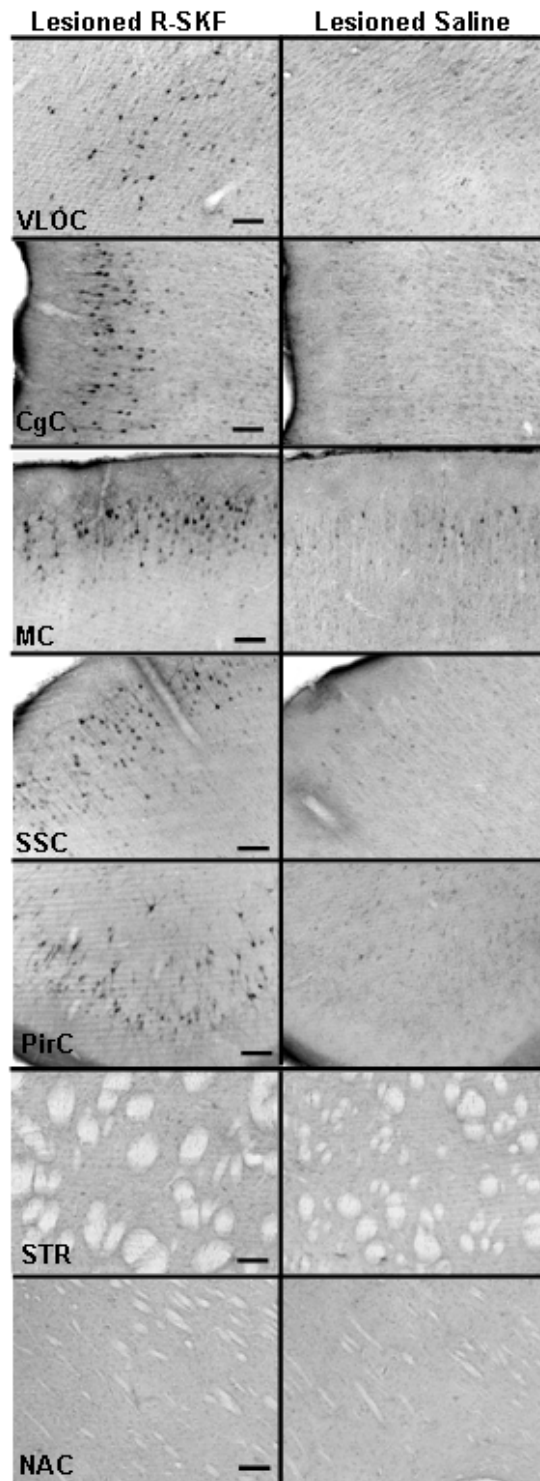
Fig. 2-5: Photomicrographs depicting ERK phosphorylation in various cortical regions, striatum, and accumbens of neonate-lesioned rats at day 7 after repeated

SKF-38393 administration (R-SKF) or saline treatment. VLOC, Ventrolateral orbital cortex, orbitofrontal cortex; CgC, Cg1, and Cg2, cingulate cortex; MC, M1, and M2, motor cortex; SSC, S1, somatosensory cortex; PirC, piriform cortex; STR, striatum; NAC, accumbens. Scale bar, 100 μm.
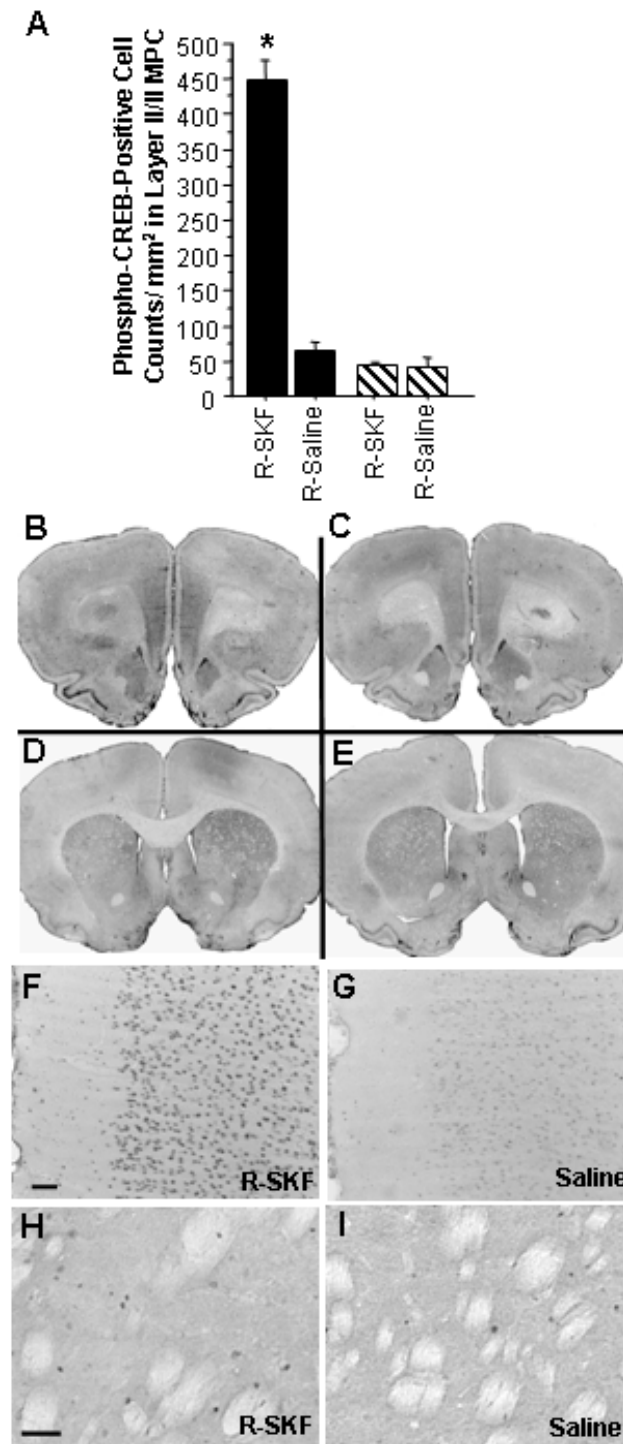
Fig. 2-6: Repeated administration of SKF-38393 to neonate-lesioned rats produces long-lasting CREB phosphorylation in mPFC. *A*, Graphic representation of layers II-III phospho-CREB-positive cell counts in mPFC at day 7 after repeated SKF-38393 or

saline treatment to neonate-lesioned (solid bars) or sham-lesioned (striped bars) rats. [*]$p < 0.05$ with Fisher's PLSD test. R-SKF, Rats administered repeated doses of SKF-38393; R-Saline, rats injected repeatedly with saline. ANOVA F test of model fit: $F_{(3,28)}$ = 82.148; $p < 0.0001$. *B,C*, Robust phospho-CREB immunostaining is observed only in mPFC of neonate-lesioned rats at day 7 after repeated SKF-38393 administration (*B*) but not in mPFC of neonate-lesioned rats treated with saline rather than the agonist (*C*). *D, E*, Only scattered phospho-CREB-positive cells were noted in striatum and accumbens of neonate-lesioned rats administered repeated SKF-38393 administration (*D*) and neonate-lesioned rats injected with saline (*E*). *F,G*, Representative low-magnification (100x) images of phospho-CREB-immunoreactive cells in mPFC of neonate-lesioned rats dosed repeatedly with SKF-38393 (*F*) or saline (*G*). Scale bar, 250 μm. *H, I*, Representative high-magnification (200x) images of phospho-CREB immunoreactive cells in striatum of neonate-lesioned rats dosed repeatedly with SKF-38393 (*H*) or saline (*I*). Scale bar, 50μm.
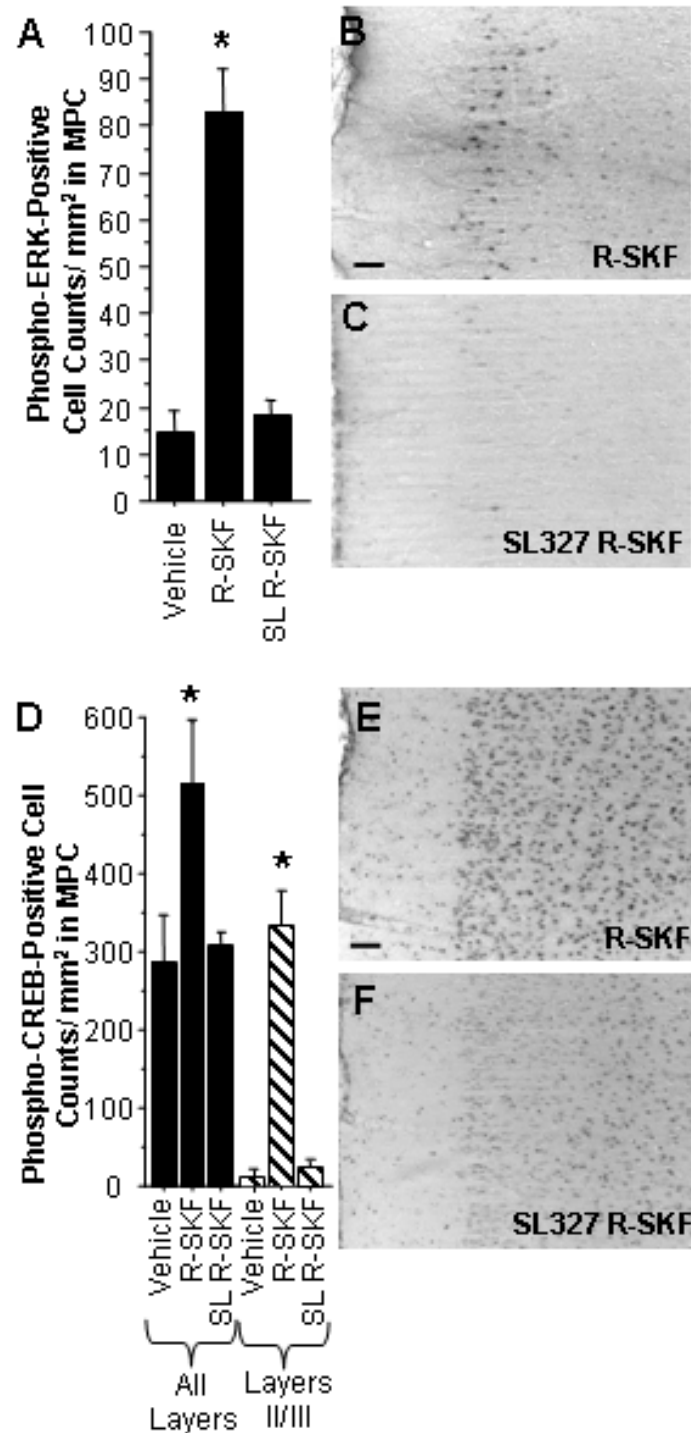
Fig. 2-7: Sustained ERK and CREB phosphorylation is blocked by pretreatment with MEK inhibitor SL327 before each weekly dose of SKF-38393. *A*, Graphic representation of phospho-ERK-positive cell counts in mPFC at day 7 after drug

treatment. Vehicle, Neonate-lesioned rats pretreated with vehicle (DMSO) before weekly saline injections; R-SKF, neonate-lesioned rats administered vehicle before SKF-38393 treatment; SL R-SKF, neonate-lesioned rats pretreated with SL327 before SKF-38393 treatment. ANOVA F test of model fit: $F_{(2,10)} = 40.604$; $p < 0.0001$. *B, C*, Representative low-magnification (100x) images of phospho-ERK-immunoreactive cells in R-SKF (*B*) and SL R-SKF (*C*) treatment groups. *D*, Graphic representation of phospho-CREB-positive cell counts across all layers (solid bars) and only layers II-III (striped bars) of mPFC after pretreatment with SL327 before each weekly dose of SKF-38393. ANOVA *F* test of model fit: $F_{(2,10)} = 35.82$; $p < 0.0001$. *E, F*, Representative low-magnification (100x) image of phospho-CREB immunoreactive cells in R-SKF (*E*) and SL R-SKF (*F*) treatment groups. Note that SL327 pretreatment appeared to reduce phospho-CREB-positive cell counts primarily in layers II-III of mPFC, where sustained phospho-ERK immunoreactivity is most prominent. [*]$p < 0.05$ with Fisher's PLSD test. Scale bar, 250 μm.
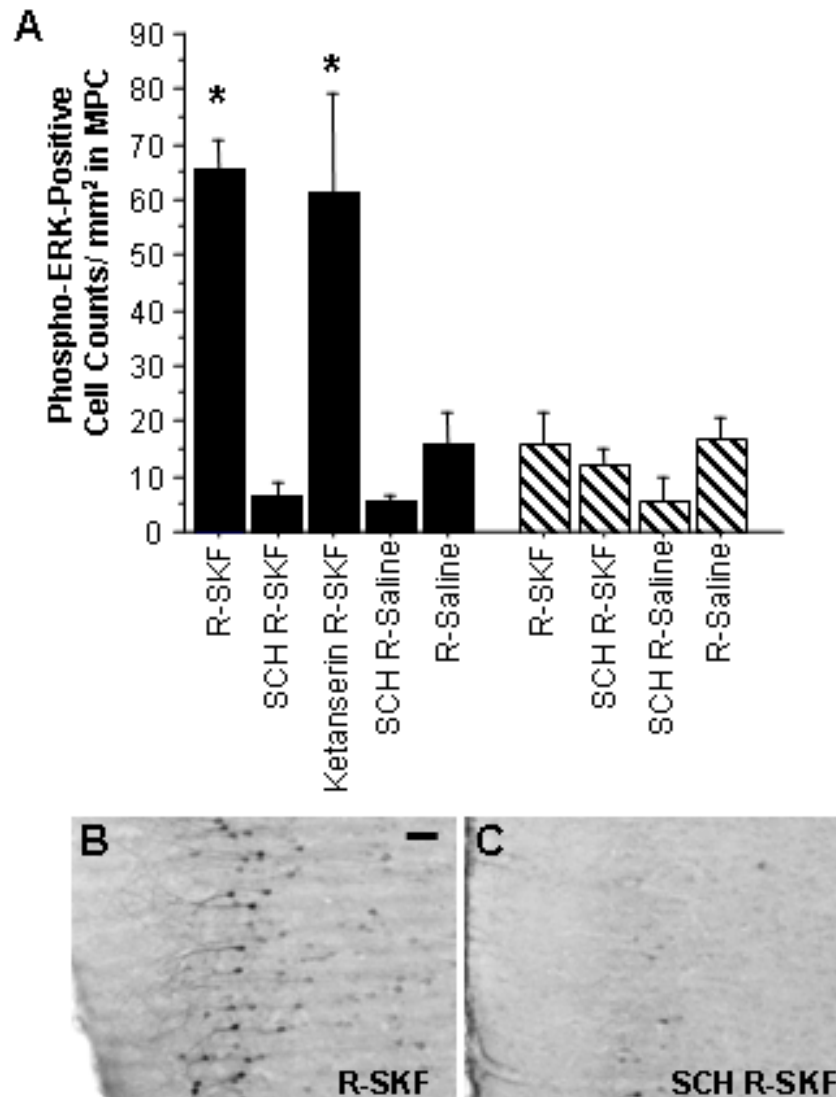
Fig. 2-8: Sustained ERK phosphorylation is blocked by pretreatment with D_1 antagonist SCH-23390 but not with 5-HT_2 antagonist ketanserin. *A*, Graphic representation of phospho-ERK-positive cell counts in mPFC of neonate-lesioned (solid bars) and sham-lesioned (striped bars) treatment groups at day 7 after drug treatment. R-SKF, Rats administered saline before SKF-38393; SCH R-SKF, rats pretreated with SCH-23390 before SKF-38393; Ketanserin R-SKF, rats pretreated with ketanserin before SKF-38393; SCH R-Saline, rats pretreated with SCH-23390 before saline injection; R-

Saline, rats pretreated with saline (vehicle) before saline injection. ANOVA F test of model fit: $F_{(8,44)} = 22.434$; $p < 0.0001$. *B, C,* Representative low magnification (100x) images of phospho-ERK immunoreactive cells in R-SKF (*B*) and SCH R-SKF (*C*) neonate-lesioned rat groups. $^{*}p < 0.05$ with Fisher's PLSD test. Scale bar, 250 μm.
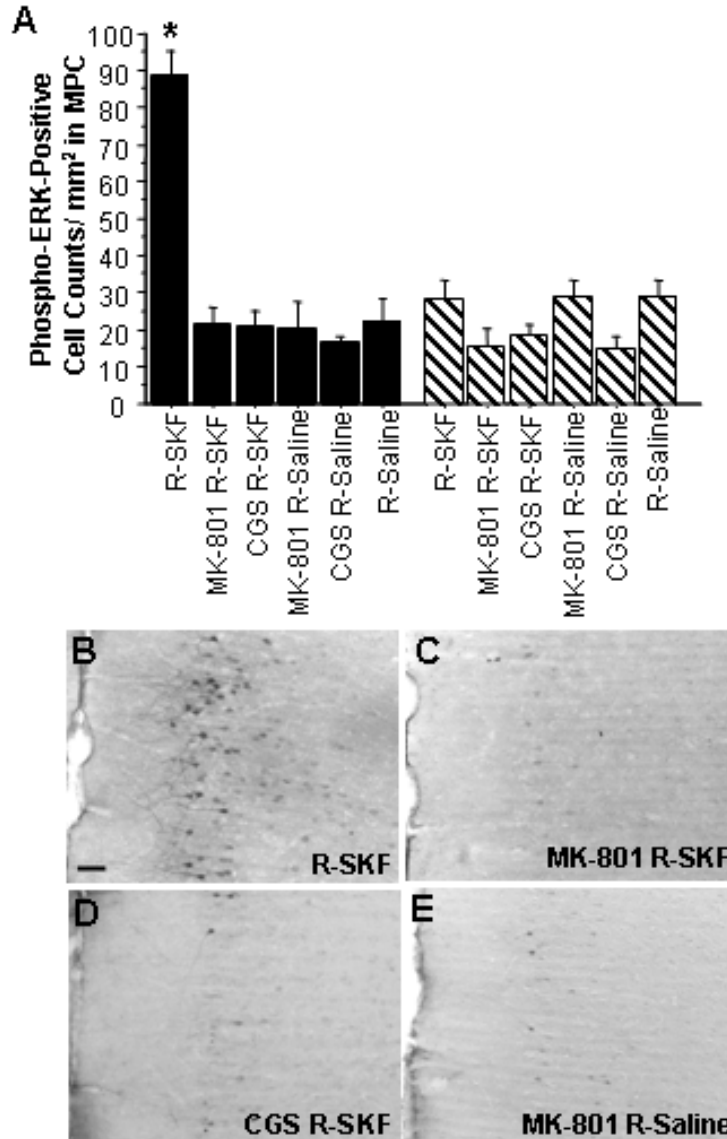
Fig. 2-9: Sustained ERK phosphorylation is blocked by pretreatment with NMDA receptor antagonists MK-801 and CGS-19755 before each repeated weekly dose of SKF-38393. *A*, Graphic representation of phospho-ERK-positive cell counts in neonate-lesioned (solid bars) and sham-lesioned (striped bars) treatment groups at day 7 after drug treatment. R-SKF, Rats administered saline before SKF-38393; MK-801 R-SKF, rats pretreated with MK-801 before SKF-38393; CGS R-SKF, rats pretreated with CGS-19755 before SKF-38393; MK-801 R-Saline, rats pretreated with MK-801 before saline

injection; CGS R-Saline, rats pretreated with CGS-19755 before saline injection; R-Saline, rats pretreated with saline (vehicle) before saline injection. ANOVA F test of model fit: $F_{(11,100)} = 10.206$; $p < 0.0001$. *B-E*, Representative low-magnification (100x) images of phospho-ERK immunoreactive cells in R-SKF (*B*), in MK-801 R-SKF(*C*), in CGSR-SKF (*D*), and in MK-801 R-Saline (*E*) neonate-lesioned rat groups. [*]$p<0.05$ with Fisher's PLSD test. Scale bar, 250 μm.

Table 2-1: Chronic time course of ERK phosphorylation in mPFC following repeated doses of SKF-38393 or saline to neonate- and sham-lesioned rats (mean ± SEM)

A. ERK phosphorylation at extended time points following SKF-38393 treatment

| Time of Sacrifice[†] | Treatment groups | | | |
	Lesioned R-Saline	Lesioned R-SKF	Sham R-Saline	Sham R-SKF
3 days	18.42 ± 7.29	94.38 ± 4.63*,a	30.08 ± 4.77	27.50 ± 5.38
7 days	19.90 ± 5.95	114.40 ± 13.37*,a	18.15 ± 5.60	16.80 ± 2.70
14 days	19.30 ± 5.95	53.59 ± 4.30*,b	19.17 ± 3.06	-----
21 days	22.78 ± 3.10	42.43 ± 7.24*,b	25.42 ± 2.64	-----
36 days	17.10 ± 3.70	37.25 ± 2.55*	15.00 ± 4.00	-----

B. ERK phosphorylation following reinstatment dose of SKF-38393 at 36 days

	Lesioned R-Saline	Lesioned R-SKF	Sham R-Saline	Sham R-SKF
7 days following additional treatment[§]	28.08 ± 4.88	96.10 ± 2.36*,a	18.50 ± 10.26	-----

ANOVA F-test of model fit: $F_{(19,117)} = 16.057$, $p < 0.0001$.

Cells counted at 100X magnification.

[†] Interval between repeated SKF-38393 or saline treatment and sacrifice.

[§] Rats were sacrificed at day 42, 7 days following an additional dose of SKF-38393 at 36 days.

*Indicates that counts are significantly different from all other counts (across all treatment groups and time points) at the $p = 0.01$ significance level with Fisher's PLSD test.

[a,b] Indicates that counts within a treatment group (column) significantly differ from each other at the $p = 0.01$ significance level with Fisher's PLSD test.

Table 2-2: Chronic time course of ERK phosphorylation in various cortical regions following repeated doses of SKF-38393 to neonate-lesioned rats (mean ± SEM)

	Time of sacrifice[†]			
Brain region	7 days	14-21 days[‖]	36 days	7 days following additional dose at 36 days (42 days)[§]
VLOC	53.21 ± 14.86*	29.53 ± 7.49	16.50 ± 7.27	39.83 ± 17.32
CgC	50.58 ± 10.28*	19.91 ± 4.18	7.90 ± 3.30	28.00 ± 9.88
MC	106.08 ± 20.05*	49.44 ± 9.60	15.10 ± 3.80	47.07 ± 18.06
SC	113.96 ± 23.44*	37.19 ± 7.99	25.50 ± 8.86	62.07 ± 23.23
PirC	135.5 ± 28.75*	53.84 ± 7.82	28.90 ± 9.82	64.07 ± 15.91

ANOVA F-test of model fit: $F_{(7,65)} = 2.863$, p = 0.0115, VLOC; $F_{(7,65)} = 5.551$, p < 0.0001, CingC; $F_{(7,65)} = 5.681$, p < 0.0001, MC; $F_{(7,65)} = 6.960$, p < 0.0001, SSC; $F_{(7,65)} = 6.090$, p < 0.0001, PirC. Cells counted at 100X magnification for each region.

[†] Interval between repeated SKF-38393 or saline treatment and sacrifice.

[‖] Values at 14-21 days did not significantly differ within treatment groups for each cortical region examined and thus collapsed.

[§] Rats were sacrificed at day 42, 7 days following an additional dose of SKF-38393 at 36 days.

* Counts within a given cortical region are significantly different from all other counts in that region at the p = 0.01 significance level, except for *Lesioned R-SKF 7 days* vs. *Lesioned-R-SKF 42 days* in VLOC.

VLOC = ventrolateral orbital cortex, orbitofrontal cortex; **CgC** = Cg1 and Cg2, cingulate cortex; **MC** = M1 and M2, motor cortex; **SSC** = S1, somatosensory cortex; **PirC** = piriform cortex.
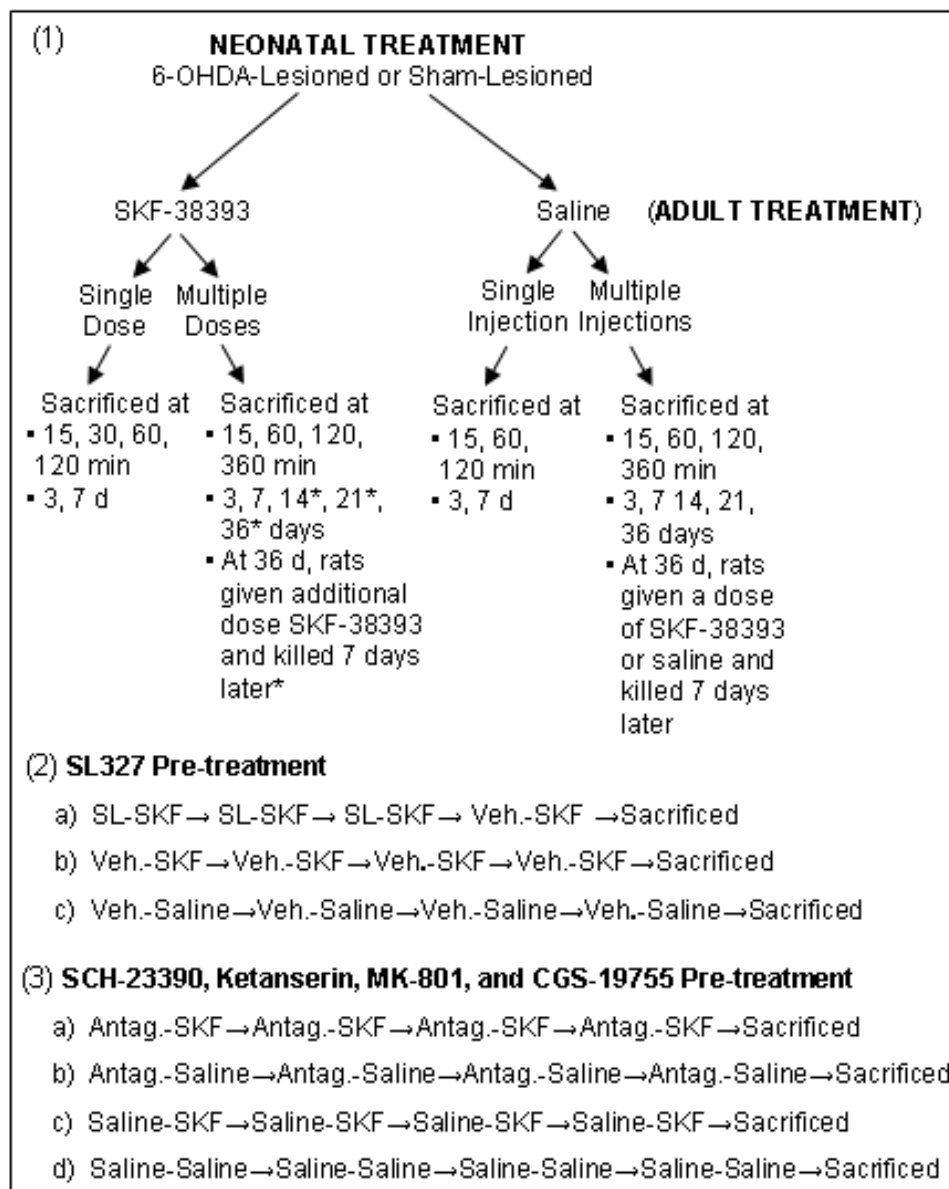
Fig. 2-1S: Experimental paradigm. *(1)* SKF-38393 dosing regimen and time of sacrifice for neonate-lesioned and sham-lesioned rats used in the acute and chronic time course experiments. * Sham-lesioned rat group not represented at these time points. *(2)* Pretreatment with SL327 prior to repeated doses of SKF-38393 to neonate-lesioned rats. *SL*, SL327; *SKF*, SKF-38393; *Veh.*, Vehicle (DMSO); *(3)* Pretreatment with SCH-23390, ketanserin, MK-801, or CGS-19755 prior to repeated doses of SKF-38393 or saline. *Antag.*, antagonist = SCH-23390, ketanserin, MK-801, or CGS-19755.

Table 2-1S: Behavioral activity at dose 1 and dose 4 following repeated weekly administration of SKF-38393 (3 mg/kg) to neonate 6-OHDA-lesioned rats

A. Horizontal Activity

Neonatal Treatment	Adult Treatment		
	Saline	Dose 1 SKF-38393	Dose 4 SKF-38393
6-OHDA-Lesioned	18,511.09 ± 7,029.31	28,161.54 ± 12,579.79	98,927.95 ± 29,997.72*
Sham-Lesioned	14,987.91 ± 4,958.53	16,792.35 ± 4,403.79	12,352.40 ± 4,728.40

B. Vertical Activity

Neonatal Treatment	Saline	Dose 1 SKF-38393	Dose 4 SKF-38393
6-OHDA-Lesioned	503.88 ± 174.57	1,100.00 ± 261.84*	1,645.00 ± 286.78*
Sham-Lesioned	584.88 ± 106.18	517.75 ± 205.38	495.75 ± 290.16

C. Stereotypical Activity

Neonatal Treatment	Saline	Dose 1 SKF-38393	Dose 4 SKF-38393
6-OHDA-Lesioned	11,629.50 ± 2,091.58[#]	11,363.75 ± 1,858.50[#]	16,324.50 ± 2,266.11*,[#]
Sham-Lesioned	6,545.38 ± 893.04	7,440.75 ± 543.45	8,347.00 ± 779.68

Anova F-test for model fit yielded $F_{(5,26)} = 8.19$, $p < 0.0001$ for horizontal activity; $F_{(5,26)} = 6.03$, $p = 0.0008$ for vertical activity, and $F_{(5,26)} = 6.67$, $p = 0.0004$ for stereotypical activity.

*Indicates values within a measured activity that are significantly different at the $p = 0.05$ significance level determined by Fisher's PLSD test. In *B*, values with astericks are also significantly different from each other.

In *C*, [#] indicates values that are significantly different than the *Sham-Lesioned Saline* treated group at the $p < 0.05$ significance level determined by Fisher's PLSD test.

CHAPTER III. **A ROLE FOR EXTRACELLULAR SIGNAL-REGULATED KINASE 1/2 IN THE SUPERSENSITIVE MOTOR RESPONSE TO REPEATED D_1 RECEPTOR AGONIST ADMINISTRATION IN THE NEONATE 6-OHDA-LESIONED RAT**

A.   Introduction

Rats given selective lesions of dopamine (DA)-containing neurons as neonates later show a unique profile of behavioral responsiveness to D_1 dopamine receptor activation (Breese et al., 1985a,b). For example, neonate 6-hydroxydopamine (6-OHDA)-lesioned rats demonstrate increased locomotor and stereotypic activity following treatment with the partial D_1 receptor agonist SKF-38393 at doses that have a minimal impact on control rats (Breese et al., 1985a,b; Criswell et al., 1989; Papadeas et al., 2004). Repeated treatment with D_1 agonists can lead to extremely high rates of behavioral activity in lesioned rats, and this sensitization, or "priming", effect can still be observed 6 months after the chronic agonist treatment (Breese et al., 1985b; Criswell et al., 1989). Supersensitivity of D_1 receptors in neonate 6-OHDA-lesioned rats has also been linked to stereotyped responses and self-injurious behavior (SIB) after treatment with apomorphine or L-DOPA, suggesting that these animals can provide a valuable model for the self-injurious behavior and DA loss associated with Lesch-Nyhan syndrome (Breese et al., 1984a,b), a metabolic disorder primarily observed in male children (Lesch and Nyhan, 1964).

Although the behavioral consequences of repeated D_1 agonist treatment to neonate-lesioned rats has been well studied, little is known about the underlying neurobiological mechanisms or brain sites responsible for priming of the behavioral responsiveness in these animals. Recently, we found a sustained increase in the phosphorylation of extracellular signal-regulated kinase 1/2 (ERK), a signaling molecule thought to play a role in neuronal adaptive responses (English and Sweat, 1996; 1997; Martin et al., 1997; Davis et al., 2000) as in well as memory formation (Atkins et al., 1998), in various cortical regions of neonate-lesioned rats behaviorally primed to the effects of repeated D_1 agonist exposure (Papadeas et al., 2004). Of all of the cortical regions examined, increased ERK phosphorylation was most remarkable in the medial prefrontal cortex (mPFC), where it lingered longest and remained most sensitive to full reinstatement with an additional dose of D_1 agonist given 36 days after the last D_1 agonist treatment.

The persistent nature of ERK phosphorylation, particularly in the mPFC, suggested that this response might facilitate priming of the behavioral responsiveness in neonate-lesioned rats to repeated D_1 agonist exposure. The development of specific inhibitors of the upstream ERK kinase MEK (mitogen-activated protein kinase/extracellular signal-regulated kinase kinase 1/2) has made it possible to examine the function of ERK phosphorylation in behaving animals (Sweatt, 2001). For example, it has been shown that blockade of ERK activity following systemic administration of the MEK inhibitor SL327 to normal rats impairs behavioral sensitization and the rewarding properties induced by cocaine (Valjent et al., 2000). Therefore, we investigated how inhibition of the ERK pathway by SL327 and the structurally dissimilar MEK inhibitor

PD98059 affects priming of the behavioral responsiveness of neonate-lesioned rats to repeated D_1 agonist treatment. Moreover, we performed microinjections with PD98059 into the mPFC to determine the precise contribution of increased mPFC phospho-ERK in the sensitized behavioral response. Ultimately, inhibitors of the ERK pathway could be valuable tools to obliterate this long-lasting D_1 receptor-induced molecular change and perhaps deepen our understanding of Lesch-Nyhan syndrome and other DA-dysfunctional states.

B.   Materials and Methods

Lesioning of dopamine-containing neurons in neonate rats

The animal protocol was conducted in accordance with the National Institutes of Health *Guide for the Care and Use of Laboratory Animals.* Pregnant Sprague Dawley rats obtained from Charles River Laboratories were individually housed, with Wayne Lab Blox laboratory chow and water available *ad libitum*. On day 3 after delivery, male and female rat pups were anesthetized with ether and then administered 100 μg (free base) of 6-OHDA (ICN; Irvine, CA) intracisternally (i.c.), 60 min after desipramine (20 mg/kg), intraperitoneally (i.p.) to protect noradrenergic neurons (Breese et al., 1984a,b). Some rats received desipramine (20 mg/kg, i.p.) and saline (i.c.) to serve as unlesioned (sham-lesioned) controls. The bilateral lesion causes over 90% loss of dopamine innervation in the striatum and disrupts basal ganglia-cortical system circuits (Smith et al., 1973). Rats treated with 6-OHDA or saline neonatally were weaned at day 30 and testing began at 35-40 d of age.

Intracerebroventricular (ICV) infusion of MEK inhibitors

Neonate 6-OHDA-lesioned and sham rats were anaesthetized with sodium pentobarbital (50 mg/kg, i.p.) and placed in a Kopf stereotaxic apparatus. Using aseptic conditions, the scalp was cleared and a small burr hole was made through which a cannula was lowered into the right lateral ventricle (from bregma; anteroposterior, -0.8 mm; mediolateral, -1.5 mm; dorsoventral, -2 mm; according to Paxinos and Watson, 1998). The animals were allowed 7 d to recover from the implant before any testing was initiated.

Prior to ICV infusion, the MEK inhibitors SL327 (α-[amino[(4-aminophenyl)thio]methylene]-2-(trifluoromethyl)benzeneacetonitrole) (kindly provided by Bristol-Myers-Squibb Company, Princeton, NJ) and PD98059 (2-(2'-amino-3'-methoxyphenyl)-oxanaphthalen-4-one) (Calbiochem, La Jolla, CA) were dissolved in dimethylsulfoxide (DMSO) at a concentration of 10 mg/kg, from which a solution containing 0.1 mg/kg with 1% DMSO was prepared in sterile saline (Choe and McGinty, 2001; Gu et al., 2001). Using a Sage infusion pump, SL327 (0.3 μg), PD98059 (0.3 μg), or vehicle (1% DMSO in saline) was infused through the cannula in a volume of 2 μl over a 5 min time period, as previously described (Gu et al., 2001). The injection needle remained in place for 1 min to reduce backflow of the solution along the injection track. Thirty minutes later, rats received an injection of SKF-38393 (2,3,4,5-tetrahydro-7,8-dihydroxy-1-phenyl-1H-3-benazepine HCl; Sigma, St. Louis, MO) (3 mg/kg, i.p.). These drug combinations were given for a total of 3 treatments at weekly intervals. Once this regimen was completed, all rats were given an additional injection of SKF-38393 (3

mg/kg, i.p.), with vehicle pretreatment, to establish whether the rats infused with MEK inhibitor demonstrated primed behavioral activity induced by the repeated D_1 agonist treatment. In order to test the effects of a single dose of SKF-38393 on behavior, a separate group of rats were given vehicle prior to each of 3 weekly injections of saline, with the fourth treatment consisting of vehicle followed by SKF-38393. Another group of rats were given vehicle prior to saline injections, once per week for 4 weeks, in order to serve as injection controls. PD98059 or SL327 was also infused ICV prior to each of 4 weekly injections of saline, to determine any non-specific effects of repeated MEK inhibitor treatment on behavior. Table 3-1 is provided as an additional guide for the experimental paradigm. Tests for behavioral activity were performed following the fourth weekly injection of SKF-38393 or saline to neonate-lesioned and sham rats.

Systemic injection of MEK inhibitor

SL327 was dissolved in 100% DMSO vehicle at 2 ml/kg (Atkins et al., 1998; Selcher et al., 1999; Yamagata et al, 2002) and administered i.p. to neonate-lesioned rats 30 min prior to injection of SKF-38393 (3 mg/kg, i.p.). Another group of neonate-lesioned rats received vehicle (100% DMSO) rather than SL327 with the SKF-38393. These combinations were given for a total of 3 treatments at weekly intervals. Once this regimen was completed, all rats were given an additional injection of SKF-38393, with only vehicle pretreatment, to assess the effects of systemic MEK inhibitor pretreatment on priming of motor activity induced by the repeated D_1 agonist treatment (see Table 3-1). A separate group of rats received vehicle prior to each of 3 weekly injections of saline, with the fourth injection consisting of vehicle followed by SKF-38393 in order to

assess the effects of a single dose of SKF-38393 on behavior. Tests for behavioral activity were performed following the fourth weekly SKF-38393 treatment to neonate-lesioned rats. The rats did not receive i.p. injections with PD98059, because this compound is unable to cross the blood-brain barrier and thus can only be administered intracranially (Alessi et al., 1995).

Microinjection of MEK inhibitor into the mPFC

Neonate-lesioned rats were anaesthetized with sodium pentobarbital (50 mg/kg, i.p.) and implanted with bilateral guide cannulas aimed at the mPFC prelimbic area (from bregma; anteroposterior, +3.2 mm; mediolateral, ±0.6 mm; dorsoventral, -2 mm; according to Paxinos and Watson, 1998). The rats were allowed to recover from surgery in their home cages for 10-12 d. During infusion, the injection needles extended 1.4 mm beyond the tips of the guides, yielding a total depth of 3.4 mm below the dura. Through the infusion cannulae, animals received bilateral 1 μl infusions of PD98059 (made of 10% PD98059 at 2 mg/ml, 40% DMSO, and 50% saline) or vehicle (made of 50% DMSO and 50% saline) over a 2 min period (Hugues et al., 2004; Blum et al., 1999). An additional 1 min period was allowed for diffusion of the drug. Thirty minutes later, rats received an injection of SKF-38393 (3 mg/kg, i.p.). These drug combinations were administered for a total of 3 cycles at weekly intervals, at which time the SKF-38393 was administered alone (see Table 3-1). Priming of behavioral activity to the D_1 agonist was determined during the fourth cycle, when all subjects received only SKF-38393. Behavioral activity was assessed as described below.

Evaluation of motor activity and behavior

To measure motor activity, rats were placed in clear 17" x 17" (43.2 cm x 43.2 cm) open field computer-monitored activity chambers (Med Associates, Inc., St. Albans, VT). Each chamber was surrounded by a 16 x 16 infrared photocell array interfaced with a computer that ran accompanying Open Field Activity software (Med Associates, Inc., St. Albans, VT). The software tabulated and processed a number of variables related to motor behavior. For the present experiment, the variables collected in 5 min bins over a 3 h testing period were horizontal counts (number of beam breaks counted across the photocell array), stereotypic counts (number of beam breaks counted at the same photocell array), vertical counts (number of periods of continuous beam breaks reported by the 'z-plane' photocell array), and vertical time (total time spent breaking beams in the 'z-plane' photocell array). On testing days, rats were placed in the activity chambers for 30 min before injections commenced. It is important to note that in neonate-lesioned rats, sensitization results in comparable levels of activity in response to SKF-38393 whether the rats are repeatedly dosed in the same or a different environment from that in which the rats are finally tested (Papadeas et al., 2004; Criswell et al., 1989).

Various behaviors were also quantified by observing whether a behavior was seen during a 1 min period at 10 min intervals, 60 min after the challenge dose of agonist was administered as previously described (Breese et al., 1985a; Criswell et al., 1988, 1989). Each 1 min period was divided into four 15 sec intervals, and behaviors from a checklist were scored for occurrence in each of the 15 sec periods. Each behavior had a maximum score of 4 for the 1 min period x 7 observation periods, for a total of 28. the behaviors that were monitored were grouped as follows: (1) horizontal behavior, e.g. running,

walking, trotting, chasing tail; (2) vertical behavior, e.g., rearing, climbing, jumping; (3) paw-fixation behavior, e.g., patting, treading, shaking paws, taffy pulling; (4) investigatory behavior, e.g., sniffing, checking, digging, (5) mouth-fixation behavior, e.g. licking, vacuous chewing, self-biting, self-injurious behavior; (6) head behavior, e.g., head shaking, head bobbing, head weaving, head jerking, head tilt; and (7) grooming behavior, e.g., grooming, scratching, licking self. Behavior was reported as a percentage of the total possible.

Histology

Following the completion of the behavioral tasks, animals were deeply anesthetized with an overdose of sodium pentobarbital (100 mg/kg) and transcardially perfused with 4% paraformaldehyde in PBS. Brains were removed, post-fixed in perfusant, and sectioned 40 μm thick with a vibrating microtome. Histological analysis was performed using cresyl violet staining and immunohistochemistry for tyrosine hydroxylase (TH) (1:4000, Calbiochem, La Jolla, CA), the rate-limiting enzyme in the biosynthesis of dopamine (Nagatsu et al., 1964). Immunohistochemical procedures were carried out as described previously (Papadeas et al., 2004). Placements of the cannulae were found to be correct in all animals (see Fig. 3-1*B*). Immunoreactivity for TH further established that the neonatal lesioning produced an adequate loss of DA-containing neurons. Lesioned rats that did not demonstrate a >90% reduction in TH immunoreactivity compared with sham control rats were eliminated from the study.

Statistical Evaluation

Previous work has shown that there are no significant behavioral differences between male and female 6-OHDA-lesioned rats (Breese et al., 1984a; Papadeas et al., 2004). Therefore, data were collapsed across sexes for analysis. Open field activity data and observer-scored behaviors were analyzed by 1-way ANOVA with treatment as a between subjects factor. For observer-scored behaviors, the scores analyzed were the percentage of 15 sec observation periods during which a given behavior occurred (Breese et al., 1984a; Criswell et al., 1988, 1989). When appropriate, post hoc comparisons were made using the Fisher PLSD test. The level of significance was set at $p < 0.05$.

C.   Results

Representative Histology

Fig. 3-1*A* illustrates the injection site for ICV infusion of MEK inhibitor on a coronal section of rat brain. Upon histological examination, placement of the cannula into the right lateral ventricle was found to be correct in all animals. Fig. 3-1*B* shows a schematic representation of a coronal brain section (Paxinos and Watson, 1998) located 3.00 mm anterior to bregma illustrating placements (shaded ovals) for 10 randomly selected 6-OHDA-lesioned rats included in the experiment involving microinjections of MEK inhibitor into the mPFC. All rats analyzed were found to have injector placements within the prelimbic area of this region.

Effects of ICV and systemic MEK inhibition on D_1 receptor-mediated priming of behavioral responses in neonate-lesioned rats

As shown in Fig. 3-2*A*, a significant main effect of treatment ($F_{(11,47)} = 9.795$, p < 0.05) was found on total horizontal counts measured in the open field. Consistent with previous studies (Papadeas et al., 2004), post hoc testing demonstrated that four weekly repeated treatments with 3 mg/kg of SKF-38393 induced a sensitized locomotor response in neonate-lesioned rats compared to saline-treated lesioned rats and sham controls (p < 0.05). More importantly, both SL327 and PD98059 compounds, when infused ICV prior to each of three of the four weekly injections with SKF-38393 in neonate-lesioned rats, augmented this effect (p < 0.05 for vs. SKF group). As shown in Fig. 3-2*B*, a disparate effect was found on measures of stereotypic counts ($F_{(11,47)} = 6.184$, p < 0.05). Priming-induced stereotypic activity in lesioned rats (p < 0.05 vs. all other groups) was reduced by SL327 and PD98059 pretreatment (both p < 0.05).

Analysis of total vertical counts (Fig. 3-2*C*) also revealed a significant main effect of treatment ($F_{(11,47)} = 2.938$, p < 0.05). Post hoc testing showed that the repeated SKF-38393 treatment enhanced vertical activity in the neonate-lesioned rats (p < 0.05 compared with saline-treated lesioned rats and sham controls). However, neither SL327 nor PD98059, when infused prior to each of three of the four weekly treatments with SKF-38393, altered this effect. Although pretreatment with these compounds had no effect on priming-induced vertical counts in lesioned rats, measures of vertical time ($F_{(11,47)} = 2.578$, p < 0.05) revealed that both SL327 and PD98059 reduced the amount of time that the primed rats spent performing behaviors in the vertical plane (p < 0.05 for both compared with SKF group). Rats that received systemic pretreatment with SL327

prior to each of three of the four weekly SKF-38393 treatments demonstrated similar behavioral effects to rats pre-treated with SL327 intraventricularly (see Fig. 3-2). No behavioral effects were observed after repeated administration of PD98059 or SL327 alone ($p > 0.05$ vs. Veh-lesion group and SKF-sham group), nor after a single dose of SKF-38393 to neonate-lesioned rats ($p > 0.05$ vs. Veh-lesion group and SKF-sham group).

In a select group of neonate-lesioned animals, observations of specific locomotor and stereotypic behaviors associated with D_1 receptor-mediated priming (Breese et al., 1985a; Criswell et al., 1989) were scored by hand. As shown in Fig. 3-3A, a significant main effect of treatment was found for observer-scored horizontal behavior ($F_{(5,20)}$ = 16.884, $p < 0.0001$). Similar to the open field activity data, post hoc testing revealed that pretreatment with SL327 or PD98059 produced augmented horizontal behavior in neonate-lesioned rats in response to an additional sensitizing dose of SKF-38393 ($p < 0.05$ vs. the Veh group). On the other hand, post hoc testing of a significant main effect of treatment for vertical behavior (i.e., rearing, climbing, jumping) ($F_{(5,20)}$ = 12.742, $p < 0.05$) and paw-fixation behavior (i.e., patting, treading, shaking paws, taffy pulling) ($F_{(5,20)}$ = 12.742, $p < 0.05$) revealed that priming of these behaviors to repeated injections of SKF-38393 was blocked by pretreatment with both MEK inhibitors ($p > 0.05$ for both vs. Veh group) (Fig. 3-3B,C). No significant main effects of treatment were found for observer-scored investigatory behavior (i.e., sniffing, checking, digging) ($F_{(5,20)}$ = 1.816, $p = 0.1554$), mouth-fixation behavior (i.e., licking, vacuous chewing, self-biting) ($F_{(5,20)}$ = 0.855, $p = 0.5279$), head behavior (i.e., head shaking, head bobbing, head weaving, head

jerking, head tilt) ($F_{(5,20)}$ = 0.954, p = 0.4687), or grooming behavior (i.e., grooming, scratching, licking self) ($F_{(5,20)}$ = 0.697, p = 0.6316) among the treatment groups.

Effects of intra-mPFC MEK antagonism on D_1 receptor-mediated priming of behavioral responses in neonate 6-OHDA-lesioned rats

Analysis of open field total horizontal counts (Fig. 3-4*A*), total stereotypic counts (Fig. 4B), and total vertical counts (Fig. 3-4*C*) revealed no significant main effects of treatment ($F_{(1,10)}$ = 0.009, p = 0.9248, $F_{(1,10)}$ = 3.058, p = 0.1109, and $F_{(1,10)}$ = 0.032, p = 0.8625, respectively). As shown in Fig. 3-4*D*, however, post-hoc comparisons of a significant main effect of treatment for total vertical time ($F_{(1,10)}$ = 9.959, p > 0.05) revealed that intra-mPFC infusions of PD98059 prior to each of three of the four weekly SKF-38393 treatments to neonate-lesioned rats reduced the amount of time that the rats spent performing behavior in the vertical plane (p < 0.05 vs. Veh group).

As shown in Fig. 3-5*A*, horizontal behavioral observations did not reveal any significant main effects of treatment in mPFC microinfused rats ($F_{(1,6)}$ = 0.006, p = 0.9417), similar to that observed with the computer-generated horizontal counts. Post hoc comparisons of a significant main effect of treatment for vertical behavior ($F_{(1,6)}$ = 9.657, p = 0 < 0.05) and paw-fixation behavior ($F_{(1,6)}$ = 39.562, p = 0 < 0.05) revealed that the intra-mPFC infusions of PD98059 inhibited the priming effect of these behaviors to repeated D_1 agonist treatment. No significant main effects of treatment were found for observations of investigatory behavior ($F_{(1,6)}$ = 0.352, p = 0.5747), mouth-fixation behavior ($F_{(1,6)}$ = 0.038, p = 0.8523), or head behavior ($F_{(1,6)}$ = 0.602, p = 0.4672). Grooming behavior was not observed in any of the rats tested.

D. Discussion

The present study demonstrates a role for ERK signaling in the sensitization, or priming, of various locomotor and stereotyped behaviors associated with repeated D_1 agonist treatment to neonate-lesioned rats. More importantly, enhanced ERK signaling in the mPFC was found to contribute to the sensitized vertical and paw-related behaviors seen in these animals.

Consistent with previous studies (Breese et al., 1985b, Criswell et al., 1989; Papadeas et al., 2004), neonate-lesioned rats primed to D_1 agonist demonstrated an increase in horizontal, stereotypic, and vertical open field activity compared with intact rats. These rats also demonstrated an increase in time spent performing behaviors in the vertical plane. Visual observations similarly showed a priming effect in the D_1 agonist-treated neonate-lesioned rats, in that the rats displayed exaggerated horizontal, vertical, and paw-fixation behaviors in response to a fourth weekly dose of SKF-38393. Some of the rats also showed sensitized investigatory, mouth-fixation, head, and grooming behaviors. Global inhibition of ERK signaling by ICV or systemic administration of MEK inhibitors altered the supersensitive motor responsiveness induced by the repeated D_1 agonist exposure. Horizontal open field activity was significantly increased during the fourth challenge dose of SKF-38393 given in the absence of MEK inhibitor, while stereotypic open field activity and vertical time were diminished. Visual observations similarly revealed that the MEK antagonism augmented horizontal behavior but inhibited vertical and paw-related behaviors. Our finding that MEK inhibitor pretreatment blocked the sensitization of vertical behavior is remarkably similar to what has been observed in mice receiving SL327 pretreatment prior to cocaine (Valjent et al., 2000). Together, these

84

data indicate that the persistent increase in forebrain ERK phosphorylation induced by repeated D_1 agonist treatment to neonate-lesioned rats (Papadeas et al., 2004) is not responsible *per se* for all priming-induced behaviors, but it does contribute to specific sensitized responses.

There are two possible explanations as to why global MEK inhibition differentially modifies motor behaviors in neonate-lesioned rats repeatedly treated with D_1 agonist. One could hypothesize that the locomotor behavior is modified by the concomitant expression of other motor behaviors (Bernardi et al., 1986; Chinen et al., 2005). More specifically, the enhanced locomotor behavior seen in the MEK inhibitor pre-treated rats could lead to the inhibition of rearing and paw-fixation behaviors in these animals. On the other hand, the opposite effects of MEK inhibitor on locomotor and stereotyped behavior might occur because these behaviors are driven by the activation of different neural systems. Microinjection of MEK inhibitors into different brain sites where phospho-ERK is persistently elevated could help determine precise regions and circuitry responsible for ERK pathway driven responses in primed neonate-lesioned rats.

In fact, microinjection of the MEK inhibitor PD98059 into the mPFC, where ERK phosphorylation is most robust and longest-lasting compared with other regions (Papadeas et al., 2004), specifically inhibited time spent vertical in the open field. Visual observations indicated that this inhibitory effect coincided with an actual reduction in vertical and paw-fixation behaviors. Interestingly, these stereotyped behaviors are believed to mirror psychostimulant-induced psychosis in humans and certain aspects of positive symptoms associated with schizophrenia (Robinson and Becker, 1986; Ujike 2002). Given the possible role of mPFC phospho-ERK in adaptations associated with

85

these DA-mediated disorders (Kyosseva, 2004; Valjent et al., 2004), it is not surprising that increased phospho-ERK in this region facilitates these types of behaviors in our model.

Studies have shown that $5HT_{2A}$ receptors contribute to the locomotor responsiveness caused by D_1 agonism in neonate-lesioned rats (Walker et al., 2004; Breese et al., 2005), and that the mechanism associated with the action of this receptor subtype on locomotor behavior occurs primarily within the striatum (Bishop and Walker, 2003; Walker et al., 2004). Moreover, our previous studies showed that pretreatment with the 5-HT$_{2A}$-preferring receptor antagonist ketanserin fails to block persistently elevated phospho-ERK in the mPFC of these animals. Together, these findings agree with our current observation that microinjection of PD98059 into the mPFC does not affect priming of locomotor behavior in neonate-lesioned rats to D_1 agonist, and suggest that the sensitized locomotor response is driven by mechanisms independent of ERK signaling.

We have previously demonstrated that ICV and systemic pretreatment with the MEK inhibitors SL327 or PD98059 at doses used in this study inhibits the phosphorylation of ERK in our model when compared with simultaneously treated vehicle controls (Papadeas et al., 2004; Papadeas et al., 2006). Moreover, we have shown that the phosphorylation of a related mitogen-activated protein kinase, c-Jun N-terminal kinase, remains unaffected (Papadeas et al., 2006). Although recent studies report that these compounds have no effect on a variety of other kinases, including cyclic AMP-dependent protein kinase A, Ca^{2+}/phospholipid-dependent kinase C, or calcium-calmodulin-dependent protein kinase (Atkins et al., 1998; Blum et al., 1999; Selcher et al., 1999; Valjent et al., 2000), this study cannot rule out the possibility that SL327 or

PD98059 might nonspecifically inhibit other kinases that have not been directly examined. Nonetheless, these MEK inhibitors have been found to be highly selective (Alessi et al., 1995; Favata et al., 1998; Davies et al., 2000).

In summary, the present results reveal that ERK signaling plays an important role in some of the behavioral responses exhibited by neonate-lesioned rats to repeated D_1 agonist exposure. These findings provide a new mechanism to explain aspects of priming behavior mediated by D_1 receptor pharmacology.

A. ICV placements
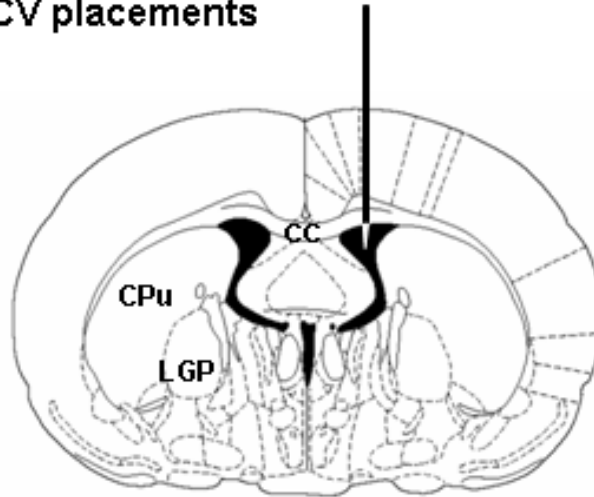
Bregma -0.80 mm

B. mPFC placements
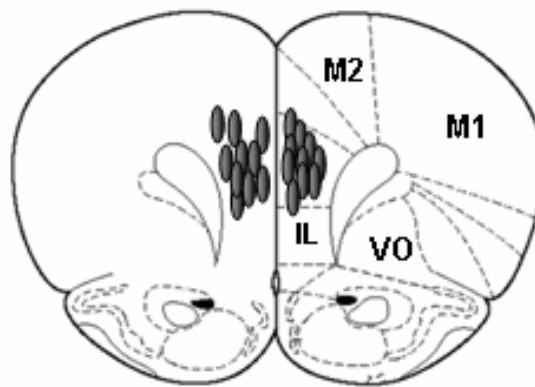
Bregma 3.20 mm

Fig. 3-1: Schematic representations of coronal sections of the rat brain depicting the ICV injection site (*A*) and the distribution of mPFC microinfusion sites (*B*). The sections were taken from Paxinos and Watson (1998). For (*A*), drugs were infused unilaterally into the right lateral ventricle. CPu, Caudate-Putamen; LGP, Lateral Globus Pallidus; CC, corpus callosum. For (*B*), shadded ovals denote placements within the striatum for selected neonate 6-OHDA-lesioned rats. M1, primary motor cortex; M2, secondary motor cortex; IL, infralimbic cortex; VO, ventral orbital cortex.

88
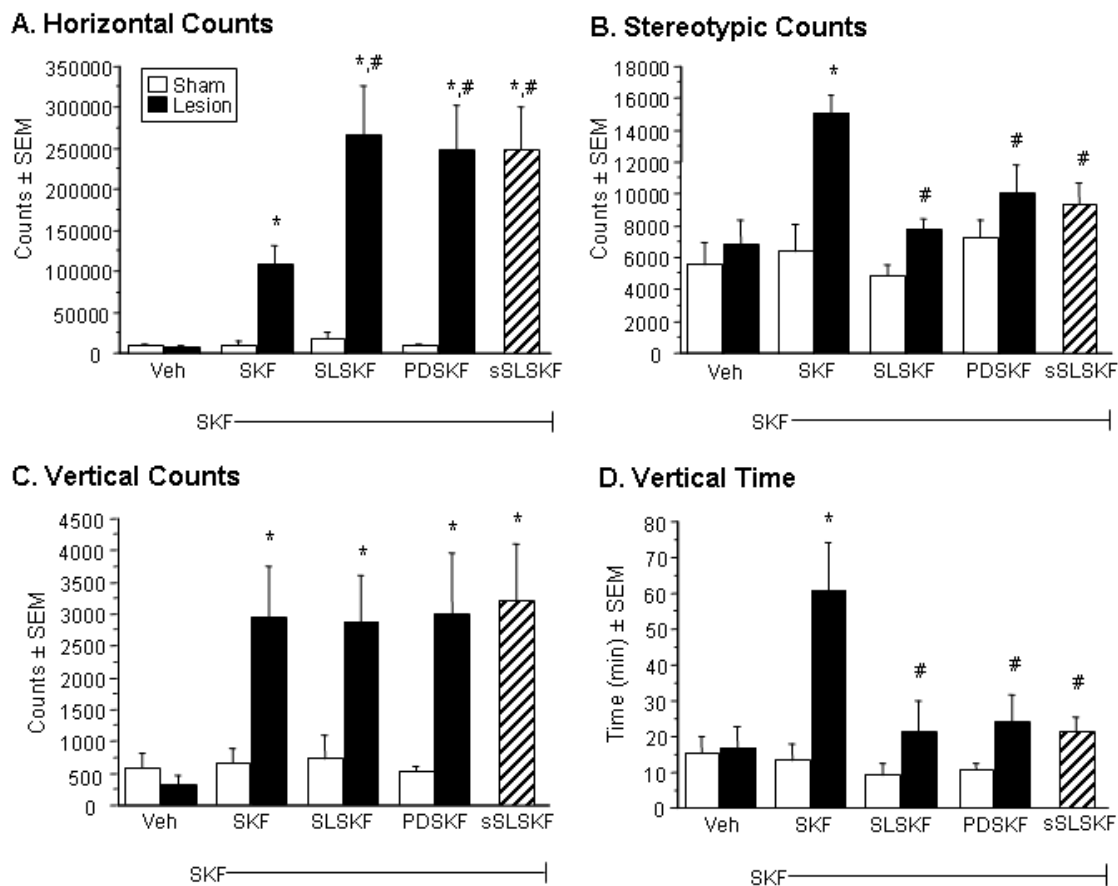
Fig. 3-2: ICV administration of SL327 or PD98059 alters sensitized locomotor activity in neonate-lesioned rats administered repeated D$_1$ agonist treatment. Graphs denote averages of thirty-six 5 min measurement periods for total horizontal counts ± SEM (*A*), stereotypic counts ± SEM (*B*), vertical counts ± SEM (*C*), and vertical time ± SEM (*D*) recorded by computer-monitored activity chambers. Data shown reflects behavioral activity following the additional dose of SKF-38393 (*x-axis*) to lesioned and sham rats at week 4. *Veh* indicates rats that were infused with vehicle prior to 4 weekly injections with saline. *SKF* indicates rats that were infused with vehicle prior to 4 weekly injections with SKF-38393. *SLSKF, PDSKF* indicate rats that were infused with SL327 or PD98059 prior to each of 3 of the 4 weekly injections with SKF-38393. Note that

lesioned rats receiving systemic pre-treatment with SL327 prior to each of 3 of the 4 weekly SKF-38393 treatments (*sSLSKF*) (*striped bars*) demonstrated similar behavioral effects to rats pre-treated with SL327 intraventricularly ($p > 0.05$). *Not shown*, lesioned rats that received a single SKF-38393 treatment demonstrated $4{,}718 \pm 616$ total horizontal counts, $7{,}868 \pm 677$ total stereotypic counts, 436 ± 79 total vertical counts, and 17 ± 8 total vertical time (min), similar to what was recorded for the Veh-lesion group and sham control groups ($p > 0.05$ for each comparison). Statistical differences were determined by 1-way ANOVA analyzing treatment effects. Significant post hoc differences are denoted by the following symbols: ***** $p < 0.05$ vs. Lesion-Veh and Sham-SKF, # $p < 0.05$ vs. Lesion-SKF.

Observer-Scored Behaviors

A. Horizontal Behavior **B. Vertical Behavior** **C. Paw-Fixation Behavior**
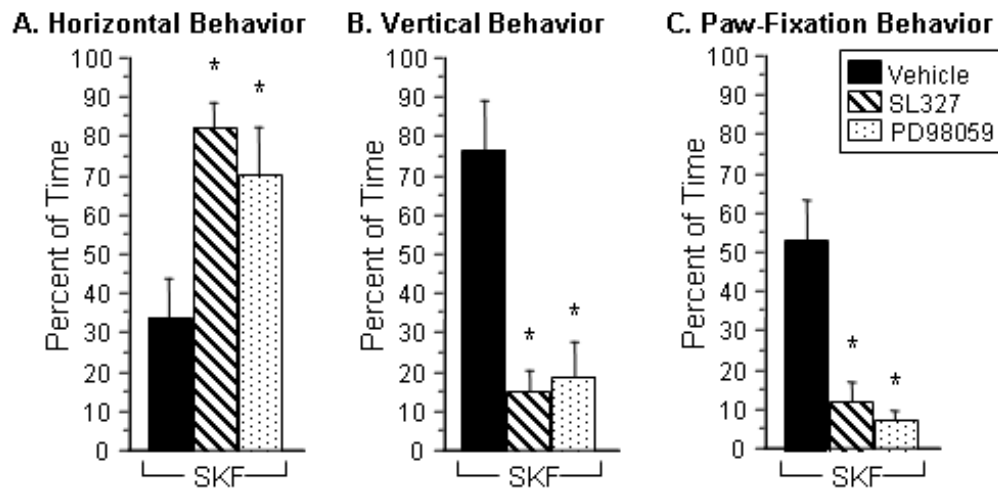
Fig. 3-3: ICV administration of SL327 or PD98059 alters D$_1$ receptor-mediated priming of behavioral responses in neonate-lesioned rats. Graphs denote average percentage of 15 sec observation periods during which horizontal behavior, e.g. running, walking, trotting (*A*), vertical behavior, e.g. rearing, climbing, jumping (*B*), and paw-fixation behavior, e.g. patting, treading, taffy pulling (*C*) occurred in lesioned rats. *Vehicle*, lesioned rats infused with vehicle prior to each of 3 weekly doses of SKF-38393; *SL327*, lesioned rats infused with SL327 prior to each of three weekly doses of SKF-38393; PD98059, lesioned rats infused with PD98059 prior to each of 3 weekly doses of SKF-38393. Data shown reflects behavioral responses after the additional dose of SKF-38393 at week 4 (indicated by *SKF* on x-axis). Lesioned rats administered a single dose of SKF-38393 or those infused with vehicle prior to each of 4 weekly injections with saline did not demonstrate any significant behavioral activity over the course of the testing period, nor did any of the sham control groups (average percentage of time spent for each behavior measured was <1%). Statistical differences were determined by 1-way ANOVA analyzing treatment effects. Significant post hoc differences are denoted by the following symbols: * $p < 0.05$ vs. Veh group.
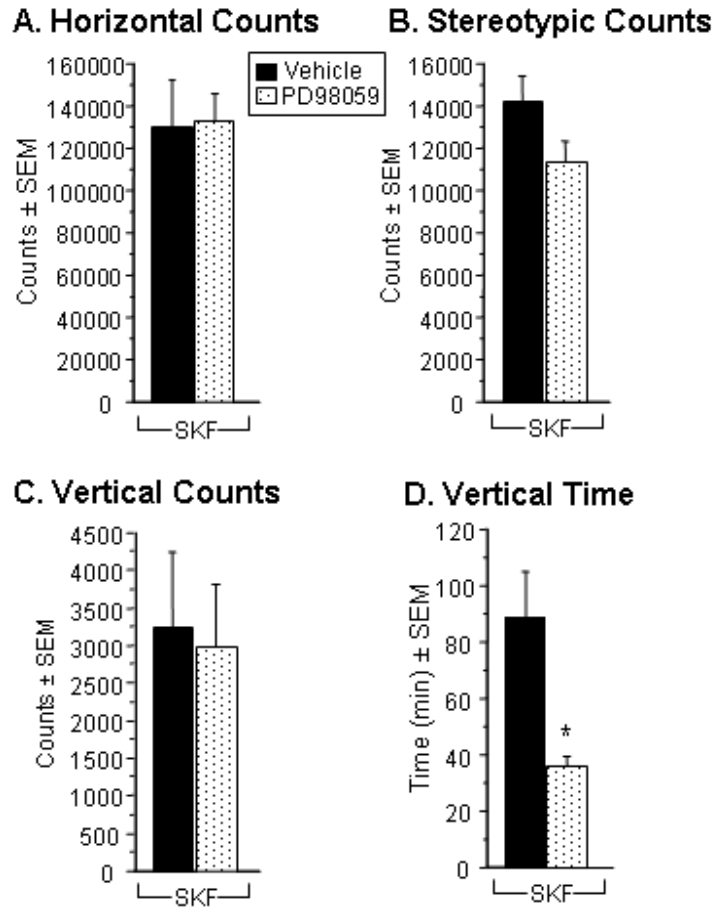
Fig. 3-4: Intra-mPFC infusions with PD98059 reduces vertical time in neonate-lesioned rats administered repeated D₁ agonist treatment. Graphs denote averages of thirty-six 5 min measurement periods for total horizontal counts ± SEM (*A*), stereotypic counts ± SEM (*B*), vertical counts ± SEM (*C*), and vertical time ± SEM (*D*) recorded by computer-monitored activity chambers. *Vehicle*, lesioned rats microinjected with vehicle prior to each of 3 weekly doses of SKF-38393; *PD98059*, lesioned rats microinjected with PD98059 prior to each of 3 weekly doses of SKF-38393. Data shown reflects behavioral activity following the additional SKF-38393 treatment at week 4 (indicated by *SKF* on x-axis). Statistical differences were determined by 1-way ANOVA analyzing treatment effects. Significant post hoc differences are denoted by the following symbols: * $p < 0.05$ vs. Veh group.

Observer-Scored Behaviors

A. Horizontal Behavior   B. Vertical Behavior   C. Paw-Fixation Behavior
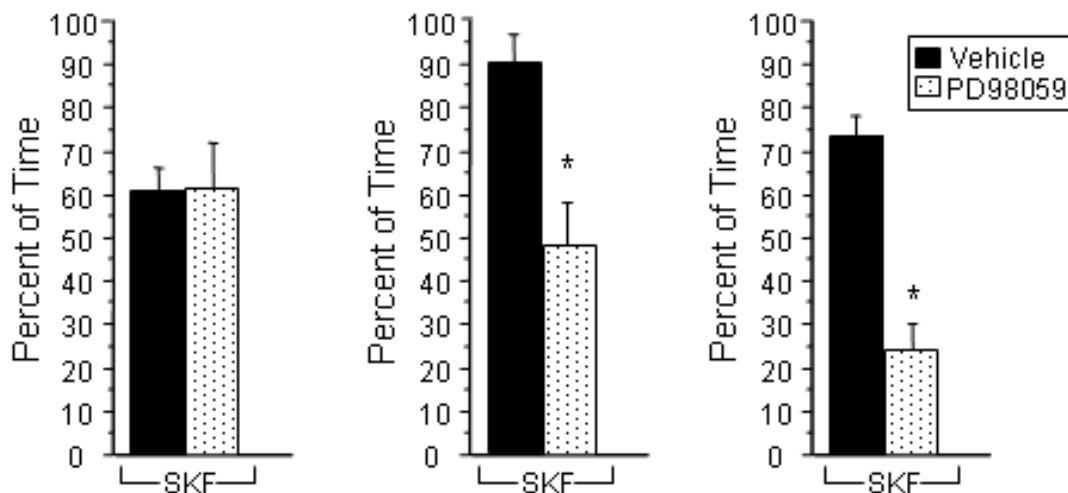
Fig. 3-5: Intra-mPFC infusion with PD98059 inhibits priming of vertical and paw-fixation behavior in neonate-lesioned rats administered repeated doses of SKF-38393. Graphs denote averages of the percentage of 15 sec observation periods during which horizontal behavior, e.g. running, walking, trotting (A), vertical behavior, e.g. rearing, climbing, jumping (B), and paw-fixation behavior, e.g. patting, treading, taffy pulling (C) occurred. Data shown reflects behavioral responses after the additional dose of SKF-38393 at week 4 (indicated by *SKF* on x-axis). Statistical differences were determined by 1-way ANOVA analyzing treatment effects. Significant post hoc differences are denoted by the following symbols: * $p < 0.05$ vs. Veh group.

Table 3-1: Experimental Paradigm

Experiment	Number of Rats	
ICV MEK Inhibitor Infusion	**Lesioned**	**Sham**
PD-SKF→PD-SKF→PD-SKF→Veh-SKF	5	4
SL-SKF→SL-SKF→SL-SKF→Veh-SKF	5	3
Veh-SKF→Veh-SKF→Veh-SKF→Veh-SKF	6	4
Veh-Sal→Veh-Sal→Veh-Sal→Veh-SKF	3	0
PD-Sal→PD-Sal→PD-Sal→PD-Sal	5	2
Veh-Sal→Veh-Sal→Veh-Sal→Veh-Sal (injection control)	5	4
Systemic MEK Inhibitor Injection		
SL-SKF→SL-SKF→SL-SKF→Veh-SKF	5	0
Veh-SKF→Veh-SKF→Veh-SKF→Veh-SKF*	4	0
Veh-Sal→Veh-Sal→Veh-Sal→Veh-SKF*	4	0
Intra-mPFC Infusion		
PD-SKF→PD-SKF→PD-SKF→SKF[§]	4	0
Veh-SKF→Veh-SKF→Veh-SKF→SKF	4	0

PD, PD98059; *SL*, SL327; *Veh*, Vehicle, *SKF*, SKF-38393, *Sal*, Saline.

(**-**) = 30 min between treatments

(→) = 1 week between treatments

*Behavioral data from these two treatment groups did not significantly differ from that of similar treatment groups in the ICV MEK Inhibitor experiment. Thus, data collected from these two groups were collapsed into the corresponding treatment groups in the ICV MEK inhibitor experiment.

[§]SKF-38393 was administered on its own to prevent any additional damage induced by the injector within the mPFC.

CHAPTER IV. **PHOSPHORYLATED ERK1/2 MODIFIES APICAL DENDRITIC STRUCTURE OF MEDIAL PREFRONTAL CORTEX PYRAMIDAL NEURONS IN A RAT MODEL OF DOPAMINE D$_1$ RECEPTOR AGONIST SENSITIZATION**

A.   Introduction

Dendrites receive multiple and diverse synaptic inputs, processing and integrating them into signals that convey information to the soma and axon. Neuronal identity largely dictates basic dendrite structure, but environmental signals further shape dendrites during development and in adulthood (Miller and Kaplan, 2003). Reciprocally, dendritic morphology impacts spatial and temporal neurotransmission by affecting the propagation and patterning of action potentials (Mainen and Sejnowski, 1996; Vetter et al., 2001). This interdependence of form and function advances the notion that dendritic morphological changes accompany neuroadaptation and plasticity (Greenough et al., 1990; Kolb and Wishaw, 1998). Accordingly, the structural remodeling of dendrites and their spines is thought to coordinate with physiological processes such as learning and memory (Lamprecht and LeDoux, 2004) and behavioral sensitization to psychostimulants (Robinson and Kolb, 1997; 1999). While recent discoveries have elucidated many of the signaling mechanisms that regulate dendritic spine plasticity and the formation of dendrites during development, relatively little is known about the capacity and mechanisms of maintenance and resculpting of the mature dendritic tree.

Microtubule-associated protein 2 (MAP2), a neuron-specific cytoskeletal protein, affects the shape, polarity and plasticity of dendrites by controlling assembly and stability of microtubules (Aoki and Siekevitz, 1985; Matus, 1988; Johnson and Jope, 1992). The phosphorylation of MAP2 by several kinases, including Ca^{2+}/calmodulin-dependent protein kinase II (CaMKII), cyclic AMP-dependent protein kinase (PKA), Ca^{2+}/phospholipid-dependent kinase (PKC), and extracellular signal-regulated kinases 1 and 2 (ERK1/2), modulates its binding to microtubule protofilaments (Sanchez et al., 2000; Hirokawa et al., 1988; Audesirk et al., 1997). Typically, activated ERK translocates to the nucleus, where it phosphorylates transcription factors to control biological processes such as cell proliferation, survival and plasticity (Seger and Krebs, 1995; Sweatt, 2004). Through interaction with MAP2 however, phosphorylated ERK1/2 may be retained in the cytoplasm in association with the microtubule cytoskeleton (Morishima-Kawashima and Kosik, 1996; Reszka et al., 1995).

Recently, we demonstrated the persistent phosphorylation of ERK1/2 in neurons of the medial prefrontal cortex (mPFC) of neonate 6-OHDA-lesioned rats behaviorally sensitized in adulthood to the effects of a dopamine D_1 receptor-selective agonist (Papadeas et al., 2004). In these D_1-sensitized animals, doses of the partial D_1 agonist SKF-38393 that are ineffective in controls stimulate profound activation of locomotor and stereotypical behaviors. Furthermore, while the behavioral response abates within a few hours, sensitivity to a subsequent agonist challenge lasts at least 6 months (Breese et al., 1984a; Criswell et al., 1989), suggesting that long-lasting neuroadaptive changes have occurred that mediate this behavioral sensitivity. In this study, we sought to determine whether MAP2 dendritic immunostaining is altered by the prolonged presence of

96

phospho-ERK in D_1-sensitized rat mPFC. We found that D_1 sensitization produces robust and long lasting changes in MAP2 that reflect radical reshaping of dendrites. Most significant, we show that these changes are prevented by pretreatment with pharmacological inhibitors of mitogen-activated protein kinase kinase 1/2 (MEK1/2), the obligate upstream activator of ERK1/2.

B.   Materials and Methods

Drugs

6-OHDA hydrobromide (ICN; Irvine, CA) was dissolved in saline containing 0.5% ascorbic acid. Desipramine HCl (Sigma, St. Louis, MO) and SKF-38393 (2,3,4,5-tetrahydro-7,8-dihydroxy-1-phenyl-1H-3-benazepine HCl; Sigma, St. Louis, MO), were dissolved in saline. SL327 (α-[Amino[(4-aminophenyl)thiomethylene]-2-(trifluoromethyl)benzene-acetonitrile; a gift from Bristol-Myers-Squibb Company, Princeton, NJ) and PD98059 (2-(-Amino-3-methoxyphenyl)-4H-1benzopyran-4-one; Calbiochem, La Jolla, CA) were dissolved in dimethylsulfoxide (DMSO) at a concentration of 10 mg/kg, from which a solution containing 0.1 mg/kg with 1% DMSO was prepared in sterile saline (pH 7.3) prior to intracerebroventricular (ICV) infusion (Choe and McGinty, 2001; Gu et al., 2001). For intraperitoneal (i.p.) administration, SL327 was dissolved in DMSO at 2 ml/kg (Atkins et al., 1998; Selcher et al., 1999; Yamagata et al, 2002). Kainic acid (1 ml/kg) (Sigma, St. Louis, MO) was dissolved in saline.

Preparation and sensitization of neonate 6-OHDA-lesioned rats

Neonate-lesioned and sham-lesioned rats were prepared at postnatal day (PND)3-4 as described previously (Papadeas et al., 2004). The bilateral lesion causes over 90% loss of dopamine innervation into the striatum and disrupts basal ganglia-cortical system circuits (Smith et al., 1973). All animals were treated and used in accordance with the *NIH Guide for the Care and Use of Laboratory Animals* with approval from the University of North Carolina School of Medicine Institutional Animal Care and Use Committee.

Neonate-lesioned rats do not show maximal sensitivity to the partial D_1 agonist SKF-38393 unless repeatedly exposed to this agonist (Breese et al., 1985; Criswell et al., 1989). Therefore, beginning at PND40-50, neonate-lesioned rats in this treatment group received repeated treatments with the partial D_1 agonist SKF-38393, sufficient to allow the animals to reach a plateau of maximal behavioral supersensitivity (Criswell et al., 1989, 1990). To accomplish D_1 sensitization, lesioned rats were administered a total of 12 mg/kg SKF-38393, divided into 4 doses of 3 mg/kg; each spaced one-week apart as previously described (*Lesioned R-SKF, D_1-sensitized*) (Papadeas et al., 2004). A separate group of sham rats received the same agonist dosing regimen (*Sham R-SKF*). Additional groups of neonate- and sham-lesioned rats received saline vehicle (*Lesioned R-Sal* and *Sham R-Sal*, respectively) and served as injection controls. To assess the effects of a single dose of SKF-38393, lesioned and sham rats were injected with a single 3 mg/kg dose of SKF-38393 following weekly doses 1-3 of saline.

In the neonate-lesioned rat, D_1 agonist sensitization is characterized by augmented behavioral responses to the locomotor and stereotypical effects of a sub-threshold dose of

selective D_1 agonists. Importantly, control animals do not display these behaviors in response to SKF-38393 administration, nor do they sensitize with repeated dosing. Therefore, upon dosing on weeks 1 through 4, behavioral activity was assessed to assure maximal responsiveness of lesioned rats to the D_1 agonist. Rats were placed in clear 17 × 17 inch computer-monitored activity chambers (Med Associates, St. Albans, VT) and their behavioral activity was recorded as previously described (Papadeas et al., 2004). Neonate-lesioned rats included in this study exhibited ≥80,000 total horizontal locomotor counts/180 min following the final SKF-38393 treatment. All rats were euthanized either 7 or 21 d after the final SKF-38393 treatment (i.e., weeks 5 or 7, respectively). Three replicates of each experiment were done, and a representative experiment is shown in each figure.

Intracerebroventricular (ICV) Infusion of MEK1/2 Inhibitors

At PND35-40, neonate- and sham-lesioned rats were anesthetized with sodium pentobarbital (50 mg/kg, i.p.) and placed in a Kopf stereotaxic apparatus. Using aseptic conditions, the scalp was cleared and a small burr hole was made through which a cannula was lowered into the right lateral ventricle (from bregma; anteroposterior, -0.8 mm; mediolateral, -1.5 mm; dorsoventral, -2 mm; according to Paxinos and Watson, 1998; supplemental Fig. 4-1S*C*). The animals were allowed 7 d to recover from the implant before any testing was initiated. Using a 32-gauge stainless steel microinjector needle and Sage syringe pump (Thermo Electron Corporation, Beverly, MA), vehicle (1% DMSO in saline), PD98059 or SL327 was infused through the cannula in a volume

of 2 μl over 5 min, as previously described (Gu et al., 2001). The needle was allowed to remain in place for 1 min to reduce backflow of the solution along the injection track.

Groups of neonate- and sham-lesioned rats received four ICV infusions with SL327 or PD98059 30 min prior to each dose of SKF-38393 (3 mg/kg) or saline. Some rats received vehicle prior to doses 1 through 3 of agonist, followed by SL327 or PD98059 prior to the fourth and final dose of SKF-38393. All rats were euthanized 7 d after the final dosing.

AAV-GFP Vector Infusions

Preparation and infusion of the adeno-associated viral (AAV) vector construct were described previously (McCown et al., 1996). Briefly, neonate- and sham-lesioned rats were anesthetized with sodium pentobarbital (50 mg/kg, i.p.), and placed in a stereotaxic frame. Using the method described above, 2.0 μl of a recombinant AAV vector (titer, 1×10^{13} viral particles/ml) was microinfused over a 20 min period into the mPFC (from bregma; anteroposterior, 3.2 mm; mediolateral, -0.6 mm; dorsoventral, -2.0 mm; according to Paxinos and Watson, 1998), where expression of green fluorescent protein (GFP) was driven by a hybrid chicken beta-actin promoter. The injector was left in place for 3 min post-infusion to allow diffusion from the site and to prevent backflow of solution. The animals were allowed 12 d to recover from the infusions before any testing was initiated and to allow transduction and expression. AAV-GFP-transduced cells continue to express GFP for months (Klein et al., 2002). Expressed GFP was visualized using confocal microscopy (see below) revealing predominant labeling in neuronal somata and dendrites (McCown et al., 1996). Labeling of GFP-positive somata

demonstrated that most of the microinjections were centered in layer V of the prelimbic cortex, however a few injections labeled somata in layer II/III.

Immunohistochemistry: tissue preparation and immunostaining

Standard immunohistochemical methods were employed as previously described (Papadeas et al., 2004). Tyrosine hydroxylase immunoreactivity was determined with affinity-purified polyclonal anti-tyrosine hydroxylase (1:4000; Calbiochem, San Diego, CA) to establish that the neonate 6-OHDA-lesioning induced an adequate loss of DA-containing neurons (Papadeas et al., 2004). Monoclonal anti-MAP2 (1:500; Chemicon, Temecula, CA) recognizes the high molecular weight isoforms MAP2A and MAP2B, and is insensitive to phosphorylation state. MAP2 is considered a suitable marker for dendrites based on evidence that closely correlates dendritic growth with an increase in MAP2 immunostaining (Philpot et al., 1997; Sanchez et al., 2000; Bury and Jones, 2002). Anti-phospho-ERK1/2 (phospho-p44/42 MAP Kinase (Thr202/Tyr204)) (1:500, Cell Signaling Technology, Beverly, MA) primary antibodies were used and quantified as previously described (Papadeas et al., 2004). Tissue sections were further processed using Vectastain Elite ABC kits (Vector Laboratories, Burlingame, CA) per the manufacturer's instructions with immunochemical detection using nickel-cobalt intensification of the 3,3'-diaminobenzidine (DAB) reaction product. Immunoreactivity was observed under a light microscope.

Double-label fluorescence

Free-floating tissue sections representative of the mPFC of AAV-GFP-injected rats were incubated with anti-MAP2 antibody (1:500), followed by incubation in AlexaFluor 594-conjugated goat anti-mouse secondary antibody (1:500; Invitrogen, Carlsbad, CA) for 45 min at 4°C with agitation. The intensity of the GFP and labeled secondary antibodies were visualized by fluorescence microscopy with FITC, rhodamine and dual pass filters. Confocal microscopy, digital imaging, and accompanying software manipulation are described below.

Morphological analysis of MAP2 immunoreactive dendrites

A strategy was devised to analyze MAP2 positive dendrites in processed sections using NIH Image (ImageJ software version 1.34s, http://rsb.info.nih.gov/ij/). Within layers II/III and V of mPFC and visual cortex (VC), 12 samples per layer were chosen that consisted of three samples from each of four sections, spaced approximately 250 μm apart. Each sample was digitized to 657 pixels × 516 pixels in 8-bit grayscale images using an Olympus BX50 microscope outfitted with a Sony DCX-390 video camera. Light levels were normalized to preset values to ensure fidelity of the data acquisition. Nissl-stain was performed on adjacent tissue sections for estimation of laminar thickness (supplemental Fig. 4-3S). Laminar thickness was measured using a method similar to the technique of Wang et al. (1995c). Using a grayscale morphology plugin created for ImageJ (available at http://rsb.info.nih.gov/ij/plugins/gray-morphology.html) a closing operator with an arbitrary radius of 6 pixels was applied to each of the digitized images, enabling us to omit MAP2-stained somata without disturbing the MAP2-positive

dendritic processes in the image. The images were then consistently thresholded such that all MAP2-stained dendrites were black and the background was white. Threshold levels were individually set to ensure all MAP2-stained dendrites were identified. Image analysis was performed using the 'Analyze Particles' function in Image J and the software was calibrated to ensure that all staining was included in surface area fraction determinations while background staining was excluded. The percent difference in area fraction of MAP2-stained dendrites between treatment groups was calculated using saline-injected sham-lesioned rats as the control group. Values obtained from layers II/III and V in each section were averaged for each animal, and a mean was determined across all animals within each treatment group. Statistical comparisons between treatment groups were carried out with ANOVA. Where appropriate, post-hoc comparisons between groups were performed using a Fisher's PLSD test. A probability of < 0.05 was accepted as significant.

Laser Scanning Confocal Microscopy

For GFP-labeled dendrites, sections were imaged with a Zeiss Axiovert LSM510 laser confocal microscope equipped with argon (488 nm) and HeNe (543) lasers, using a 40x objective. Qualitative analysis was performed using Zeiss LSM Image Browser and Adobe Photoshop software. Thirty images through a Z-series were taken at approximately 1 μm intervals through each mPFC section, and the images were merged to obtain an image as close as possible to a complete dendritic tree. To calculate the length of dendrites, three dendrites were selected from one section that appeared to extend from the cell body to the tip of the dendrite. As described in detail by Harada et al.

(2002), lengths of representative dendrites were measured and averaged within each of the treatment groups.

For double-label immunofluorescence, dually labeled GFP and MAP2 immunoreactive neurons identified with the fluorescence microscope were confirmed using laser scanning confocal microscopy. Cells were considered double-labeled when expression of GFP and phospho-ERK1/2 or MAP2 were co-localized in a minimum of three consecutive steps in a Z-series taken at 1 μm intervals through the section of interest using a 40x objective.

SL327 Effects on JNK Phosphorylation Elicited by Kainic Acid-Induced Seizures

During the preparation of this manuscript, a report by Bjorkblom et al. (2005) described an enhanced role for cJun N-terminal kinase (JNK) relative to ERK1/2 in modifying cortical dendritic architecture. We thus investigated whether MEK inhibitors administered *in vivo* affect JNK phosphorylation, a possibility that might suggest that our observations were phospho-JNK-dependent. Unlesioned rats were administered SL327 (100 mg/kg, i.p.) or DMSO vehicle (100%) 30 min prior to injections with kainic acid (KA, 12 mg/kg). Control treatment groups included SL327 followed by saline and DMSO vehicle followed by saline. Following KA administration, rats were monitored continuously for 3 h for the onset and extent of seizure activity and seizures were rated according to a previously defined scale (Racine et al., 1972). All rats included in the study exhibited seizures. Three hours after KA administration (Jeon et al., 2000), animals were decapitated and their brains processed for Western blotting with antibodies to stress-activated protein kinase (SAPK)/JNK and phospho-SAPK/JNK as described below.

104

Average integrated signal intensity measurements revealed that pretreatment with SL327 did not alter the immunoreactive density of phosphorylated JNK or total JNK protein in hippocampus compared to saline-pretreated controls (phospho-JNK *ANOVA*: $F_{(1,7)} = 0.028$, p = 0.8708; total JNK *ANOVA*: $F_{(1,7)} = 0.068$, p = 0.4373; blots not shown).

Western blot analysis: tissue preparation, immunoblotting, and quantification

For Western blotting, brains were rapidly removed immediately following decapitation, and the mPFC and hippocampus were dissected on ice and stored at -80°C until use. Tissues were homogenized by sonification in solubilization buffer (10 mM Tris-HCl, 50 mM NaCl, 1% Triton X-100, 30 mM sodium pyrophosphate, 50 mM NaF, 5 nM $ZnCl_2$, 100 μM Na_3VO_4, 1 mM DTT, 5 nM okadaic acid, 2.5 ng/ml aprotinin, 2.5 ng/ml pepstatin, and 2.5 ng/ml leupeptin). Insoluble material was removed by centrifugation (13,000 rpm for 20 min at 4°C), and protein concentration determined using a BCA protein assay kit (Pierce, Rockford, IL). Samples were mixed with Novex 2X Tris-glycine SDS sample buffer (San Diego, CA) containing 5% 2-mercaptoethanol and heated to 90°C for 3 min. Aliquots of 20 μg of protein/lane were separated on Novex 8-16% gradient Tris-glycine gels under reducing conditions. Proteins were transferred to polyvinylidene difluoride membranes (Immobilon-P, Millipore, Bedford, MA), rinsed 3 times in PBS for 5 min, and incubated with one of the following: monoclonal anti-MAP2 antibody (1:500; Chemcion, Temecula, CA); polyclonal anti-phospho-SAPK/JNK antibody (1:500, Cell Signaling Technology, Beverly, MA); anti-SAPK/JNK antibody (1:500, Cell Signaling Technology); or polyclonal β-actin antibody (1:5000; Sigma, St. Louis, MO). Antibodies were diluted 1:1 in Odyssey Blocking Buffer (LI-COR

105

Biosciences, Lincoln, NE) in PBS containing 0.1% Tween-20. Binding of the primary antibodies to proteins was detected using either IRDye800 goat anti-rabbit (1:5000; Rockland Immunochemicals, Gilbertsville, PA) or AlexaFluor 680 goat anti-mouse secondary antibodies (Invitrogen, Carlsbad, CA). Fluorescent signals were detected using the Odyssey Infrared Imaging System (LI-COR Biosciences, Lincoln, NE). Average integrated signal intensity measurements for MAP2 were calculated using Odyssey image analysis software after normalization to β-actin.

C.   Results

D_1-sensitized rats exhibit altered MAP2 immunostaining in medial prefrontal but not in visual cortex

Previously, we demonstrated the persistent ($\geq$36 d) phosphorylation of ERK1/2 in mPFC of D_1-sensitized rats (Papadeas et al., 2004). In an effort to identify potential downstream signaling effects of sustained ERK activation in this region, we examined the immunohistochemical profile of an ERK1/2 target protein, MAP2. In rat brain coronal sections, apical dendrites of layers II/III and V pyramidal neurons were stained intensely throughout the cortex with anti-MAP2A/B. In agreement with descriptions by Gabbot and Bacon (1996), Figs. 4-1*A*, *B*, and *C* demonstrate that first-order MAP2-immunoreactive dendritic shafts in mPFC of sham control and saline-injected lesioned rats were long and straight, traversing from deeper layers of the cortex to the pial surface in well-delineated bundles (region of interest depicted in supplemental Fig. 4-1S*A*). In contrast, repeated SKF-38393 treatments to neonate-lesioned rats resulted in mPFC apical dendritic processes that appeared short and bent, and bundling was far less

prominent at day 7 (Lesioned R-SKF, Fig. 4-1D). Bundles containing at most 2 to 3 visible shafts were observed, suggesting a loss of normal dendritic fasciculation. The altered pattern of MAP2 immunostaining persisted for at least 21 days after repeated agonist treatment (Figure 4-1E), thus coinciding temporally with the sustained presence of phosphorylated ERK1/2 in these animals (Papadeas et al., 2004). Quantitative analysis of the MAP2-stained dendritic profiles revealed that the surface area fraction was decreased by 40 to 50% in mPFC of D_1-sensitized rats at both time points ($p < 0.0001$ compared to Lesioned R-Saline, Sham R-SKF, and Sham R-Saline treatment groups) (Fig.4-1F). On the other hand, a single dose of SKF-38393 administered to neonate-lesioned rats caused no significant change in mPFC MAP2 immunostaining compared to saline-treated rats ($p > 0.05$) (Fig. 4-1F).

Relative to mPFC, dopaminergic innervation in the visual cortex (VC) is relatively low (Descarries et al., 1987). MAP2-stained dendritic profiles in VC were long and relatively straight and exhibited well-delineated bundling in all groups (supplemental Figs. 4-1SB and 4-2SA). In contrast to mPFC, surface area fraction of apical dendrites in VC did not differ among any of the treatment groups at the time points examined (day 7 after treatment, *ANOVA*: $F_{(4,16)} = 1.469$, $p = 0.2578$; day 21 after treatment, *ANOVA*: $F_{(4,16)} = 0.6690$, $p = 0.6227$). Correspondingly, phospho-ERK was not present in visual cortex after treatment with the D_1 agonist (supplemental Fig. 4-2SB). Together, these results are consistent with the hypothesis that the altered appearance of MAP2 immunostaining in mPFC of neonate-lesioned rats sensitized to a D_1 agonist is related to the presence of persistent ERK1/2 phosphorylation in this region.

Decreased expression of MAP2 protein is not involved in the altered appearance of immunostaining in D_1-sensitized mPFC

Despite the profound effects on MAP2 immunostaining, the cytoarchitecture of D_1-sensitized rat mPFC was similar to controls in Nissl-stained sections (supplemental Fig. 4-3S). This result seemed to reduce the likelihood that neurodegenerative effects were responsible for the decrease in visible MAP2. We thus considered whether MAP2 protein expression might be diminished, either by reduced transcription/translation or by calpain-mediated proteolysis (Buddle et al., 2003). Alternatively, the dendrites might have undergone extensive pruning, with subsequent depletion of MAP2 due to significant loss of dendritic elaboration. Immunoblotting of mPFC homogenates with anti-MAP2 identified a high molecular weight protein as MAP2A/B with the characteristic, broad band or closely associated doublet of approximately 300kD (Fig. 4-2*A*). Fainter bands of increased electrophoretic mobility were presumably MAP2 degradation products (Quinlan and Halpain 1996a). Similar intensities of the 300kD and lighter bands appeared across lanes containing samples from each of the neonate- and sham-lesioned groups treated with SKF-38393 or saline. Quantitative analysis revealed that the MAP2 immunoreactive band intensities were not significantly different among these groups (Fig. 4-2*B*, $p > 0.05$). These results suggest that normal expression levels of MAP2 protein are preserved in D_1-sensitized rat mPFC. They furthermore make improbable the conclusion that the depleted appearance of MAP2 was brought about by proteolysis or extensive dendritic retraction, and thus a qualitative, rather than quantitative adaptation to D_1 sensitization seems likely.

AAV-GFP transduction of mPFC neurons reveals abnormal morphology of apical dendrites in mPFC of D_1-sensitized rats

To further explore qualitatively the nature of the MAP2 changes in D_1-sensitized rat mPFC, a recombinant AAV vector with GFP as the transgene was microinjected bilaterally for visualization of the neurons and their processes. Overlapping patterns of MAP2-stained profiles and GFP-labeled dendrites were observed using double-label fluorescence for expressed GFP and MAP2 immunohistochemical staining (Fig. 4-3). By adjusting the focal plane of the microscope, the soluble, cytosolic GFP and MAP2 immunoreactive staining could be observed along the length of dendrites in mPFC sections from all groups. This colocalization thus suggests that MAP2 is not redistributed into specific dendritic domains, as has been described in synaptically stimulated hippocampal laminae (Steward and Halpain, 1999), but remains dispersed along the entire dendritic shaft. Rather, the meandering course of thinner- and thicker-appearing apical dendritic segments gives the perception of shortened dendrites with MAP2 immunohistochemistry and light microscopy (Fig. 4-3).

GFP-expressing neurons were assessed qualitatively in detail using confocal images of single 1 μm optical sections, and images reconstructed from stacks of approximately 30 optical sections. Apical dendrites of sham controls were relatively straight and thick and were present in distinct bundles (Fig. 4-4*A*). These dendrites typically extended to the marginal zone and could be traced from the soma to pial surface in single optical sections or stacked projections, indicative of outgrowth in a straight path (Fig. 4-4*A.a*, *A.b*, *A.c*). This was not the case with the apical dendrites observed in sections prepared from D_1-sensitized rats (Fig. 4-4*B*). The dendrites of these animals also

reached the marginal zone, but could only be followed from the soma to the pial surface

in stacked projections (i.e., by focusing through several different focal planes) (Fig. 4-

4$B.a$, $B.b$, $B.c$). These dendrites were not only wavier, but dendritic length measurements

indicated that they were also approximately 25% longer in D_1-sensitized mPFC than in

controls (Table 4-1), despite no change in laminar thickness (Nissl stain, *ANOVA*: $F_{(3,12)}$

= 1.206, p = 0.3494; p > 0.05 compared with *Sham R-Saline* group with Fisher's PLSD

test). Finally, consistent with the MAP2 immunohistochemical results, apical shafts of

GFP-expressing dendrites displayed smaller, infrequent bundles in D_1-sensitized mPFC.

The waviness and loss of bundling were most readily apparent in dendrites extending

from deeper layers to layer I, although these aspects could be visualized in layer II/III

neurons when AAV-GFP microinjections were centered closer to this layer (not shown).

These data indicate that despite the appearance of short discontinuous segments of MAP2

immunostained apical dendrites in mPFC of D_1-sensitized animals, the dendrites actually

plunged into and out of the plane of the tissue section in a tortuous fashion. A similar

dendritic phenomenon has been described in mPFC of D_1 receptor knockout mice

(Stanwood et al., 2005) and following prenatal cocaine exposure in rodents (Jones et al.,

1996, 2000; Stanwood et al., 2001a,b).

Inhibition of ERK1/2 phosphorylation prevents the development of morphological

dendritic changes in mPFC of rats sensitized to a D_1 agonist

While an established role for ERK1/2 in neuronal plasticity is evolving rapidly,

the influence of ERK activity on dendritic architecture has been appreciated only recently

(reviewed by Miller and Kaplan, 2003). MAP2 is a widely recognized substrate for

phosphorylation by ERK1/2, and this modification regulates MAP2 interaction with the cytoskeleton (Sanchez et al., 2000). To determine whether sustained activation of ERK1/2 is involved in the altered morphology of dendrites in D_1-sensitized mPFC, we utilized two structurally and mechanistically dissimilar inhibitors of MEK1/2, the upstream kinase activator of ERK1/2. In neonate-lesioned rats infused with either PD98059 or SL327 prior to each sensitizing dose of D_1 agonist, phospho-ERK1/2-positive cell counts were similar to background when observed on day 7 following the final treatment (Fig. 4-5*A, C, D*) (p > 0.05 compared with *R-Saline*). Consistent with our previous results (Papadeas et al., 2004), D_1-sensitized rats pretreated with vehicle demonstrated robust ERK phosphorylation at this time point (Fig. 4-5*A, B*). On the other hand, when MEK inhibitors were infused prior only to the final dose of agonist, inhibition of phospho-ERK1/2 immunostaining was incomplete (Fig. 4-5*A*). No differences in phospho-ERK1/2 were found in visual cortex among treatment groups (*ANOVA*: $F_{(11,36)} = 0.4340$, p = 0.9299).

We next examined the effect of MEK1/2 inhibitor pretreatment on MAP2 immunostaining in sections adjacent to those stained for ERK1/2. ICV infusions with either PD98059 or SL327 prior to each weekly D_1 agonist injection in neonate-lesioned rats inhibited the alterations in dendritic immunostaining of MAP2 in mPFC (Figure 4-6*A, B, C;* see also cannula placement, supplemental Fig. 4-1S*C*). Quantification of the MAP2-stained dendritic profiles showed that preinfusions of MEK1/2 inhibitors prevented the change in area fraction of apical dendrites in D_1-sensitized rats (p < 0.0001 for both Lesioned R-PDSKF and Lesioned R-SLSKF groups compared with Lesioned R-SKF) (Fig. 4-6*E*). Interestingly, incomplete recovery of normal dendritic bundling and

length were observed when a single infusion of PD98059 or SL327 was administered only prior to the final dose of SKF-38393 (Fig. 4-6*D*), consistent with the partial inhibition of phospho-ERK in the same animals (Fig. 4-5*A*). The decrease in surface area fraction of dendritic MAP2 in rats challenged with one dose of MEK inhibitor was half that of D_1-sensitized animals receiving no inhibitor treatment (*Lesioned R-SKF, PDSKF challenge*, approximately 20% decrease from *Sham R-SKF* control *vs. Lesioned R-SKF*, 40% decrease from *Sham R-SKF* control; $p < 0.001$; Fig. 4-6*E*). Infusion of PD98059 alone had no effect on MAP2-stained dendritic profiles (Fig. 4-6*E*) and area fraction was not altered in visual cortex following ICV infusion with either PD98059 or SL327 (*ANOVA*: $F_{(12,41)} = 0.7420$, $p = 0.7035$).

In a separate group of animals, GFP-positive mPFC neurons were examined for the effect of MEK1/2 inhibitor pretreatment on apical dendritic architecture. Similar to our results with MAP2 immunostaining, systemic administration of SL327 prior to each dose of SKF-38393 prevented the loss of bundling and tortuous course of dendrites in mPFC of D_1-sensitized rats (Fig. 4-7). In addition, SL327 blocked the lengthening of dendritic processes seen in these animals ($p > 0.05$ for Lesioned R-SL327 compared with Sham R-SKF group) (Table 4-1).

D.   Discussion

The results presented here demonstrate *in vivo* that mature dendrite morphology in mPFC may be modified by the degree of ERK1/2 activation, a finding that strengthens recent in vitro studies proposing a role for ERK in regulation of dendritic structure and plasticity (reviewed by Sanchez et al., 2000, Miller and Kaplan, 2003, Chen and Ghosh,

112

2005). Apical dendrite remodeling in pyramidal neurons of mPFC coincided with persistent ERK1/2 phosphorylation after rats lesioned as neonates with 6-OHDA were behaviorally sensitized to D_1 agonists. The lengthening, waviness and decreased bundling of affected dendrites in these animals were reflected immunohistochemically as sparse short and bent profiles with an antibody to the somatodendritic marker MAP2. Finally, the robust dendritic alterations found in D_1-sensitized mPFC persisted for at least 21 days after the final agonist treatment and were not found in the phospho-ERK-negative and relatively D_1 receptor-deficient visual cortex. Together, these results suggest that a long-lasting and regionally specific structural adaptation occurred because of the repeated SKF-38393 exposure.

Subcellular fractionation and immunocytochemistry have revealed that a considerable portion of cellular ERK associates with the cytoskeleton (Fiore et al., 1993; Reszka et al., 1995). Furthermore, in primary neuronal cultures and tissue slices ERK1/2 mediates changes in dendrite structure that are dependent upon neuronal activity (Quinlan and Halpain, 1996b; Wu et al., 2001; Vaillant et al., 2002), neurotrophins (Miller and Kaplan, 2003) and extracellular matrix and adhesion proteins (Mantych and Ferreira, 2001; Karasewski and Ferreira, 2002). Both increased phosphorylation of cytoskeletal proteins by ERK1/2 (Holzer et al., 2001), and enhanced dendritic length and complexity (Alpar et al., 2003) are characteristics found in cortical pyramidal neurons of transgenic mice expressing a constitutively active form of the upstream MEK/ERK activator p21H-ras. Among the cytoskeletal proteins phosphorylated by activated ERK1/2, MAP2 binds to and stabilizes microtubule bundles (Sanchez et al., 2000). Phosphorylation of MAP2 by ERK1/2, CaMKII and other kinases decreases its affinity for microtubules, thus

113

altering microtubule stability and increasing neural plasticity (Quinlan and Halpain, 1996a,b; Redmond et al., 2002). Together, these studies provide significant evidence supporting a role for ERK1/2 in the modulation of dendrite morphology. Although our data do not allow us to conclude that the specific phospho-ERK1/2-positive cells that were identified immunohistochemically in mPFC drive directly the modifications in MAP2 and dendritic morphology, the disruption of these modifications by MEK inhibitors strongly suggests that ERK is by some means involved in their genesis.

Calculating the surface area fraction of MAP2 immunostaining disclosed a significant reduction of dendritic MAP2 in mPFC of D_1-sensitized *vs.* control rats, whereas immunoblotting suggested that total MAP2 protein did not differ across groups. These seemingly conflicting results were resolved by virally transducing mPFC neurons with GFP. These experiments revealed an undulating pattern of pyramidal apical dendrites in D_1-sensitized mPFC, which we have subsequently confirmed using Golgi-Cox histochemical staining (unpublished observations). By confocal reconstruction of GFP-labeled dendrites, we illustrated that this waviness likely contributed to the MAP2 immunohistochemical appearance of short dendritic segments when viewed within a single microscopic plane, and to the reduction in surface area fraction of D_1-sensitized mPFC dendrites. Whether multi-dimensional effects account for the difference in area fraction in its entirety, however, is unclear. For example, some of the apparent loss might be related to the phospho-ERK1/2-dependent disassembly of MAP2-microtubule bundled complexes described above. Consequently, either dispersion of MAP2 monomers within the neurons, or altered availability of specific epitopes *in situ* could account for the apparent loss of MAP2 immunostaining selectively in tissue sections but not with

114

immunoblotting. Studies underway are investigating the phosphorylation state of MAP2 at extended time points following D_1 sensitization, and investigating additional kinase and phosphatase pathways that may bring about these modifications.

Although the involvement of ERK1/2 in neuronal injury (Stanciu et al., 2000; Pei et al., 2002; Chu et al., 2004) and neuroprotection (Kaplan and Miller, 2000; Troadec et al., 2002; Zhu et al., 2005) is widely appreciated, we hypothesize that the structural modifications observed herein may be more closely reflective of a reversible, perhaps even beneficial adaptation to an altered signaling environment in the mPFC than to pathological indications of toxicity. For example, the apical dendritic alterations persist for at least 21 days, yet overt changes in the spontaneous behavior of D_1 sensitized rats are absent over time except for a heightened locomotor sensitivity to D_1 agonist challenge (Breese et al., 1985b). In addition, the morphological effects were significantly ameliorated by a single dose of a MEK inhibitor administered at the end of the dosing sequence. The latter finding suggests that continuous MEK1/2 activity may be required to maintain the condition over time, consistent with our observation that MEK-driven phosphorylation of ERK is also sustained in mPFC. Stable changes in cellular signaling and the maintenance of constant MAP2 protein levels imply that the neurons retain at least the ability to synthesize proteins and orchestrate signaling processes. As further support for the idea that neurodegenerative changes are minimal, we note elongated, rather than retracted apical dendrites, absence of dendritic swelling or beading, and no changes in laminar thickness or cellular architecture in Nissl-stained sections. In addition, histological and immunochemical analyses of Fluoro-Jade neurodegenerative marker (Schmued and Hopkins, 2000), phospho-JNK, p38-MAPK, JunD, glial fibrillary acidic

protein (GFAP) and Bcl-2 were negative in mPFC of D_1-senstized animals (unpublished observations).

Our results show that non-specific effects on JNK phosphorylation are absent with SL327 administered in vivo, corroborating previous studies showing that PD98059, SL327 and its structural analog, U0126 are selective inhibitors of MEK1/2 (Alessi et al., 1995; Seger and Krebs, 1995; Favata et al., 1998; Blum et al., 1999; Davies et al., 2000; Valjent et al., 2000; Pearson et al., 2001; Kohno and Pouyssegur, 2003). Furthermore, we employed two structurally dissimilar MEK inhibitors with distinct mechanisms of action (Davies et al., 2000), lessening the possibility that the two inhibitors would have similar nonspecific effects. Nonetheless, it was recently reported that PD98059 prevents activation of ERK5, a related MAPK family member (Kamakura et al., 1999). Since there is negligible expression of ERK5 in adult rat brain however (Liu et al., 2003), neither ERK5 nor JNK are likely to mediate the dendritic effects observed.

The wavy, disorganized character of mPFC pyramidal apical dendrites in D_1-sensitized rats bears a remarkable morphological similarity to lengthening and tortuous dendritic alterations described by the Levitt group in the frontal cortices of D_1 receptor knockout mice and animals exposed prenatally to cocaine (Jones et al., 1996, 2000; Murphy et al., 1997; Stanwood et al., 2001a, b; Lloyd et al., 2003). In these developmental models of dopaminergic system dysfunction, the anomalous morphology appears to develop endogenously from birth, rather than arise from drug exposure during adulthood as found in the present study. In other studies, D_1 receptor stimulation has been linked to decreased MAP2 phosphorylation, spontaneous neurite outgrowth, and dendrite length and branching (Lankford et al., 1988; Todd, 1992; Spencer et al., 1996; Reinoso et

al., 1996, Song et al., 2002), although there are some exceptions (Schmidt et al., 1996). In agreement with these findings, evidence from the prenatally cocaine-exposed and D_1 receptor-null animals suggests that reduced D_1 receptor coupling to $G\alpha s$ mediates the observed dendritic structural effects (Wang, et al., 1995a; Jones et al., 2000). Together, these data would seem to support the notion that insufficient signaling through D_1 receptors is responsible for the lengthening and waviness of mPFC apical dendrites.

Superficially, our observations in the D_1-sensitized rat model, in which repeated D_1 agonist treatments induce similar morphological changes, would seem to conflict with such a mechanism. Why would these animals, made dopamine-deficient from PND3, develop effects similar to those found in D_1 receptor insufficiency only upon repeated dosing with a D_1 agonist? Part of the answer may lie in the fact that the agonist treatment is intermittent (i.e., weekly), whereas throughout postnatal development and during the periods in between doses, D_1 receptor stimulation in mPFC presumably is precluded because dopaminergic afferents have been lesioned. It is likely to be during these intervening periods between doses that adaptive changes in other neurotransmitter receptor systems (e.g., glutamate, GABA, serotonin), neurotrophic factors, and intracellular signaling pathways occur that profoundly influence the structural outcome.

Unlike the signs of Parkinsonism that develop in animals lesioned with 6-OHDA as adults, neonate-lesioned rats exhibit normal spontaneous motor behavior in adulthood, suggesting that neuroadaptive changes compensate for the early loss of dopamine (Breese et al., 2005). Repeated D_1 agonist dosing to neonate-lesioned rats may induce additional changes to a system already delicately counterbalancing the loss of D_1 stimulation, thus resulting in malfunction of the compensatory system. The alterations in dendritic

morphology observed in the present study may serve to dampen these malfunctioning signals, providing a protective, beneficial effect. Alternatively, the changes may merely reflect reduced or excessive levels of critical neuronal signals. In any case, the periods of adaptation that occur between agonist exposures in neonate-lesioned rats are perhaps when a radically altered signaling environment in mPFC provides the force that drives these changes in dendritic morphology, with the loss of D_1 receptor activity assuming a facilitating role.
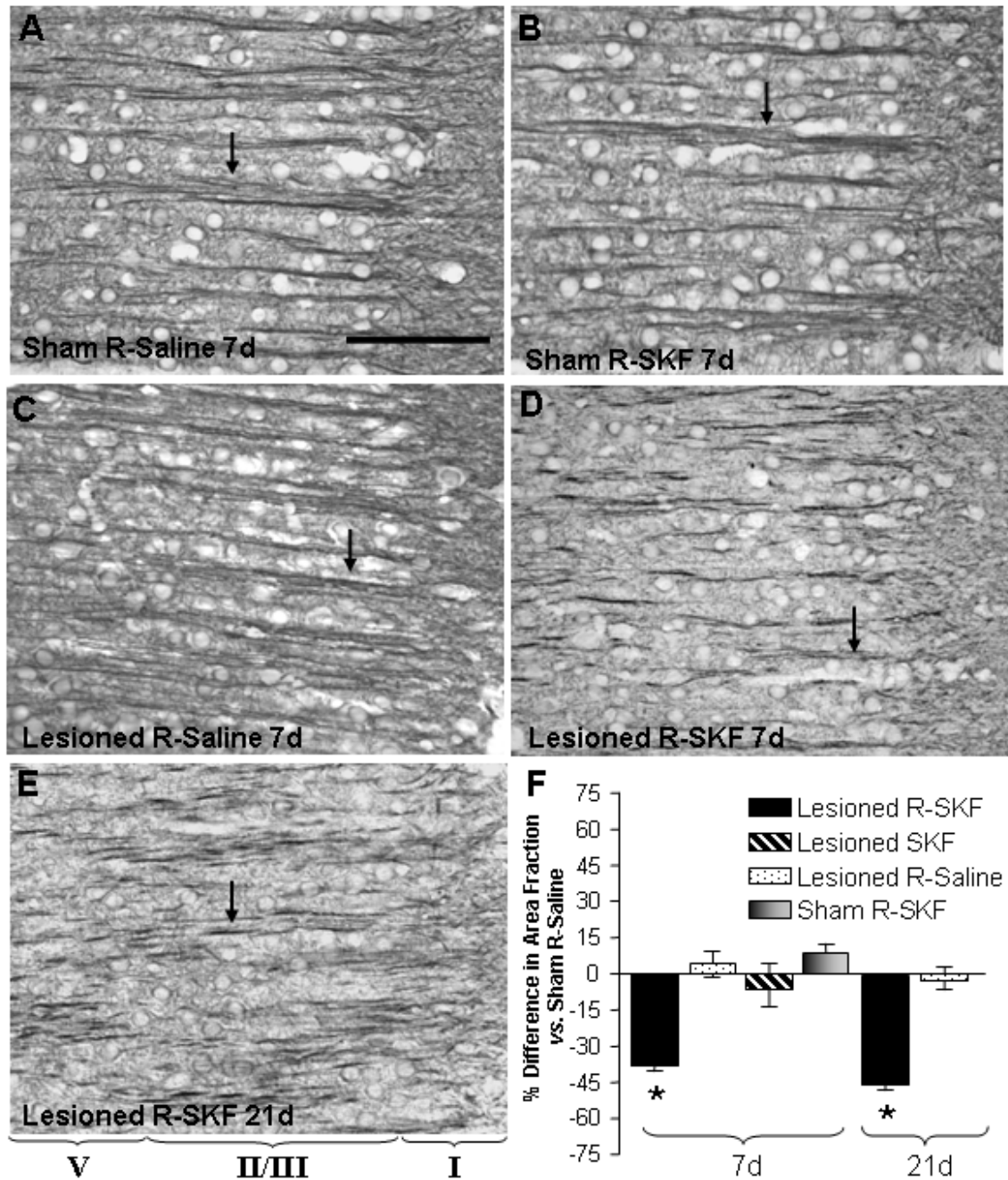
Fig. 4-1: Repeated administration of SKF-38393 to neonate-lesioned rats produces long-lasting alterations in the appearance of MAP2 immunoreactivity in mPFC relative to controls. *A-E*, Representative high magnification (400×) photomicrographs of MAP2 immunoreactivity in the mPFC of neonate-lesioned (*Lesioned*) or sham-lesioned

119

(*Sham*) rats administered repeated injections of either saline (*R-Saline*) or SKF-38393 (*R-SKF*) and euthanized at day 7 (*7d*) or day 21 (*21d*) after the final injection. Roman numerals (*I, II/III*, and *V*) underneath *E* represent approximate laminar boundaries for all five photomicrographs. *Black arrows* identify MAP2-stained apical dendrites. Scale bar, 100 μm. *F*, Graph depicting the average percent difference ±SEM of MAP2 dendritic area fraction (compared to *Sham R-Saline* group) in rats euthanized at days 7 or 21 after the final agonist treatment (*Lesioned SKF*, neonate-lesioned rats administered a single dose of SKF-38393). *ANOVA*, 7d after treatment: $F(4,16) = 10.936$, $p = 0.0002$; *ANOVA*, 21d after treatment: $F(2,17) = 18.409$, $p < 0.0001$. *$p < 0.05$ compared with saline-injected sham rats with Fisher's PLSD test.
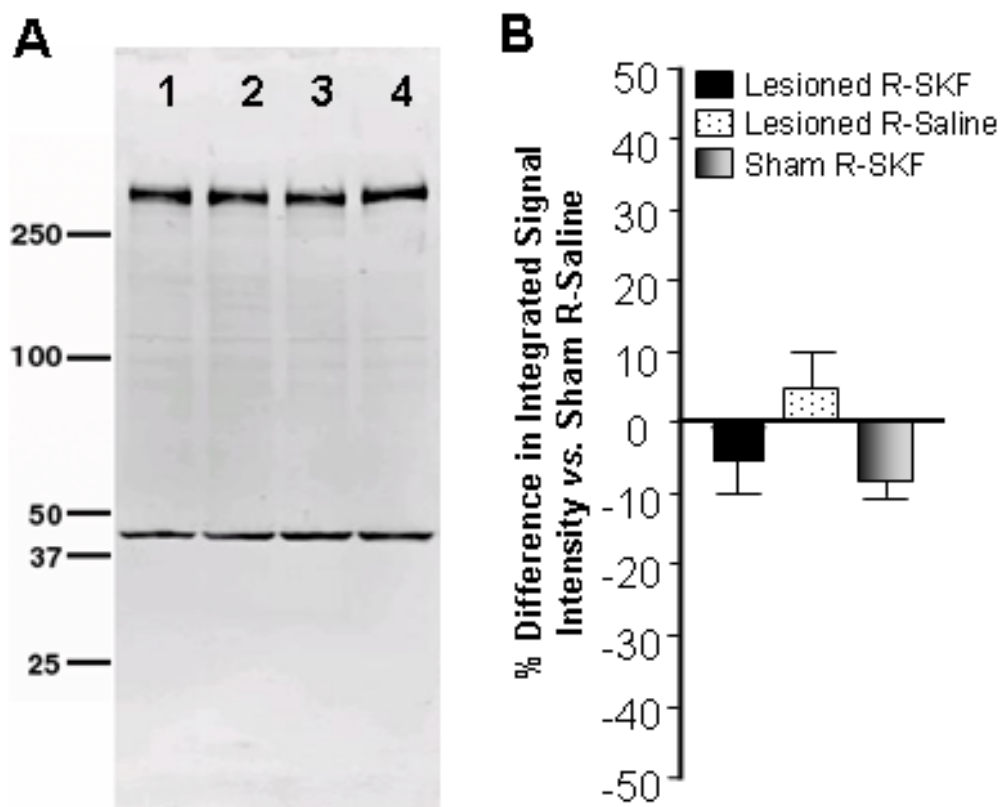
Fig. 4-2: MAP2 total protein levels in mPFC homogenates from D$_1$ sensitized rats are not significantly different from controls. *A,* Immunoblot of MAP2A/B (upper band) and β-actin (lower band) 7d after the final agonist or saline treatment: *Lane 1*, Sham R-Saline; *Lane 2*, Lesioned R-SKF; *Lane 3*, Lesioned R-Saline; *Lane 4*, Sham R-SKF. Treatment groups abbreviated as described in legend, Fig. 4-1. Note the small but consistent amount of MAP2 degradation product across all samples. *B,* Average integrated signal intensity measurements for MAP2 were calculated after normalization to β-actin and are represented as percent difference *vs.* Sham R-Saline. *ANOVA*: F(3,14) = 0.359, p = 0.7836.

Fig. 4-3: Double fluorescence labeling of MAP2 immunostaining and GFP in apical dendrites of D$_1$-sensitized rat mPFC. Photomicrographs are representative of neonate-lesioned rats systemically pre-treated with SL327 prior to each repeated dose of SKF-38393. Representative confocal images of *A*, GFP (green); *B*, MAP2 immunofluorescence (red); *C*, GFP + MAP2 overlay. Note that the morphological pattern of MAP2 immunolabeling is identical to that of GFP-labeled apical dendrites (yellow). mPFC layers depicted are similar to those indicated in Fig. 4-1*E*. Scale bar, 50 µm.
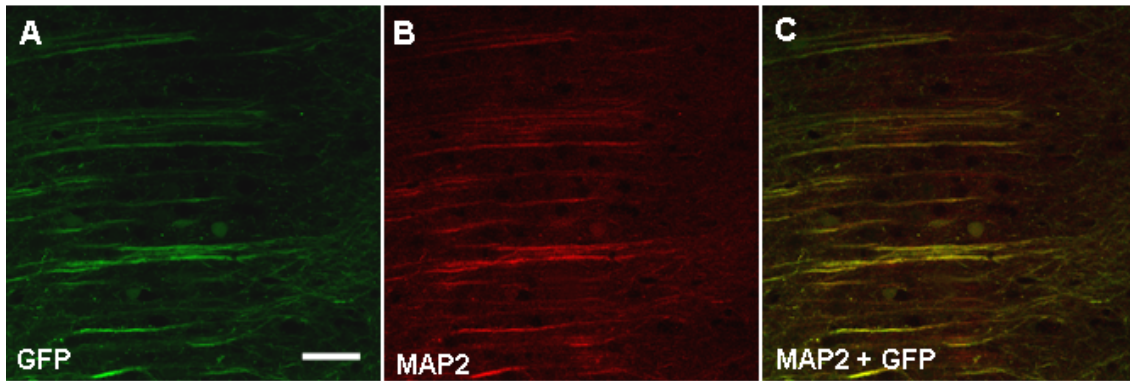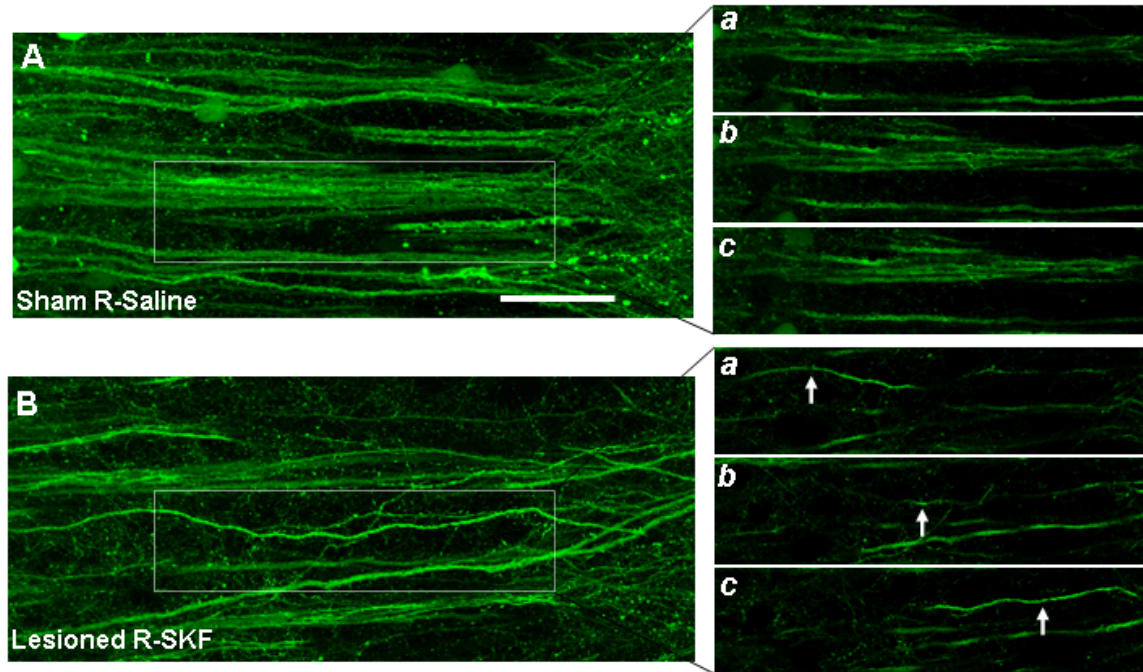
Fig. 4-4: Repeated administration of SKF-38393 to neonate-lesioned rats produces long-lasting alterations in apical dendrites of mPFC. *A*, *B*, Representative projected images of GFP-labeled dendrites in mPFC of *A*, Sham R-Saline and *B*, Lesioned R-SKF rats. *Lowercase letters*, serial 1 µm optical sections representing those used to reconstruct the corresponding projection (spanning 30 µm) on the left. Note that whereas GFP-labeled dendrites in *Sham R-Saline* mPFC are visible across nearly the entire length of *A.a*, *A.b* and *A.c*, the *Lesioned R-SKF* apical dendrite indicated by *white arrows* in *B.a*, *B.b* and *B.c* appears alternately to descend into and emerge from the optical section. Scale bar, 50 µm.
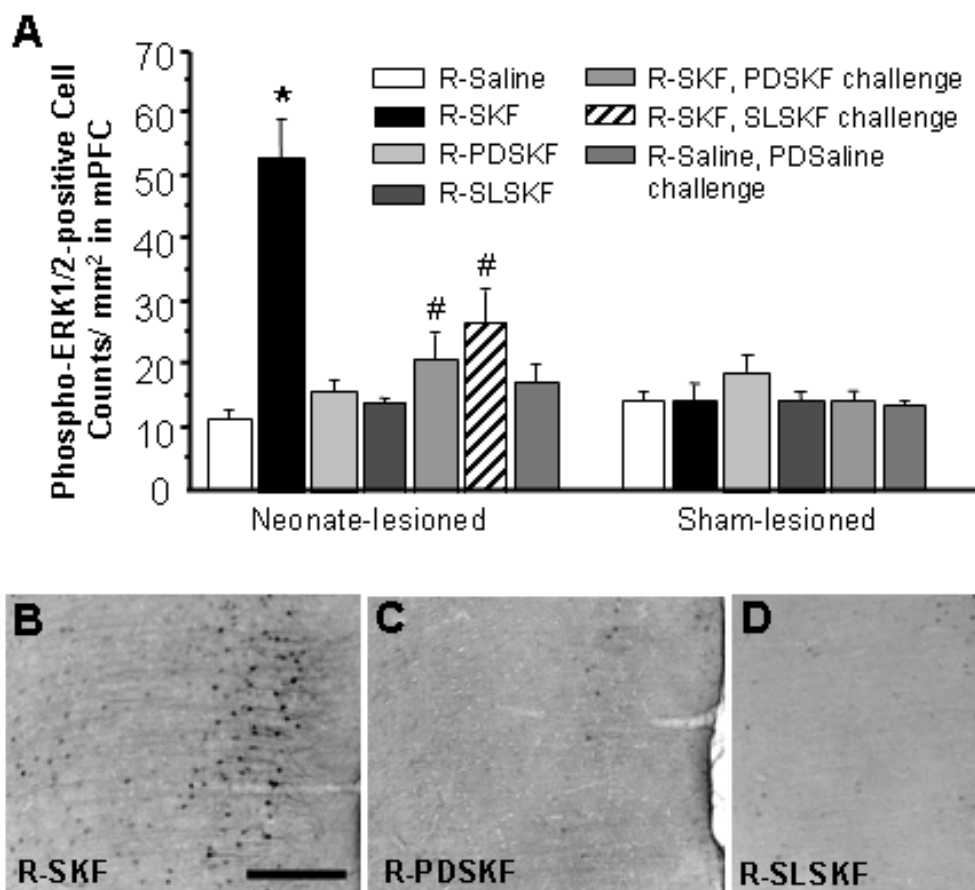
Fig. 4-5: **Pretreatment with the MEK1/2 inhibitors PD98059 and SL327 prevents sustained ERK1/2 phosphorylation in mPFC of neonate-lesioned rats administered repeated SKF-38393 treatments**. *A*, Graphic representation of phospho-ERK1/2-positive cell counts in neonate-lesioned and sham-lesioned rat mPFC. ICV infusions of vehicle (*R-Saline*; *R-SKF*) or MEK inhibitor (*R-PDSKF*; *R-SLSLKF)* were administered 30 min prior to systemic saline or SKF-38393 for 4 consecutive weeks and were euthanized 7 days later. Separate groups of rats received preinfusions of vehicle prior to SKF-38393 or saline for the first 3 doses, followed by a challenge dose of either PD98059 or SL327 prior to SKF-38393 (*R-SKF, PDSKF challenge*; *R-SKF, SLSKF challenge*) or saline (*R-Saline, PDSaline challenge*) on week 4, then euthanized 7 days

124

later. * p < 0.05 compared with Sham R-Saline group, # p < 0.05 compared with Lesioned R-SKF and Sham R-Saline groups with Fisher's PLSD. *ANOVA*: $F(12,41) = 10.589$, $p < 0.0001$. *B-D*, Representative low magnification (100×) photomicrographs of phospho-ERK1/2 immunoreactive cells in *R-SKF* (*B*), *R-PDSKF* (*C*), and *R-SLSKF* (*D*) neonate-lesioned rat groups. Scale bar, 200 µm.
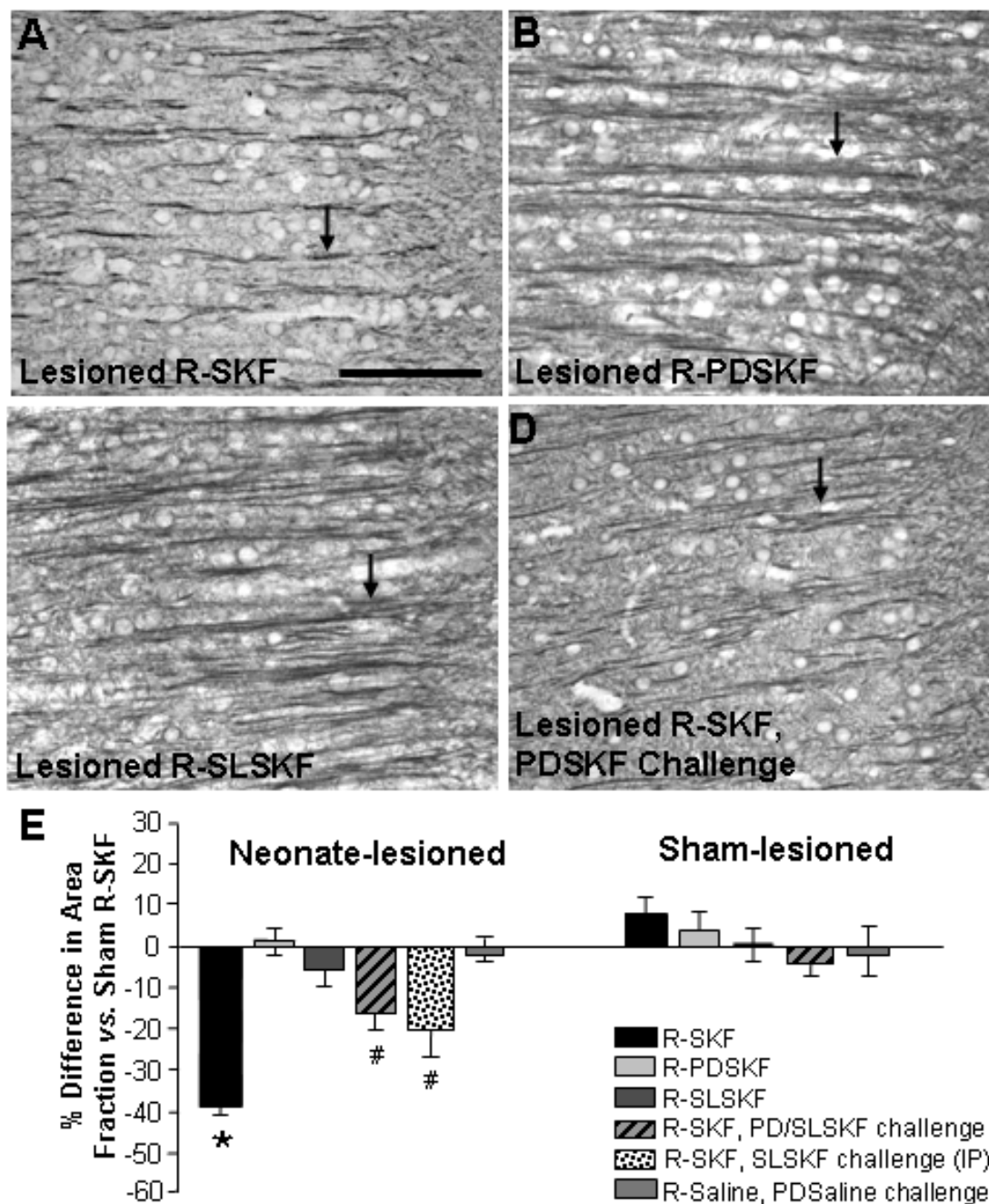
Fig. 4-6: Pretreatment with PD98059 or SL327 prior to SKF-38393 prevents long-lasting alterations in the morphology of MAP2 immunoreactive apical dendrites. *A-C*, Representative high magnification (400×) images of MAP2 immunoreactivity in neonate-lesioned rats infused with vehicle (*Lesioned R-SKF*) or MEK inhibitor (*Lesioned*

R-PDSKF; *Lesioned R-SLSKF*) prior to each repeated systemic SKF-38393 injection. *D*, A single preinfusion of PD98059 prior to the fourth, final dose of SKF-38393 (*Lesioned R-SKF, PDSKF challenge*) results in limited MAP2 immunoreactive changes (compare *D* to *A*). *Black arrows* indicate MAP2-stained apical dendrites. Scale bar, 100 μm. *E*, Mean percent difference ±SEM of dendritic MAP2 surface area fraction in various treatment groups compared to *Sham R-SKF*. Data from animals receiving ICV PD98059 or ICV SL327 on the fourth, final dose (*R-SKF, PD/SLSKF challenge*; *grey and black stripes*) were collapsed together. Note that area fraction of dendritic MAP2 from a separate group of rats challenged with systemic SL327, rather than ICV infusion (*R-SKF, SLSKF challenge (i.p.)*; *stippled*), was virtually identical to that of rats receiving ICV MEK inhibitor. All rats were euthanized 7d after the final drug treatment. *ANOVA*: $F_{(12,41)} = 6.729$, $p < 0.0001$. * $p < 0.05$ compared with Sham R-Sal. # $p < 0.05$ compared with Lesioned R-SKF and Sham R-Sal groups with Fisher's PLSD.
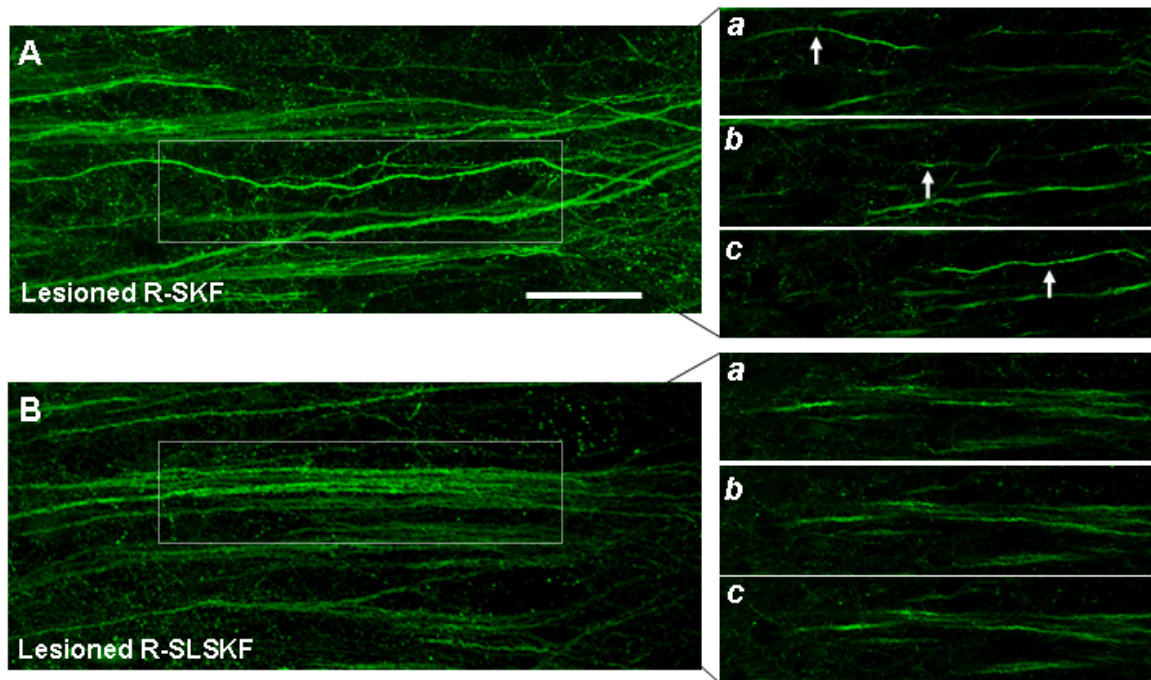
Figure 4-7: SL327 prevents long-lasting alterations in the morphology of apical dendrites in mPFC of neonate-lesioned rats administered repeated doses of SKF-38393. *A, B*, Projected images of GFP-labeled apical dendrites after mPFC infection with AAV-GFP in *A*, neonate-lesioned rats repeatedly treated with SKF-38393 (*Lesioned R-SKF*), and *B*, a neonate-lesioned rats pre-treated with systemic (i.p.) injections of SL327 prior to each SKF-38393 treatment (*Lesioned R-SLSKF*). *Lowercase letters*, serial 1 μm optical sections representing those used to reconstruct the 30 μm spanning projection on the left. *White arrows* in *A.a*, *A.b* and *A.c* indicate a single apical dendrite. Note that loss of bundling and increased waviness of apical dendrites typical of Lesioned R-SKF mPFC is prevented in Lesioned R-SLSKF mPFC. Scale bar, 50 μm.
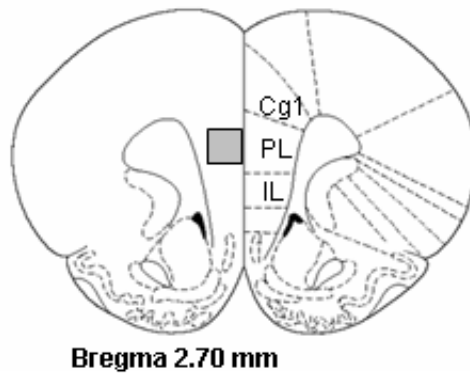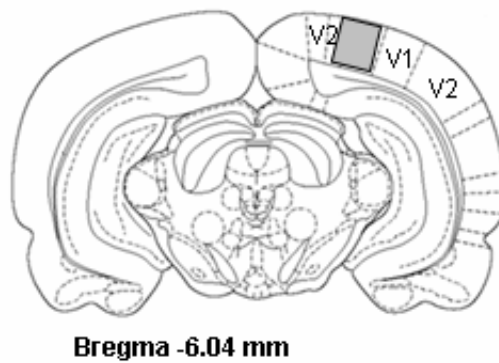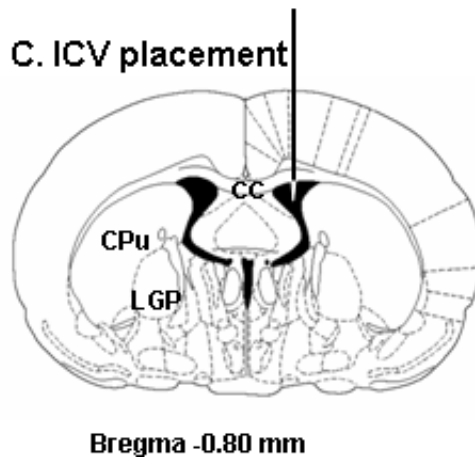
Fig. 4-1S: Schematic diagrams of regions of interest adapted from Paxinos and Watson (1998). *A*, Area of medial prefrontal (prelimbic) cortex depicted in photomicrograps and the site of AAV-GFP infusion; *B*, Visual cortex depicted in photomicrographs; and *C*, Placement of intracerebroventricular cannulae.
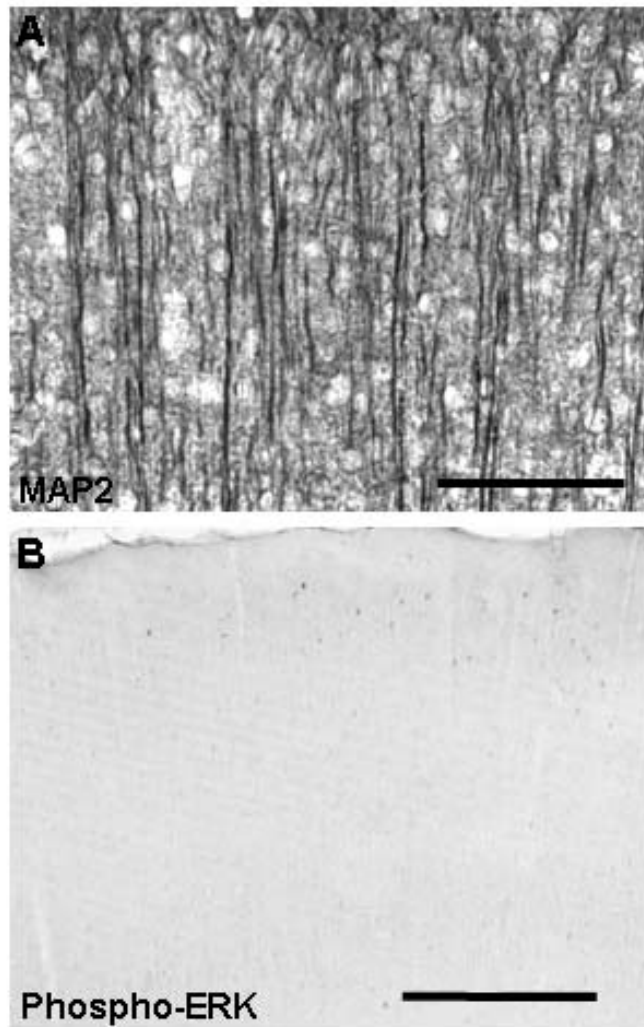
Fig. 4-2S: Repeated administration of SKF-38393 to neonate-lesioned rats has no effect on MAP2 or phospho-ERK1/2 immunoreactivity in the visual cortex. Representative *A*, high magnification (400×) photomicrograph of MAP2 immunoreactive dendrites (scale bar, 100 µm) and *B*, low magnification (100×) photomicrograph of phospho-ERK1/2 immuno-positive cells (scale bar, 200 µm) at day 7 after repeated SKF-38393 treatment to neonate-lesioned rats.
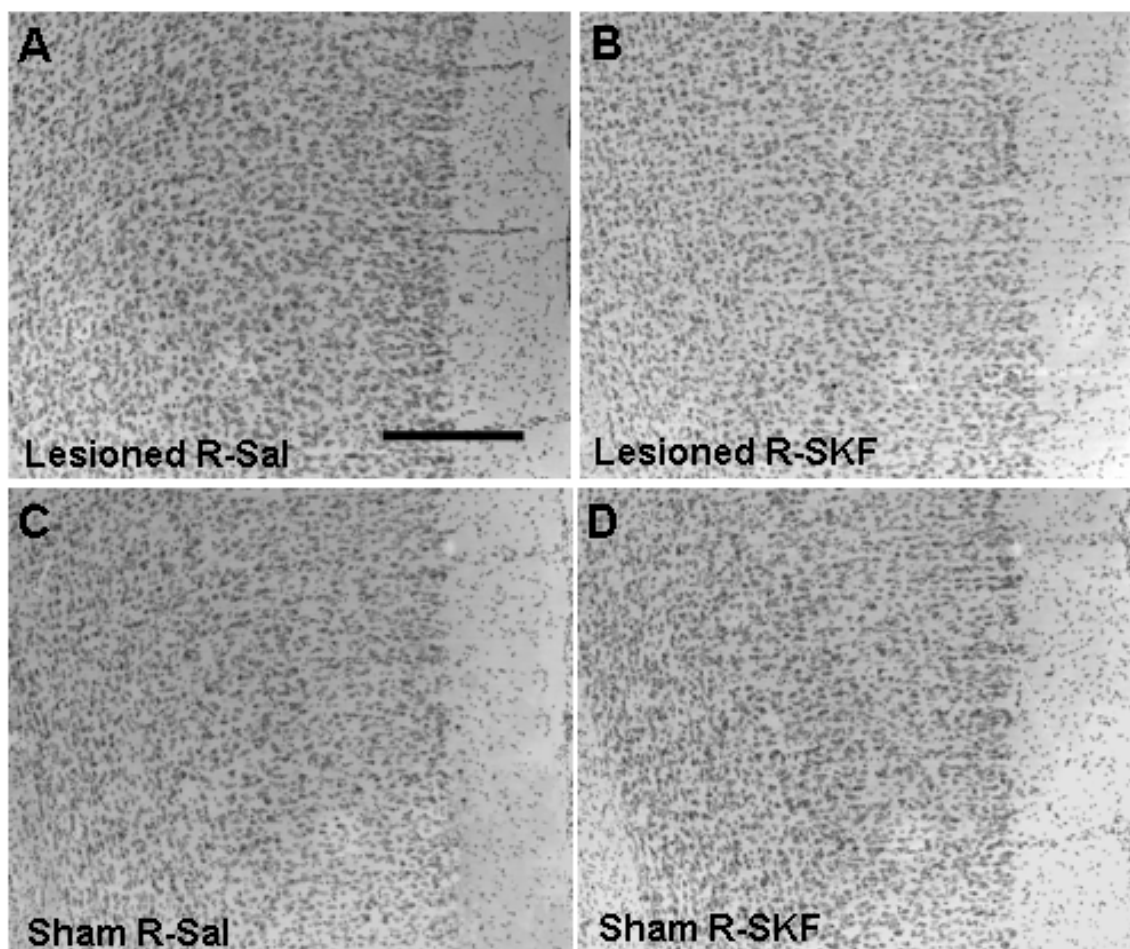
Fig. 4-3S: **Repeated administration of SKF-38393 to neonate- or sham-lesioned rats does not alter cytoarchitecture in the mPFC**. *A-D*, representative low magnification (100X) photomicrographs of Nissl-stained sections of a *A*, neonate-lesioned rat dosed repeatedly with saline, *Lesioned R-Saline*; *B*, neonate-lesioned rat dosed repeatedly with SKF-38393 (D_1-sensitized), *Lesioned R-SKF*; *C*, sham-lesioned rat dosed repeatedly with saline, *Sham R-Saline*; *D*, sham-lesioned rat dosed repeatedly with SKF-38393, *Sham R-SKF*. Scale bar, 30 μm.

Table 4-1: SL327 prevents increased dendritic length in mPFC of neonate-lesioned rats administered repeated doses of SKF-38393

RAT TREATMENT GROUP[¶]	AVERAGE DENDRITIC LENGTH (μm)[‡]
Lesioned R-SKF	206.506 ± 8.539*
Lesioned R-SLSKF	164.667 ± 4.926
Sham R-SKF	165.492 ± 5.810

ANOVA F-test of model fit: $F_{(2,11)} = 9.309$, p = 0.0043

[¶]Corresponding treatment groups are as follows: *Lesioned R-SKF*, neonate-lesioned rats administered repeated weekly doses of SKF-38393; *Lesioned R-SLSKF*, neonate-lesioned rats pretreated with SL327 prior to each weekly repeated dose of SKF-38393; *Sham R-SKF*, sham-lesioned rats administered repeated weekly doses SKF-38393.

[‡]Data are presented as mean ± SEM

*p < 0.05 compared with *Sham R-SKF* using Fisher's PLSD test

CHAPTER V.   CONCLUSIONS

A.   Summary of Major Findings

The goal of this dissertation was to determine whether the activation of ERK, a well known regulator of gene expression, occurs as a result of repeated D_1 receptor stimulation in neonate-lesioned rats, and to establish whether active ERK plays a role in behavioral priming and structural plasticity in these animals. To further knowledge of the ERK pathway and its role in D_1 receptor-mediated behavioral and structural adaptations in our model, three research objectives were formulated. First, to examine the phosphorylated (active) form of ERK after both single and repeated (i.e., sensitizing) doses of the partial D_1 receptor agonist SKF-38393 to neonate-lesioned rats; Second, to show the involvement of active ERK in the sensitization, or priming, of various motor behaviors characteristic of neonate-lesioned rats administered repeated D_1 agonist treatment; and Third, to determine if changes in dendritic morphology occur with priming and whether ERK plays a role in the changes. The findings based upon these objectives are summarized below.

Examination of Phosphorylated ERK

Using immunohistochemical techniques, a prolonged increase in phospho-ERK that accumulated primarily in layers II-III of the mPFC was found, where it declined gradually yet remained significantly elevated for at least 36 d after repeated SKF-38393

treatment to neonate-lesioned rats. A sustained (≥7 d) increase in phospho-ERK was observed for shorter periods in various other cortical regions, i.e., VLOC, CgC, MC, SSC, and PirC, but was not detectable in the striatum or nucleus accumbens. Total ERK protein levels remained unchanged in all brain regions examined. At 36 d, an additional injection of SKF-38393 to D_1-sensitized rats restored phospho-ERK to maximal levels only in the mPFC when examined 7 d later. Moreover, the phosphorylated form of transcription factor CREB, examined 7 d after the sensitizing regimen, was observed exclusively in the mPFC, where it was abundant throughout all layers. Systemic injections of SL327, an inhibitor of the upstream ERK activator MEK, attenuated both ERK and CREB phosphorylation in layers II-III of the mPFC, suggesting that the increased phospho-CREB likely represents a functional product of persistently elevated phospho-ERK in this brain region.

In addition, pretreatment with the D_1 antagonist SCH-23390 inhibited the prolonged increase in mPFC phospho-ERK, whereas the 5-HT_2 receptor antagonist ketanserin was ineffective. The NMDA receptor antagonists MK-801 and CGS-19755 also blocked the sustained increase in ERK phosphorylation. Collectively, these results demonstrate a coupling of D_1 and NMDA receptor function that is reflected by a sustained activation of the ERK signaling pathway in the mPFC of neonate-lesioned rats administered repeated SKF-38393 treatment. The long-lasting phosphorylation of ERK and CREB in the mPFC could play a pivotal role in any permanent adaptive change(s) in these animals.

Involvement of Phosphorylated ERK in Behavioral Priming

MEK inhibitors were used as a tool to show the involvement of active ERK in the priming of various motor behaviors characteristic of neonate-lesioned rats administered repeated SKF-38393 treatment. Intracerebroventricular or systemic pretreatment with SL327, and the structurally dissimilar PD98059, prior to each of three of four weekly sensitizing doses of SKF-38393 altered the character of the supersensitive motor response elicited by D_1 agonism. In particular, priming-induced horizontal behaviors (i.e., running, walking, and trotting) were augmented, while stereotyped behaviors (i.e., rearing, climbing, jumping, patting, treading, and taffy pulling) were inhibited. Intra-mPFC infusions of PD98059 prior to SKF-38393 treatments inhibited stereotyped behaviors, but did not affect horizontal behaviors. Together, these data indicate that forebrain ERK activation contributes to some but not all of the sensitized motor responses seen with D_1 agonist priming of neonate-lesioned rats, and furthermore, that mPFC ERK activation is crucial for the sensitization of specific stereotyped behaviors demonstrated by these animals.

Involvement of Phosphorylated ERK in Dendritic Alterations with Priming

Quantitative measures of dendritic processes immunoreactive for MAP2 as well as confocal rendering of pyramidal neurons locally expressing GFP by viral vector-mediated gene transfer were used to reveal dendritic remodeling in the mPFC of primed neonate-lesioned rats. Long apical dendrites of layer V neurons exhibited decreased bundling and wavy, irregular patterns as they advanced through layer II-III toward the pial surface; these modifications persisted for at least 21 days after dosing. Meanwhile, MAP2 dendritic profiles in the visual cortex were unchanged. Pretreatment with SL327

or PD98059 before the final sensitizing dose SKF-38393 resulted in diminished effects on dendritic morphology, whereas administration of these agents prior to each repeated treatment completely prevented these changes. These data reveal that dendritic remodeling emerges simultaneously with sustained ERK phosphorylation in the mPFC of rats deprived of dopamine in development and administered sensitizing doses of a D_1 agonist. Together, these findings implicate phospho-ERK in guiding dopaminergic effects on pyramidal neuron morphology, and demonstrate for the first time *in vivo* that inhibition of the ERK pathway reverses a profound structural reorganization of mature cortical dendrites.

B. Future Directions

The findings from my research have raised a number of exciting and interesting questions that can be pursued. In addition to the points mentioned in the previous chapters, the following sections provide some additional lines of future investigation:

Phosphatase Studies

In Chapter II, a persistent elevation in phospho-ERK immunoreactivity in the mPFC following repeated D_1 agonist treatment to neonate-lesioned rats was found. The persistent phosphorylation of ERK in the mPFC of D_1-sensitized rats could conceivably result from downregulation of phosphatase(s) that normally inactivate ERK, rather than plastic changes in specific receptor mechanisms. It is known that MAP kinase phosphatases (MKPs) are enriched throughout the brain (Stoker and Dutta, 1998) and play an essential role in the regulation of ERK activity. MKPs are dual specificity protein

136

phosphatases that dephosphorylate and inactivate ERK by removal of phosphate groups from both tyrosine and/or threonine residues of phosphorylated ERKs (Keyse, 1998). It is thus of interest to investigate whether MKPs are altered after neonatal 6-OHDA lesioning and whether this contributes to the persistent phosphorylation of ERK in response to repeated D_1 receptor stimulation. As an initial approach to assessing this possibility, mPFC MKP-1, -2, and -3 levels were measured and found not to differ between D_1-sensitized rats and controls (unpublished observations). This data suggested that the persistent mPFC phospho-ERK results from adaptations at the level of specific neurotransmitter receptor-signaling mechanisms. Nevertheless, because protein level, but not activity, was measured, and other phosphatases could be involved in the dephosphorylation of ERK, activity assays for MKPs should be performed in future studies along with examination of other ERK-specific phosphatases (e.g., protein phosphatase 2A) to confirm our findings.

siRNA Studies

In Chapters III and IV, MEK inhibitors SL327 and PD98059 were used to demonstrate the involvement of persistent phospho-ERK in behavioral sensitization and dendritic morphogenesis following repeated D_1 agonist treatment to neonate-lesioned rats. Because the specificity of these compounds may not be absolute, a more direct approach would involve the use of small interference RNA (siRNA) targeting ERK1 and ERK2. This technique would provide extremely important information as to whether these priming-induced phenomena are strictly dependent on long-lasting ERK activation. With regard to the behavioral studies, however, this technique could prove to be labor

intensive because ERK1/2 siRNA would have to be injected into the mPFC and a number

of other brain regions demonstrating elevated phospho-ERK.

It should also be mentioned that there are a number of caveats to the use of

siRNAs *in vivo*. For example, there are problems with the stability of siRNAs *in vivo*, for

the half-life of the knockdown effect is at best 2-4 days (Bonetta, 2004). Moreover, there

exists the possibility that the siRNAs could knock down or induce genes other than the

intended targets (Bonetta, 2004). Regardless, with the commercial availability of custom

siRNAs little effort or skill is required to test whether an siRNA is effective *in vivo*, and

thus the benefits of using ERK1/2 siRNA in our model outweigh any possible problems

of using this technique.

Further morphology studies

In Chapter IV, repeated doses of D_1 agonist to neonate-lesioned rats produced

altered morphology of apical dendrites in the mPFC, and this change was shown to

involve activation of the ERK pathway. In future studies, it will be important to extend

our observations to dendritic spines and branches, since these are the primary sites of

excitatory input and synaptic integration (for review, see Harris and Kater, 1994; Yuste

and Tank, 1996). Experiments to test this would involve the use of MEK inhibitor

followed by infusion of AAV-GFP into the mPFC, or alternatively, the use of ERK1/2

siRNA followed by rapid Golgi-Cox staining. Recent *in vitro* studies have highlighted a

necessity for ERK in stabilizing morphological changes in dendritic spines and branches

(Wu et al., 2001; Goldin and Segal, 2003), and suggest that this mechanism is relevant in

triggering long-lasting changes in neuronal circuit structure. Accordingly, persistent

ERK-dependent changes in dendritic spines and branches might disrupt normal synaptic transmission in the mPFC, impairing mPFC function and perhaps contributing to some to the long-lasting behavioral effects of repeated D_1 agonist treatment to neonate-lesioned rats. Collectively, these experiments could provide further insight into the role of ERK in the maintenance and reorganization of dendrites in our model.

C.   Final Reflections

The research that I have conducted for this dissertation has been extremely rewarding. I have explored many avenues of research and continue to gain experience in techniques for laboratory science. My findings themselves have raised several questions and future research based upon this dissertation can follow many paths. Future experiments and ideas suggested represent what I believe to be the most important based upon my research, and should provide valuable insight into neurobiological mechanisms that underlie the permanence of behavioral responses following priming of D_1 receptor function. Furthermore, results from such studies could have implications for identifying mechanisms that support the behavioral sensitization that accompanies repeated psychostimulant drug exposure, and for identifying the basis of symptoms in disorders involving dopamine dysfunction such as LNS and schizophrenia.

REFERENCES

Adams JP, Sweatt JD (2002) Molecular psychology: roles for the ERK MAP kinase cascade in memory. Annu Rev Pharmacol Toxicol 42:135-163.

Adriani W, Felici A, Sargolini F, Roullet P, Usiello A, Oliverio A, Mele A (1998) N-methyl-D-aspartate and dopamine receptor involvement in the modulation of locomotor activity and memory processes. Exp Brain Res 123:52-59.

Albin RL, Young AB, Penney JB (1989) The functional anatomy of basal ganglia disorders. Trends Neurosci 12:366-375.

Alessi DR, Cuenda A, Cohen P, Dudley DT, Saltiel AR (1995) PD 098059 is a specific inhibitor of the activation of mitogen-activated protein kinase kinase in vitro and in vivo. J Biol Chem 270:27489-27494.

Alpar A, Palm K, Schierwagen A, Arendt T, Gartner U (2003) Expression of constitutively active p21H-rasval12 in postmitotic pyramidal neurons results in increased dendritic size and complexity. J Comp Neurol 467:119-133.

Aoki C, Siekevitz P (1985) Ontogenetic changes in the cyclic adenosine 3',5'-monophosphate-stimulatable phosphorylation of cat visual cortex proteins, particularly of microtubule-associated protein 2 (MAP 2): effects of normal and dark rearing and of the exposure to light. J Neurosci 5:2465-2483.

Arvanov VL, Wang RY (1997) NMDA-induced response in pyramidal neurons of the rat medial prefrontal cortex slices consists of NMDA and non-NMDA components. Brain Res 768:361-364.

Atkins CM, Selcher JC, Petraitis JJ, Trzaskos JM, Sweatt JD (1998) The MAPK cascade is required for mammalian associative learning. Nat Neurosci 1:602-609.

Audesirk G, Cabell L, Kern M (1997) Modulation of neurite branching by protein phosphorylation in cultured rat hippocampal neurons. Brain Res Dev Brain Res 102:247-260.

Bading H, Greenberg ME (1991) Stimulation of protein tyrosine phosphorylation by NMDA receptor activation. Science 253:912-914.

Basura GJ, Walker PD (1999) Serotonin 2A receptor mRNA levels in the neonatal dopamine-depleted rat striatum remain upregulated following suppression of serotonin hyperinnervation. Brain Res Dev Brain Res 116:111-117.

Berger TW, Kaul S, Stricker EM, Zigmond MJ (1985) Hyperinnervation of the striatum

by dorsal raphe afferents after dopamine-depleting brain lesions in neonatal rats. Brain Res 336:354-358.

Berke JD, Hyman SE (2000) Addiction, dopamine, and the molecular mechanisms of memory. Neuron 25:515-532.

Bernardi MM, Scavone C, Frussa-Filho R (1986) Differential effects of single and long-term amphetamine and apomorphine administrations on locomotor activity of rats. Gen Pharmacol 17:465-468.

Bi R, Foy MR, Thompson RF, Baudry M (2003) Effects of estrogen, age, and calpain on MAP kinase and NMDA receptors in female rat brain. Neurobiol Aging 24:977-983.

Bischoff S, Heinrich M, Krauss J, Sills MA, Williams M, Vassout A (1988) Interaction of the D1 receptor antagonist SCH 23390 with the central 5-HT system: radioligand binding studies, measurements of biochemical parameters and effects on L-5-HTP syndrome. J Recept Res 8:107-120.

Bishop C, Tessmer JL, Ullrich T, Rice KC, Walker PD (2004) Serotonin 5-HT2A receptors underlie increased motor behaviors induced in dopamine-depleted rats by intrastriatal 5-HT2A/2C agonism. J Pharmacol Exp Ther 310:687-694.

Bishop C, Walker PD (2003) Combined intrastriatal dopamine D1 and serotonin 5-HT2 receptor stimulation reveals a mechanism for hyperlocomotion in 6-hydroxydopamine-lesioned rats. Neuroscience 121:649-657.

Bjorkblom B, Ostman N, Hongisto V, Komarovski V, Filen JJ, Nyman TA, Kallunki T, Courtney MJ, Coffey ET (2005) Constitutively active cytoplasmic c-Jun N-terminal kinase 1 is a dominant regulator of dendritic architecture: role of microtubule-associated protein 2 as an effector. J Neurosci 25:6350-6361.

Blanchard DC, Blanchard RJ, Carobrez Ade P, Veniegas R, Rodgers RJ, Shepherd JK (1992) MK-801 produces a reduction in anxiety-related antipredator defensiveness in male and female rats and a gender-dependent increase in locomotor behavior. Psychopharmacology (Berl) 108:352-362.

Blum S, Moore AN, Adams F, Dash PK (1999) A mitogen-activated protein kinase cascade in the CA1/CA2 subfield of the dorsal hippocampus is essential for long-term spatial memory. J Neurosci 19:3535-3544.

Bonetta L (2004) RNAi: silencing never sounded better. Nature Methods 1:79-86.

Bourtchuladze R, Frenguelli B, Blendy J, Cioffi D, Schutz G, Silva AJ (1994) Deficient long-term memory in mice with a targeted mutation of the cAMP-responsive element-binding protein. Cell 79:59-68.

Brami-Cherrier K, Valjent E, Garcia M, Pages C, Hipskind RA, Caboche J (2002) Dopamine induces a PI3-kinase-independent activation of Akt in striatal neurons: a new route to cAMP response element-binding protein phosphorylation. J Neurosci 22:8911-8921.

Breese GR, Knapp DJ, Criswell HE, Moy SS, Papadeas ST, Blake BL (2005) The neonate-6-hydroxydopamine-lesioned rat: a model for clinical neuroscience and neurobiological principles. Brain Res Brain Res Rev 48:57-73.

Breese GR, Criswell HE, Johnson KB, O'Callaghan JP, Duncan GE, Jensen KF, Simson PE, Mueller RA (1994) Neonatal destruction of dopaminergic neurons. Neurotoxicology 15:149-159.

Breese GR, Duncan GE, Napier TC, Bondy SC, Iorio LC, Mueller RA (1987) 6-hydroxydopamine treatments enhance behavioral responses to intracerebral microinjection of D1- and D2-dopamine agonists into nucleus accumbens and striatum without changing dopamine antagonist binding. J Pharmacol Exp Ther 240:167-176.

Breese GR, Baumeister A, Napier TC, Frye GD, Mueller RA (1985) Evidence that D-1 dopamine receptors contribute to the supersensitive behavioral responses induced by L-dihydroxyphenylalanine in rats treated neonatally with 6-hydroxydopamine. J Pharmacol Exp Ther 235:287-295.

Breese GR, Napier TC, Mueller RA (1985) Dopamine agonist-induced locomotor activity in rats treated with 6-hydroxydopamine at differing ages: functional supersensitivity of D-1 dopamine receptors in neonatally lesioned rats. J Pharmacol Exp Ther 234:447-455.

Breese GR, Baumeister AA, McCown TJ, Emerick SG, Frye GD, Crotty K, Mueller RA (1984) Behavioral differences between neonatal and adult 6-hydroxydopamine-treated rats to dopamine agonists: relevance to neurological symptoms in clinical syndromes with reduced brain dopamine. J Pharmacol Exp Ther 231:343-354.

Breese GR, Baumeister AA, McCown TJ, Emerick SG, Frye GD, Mueller RA (1984) Neonatal-6-hydroxydopamine treatment: model of susceptibility for self-mutilation in the Lesch-Nyhan syndrome. Pharmacol Biochem Behav 21:459-461.

Brus R, Kostrzewa RM, Nowak P, Perry KW, Kostrzewa JP (2003) Ontogenetic quinpirole treatments fail to prime for D2 agonist-enhancement of locomotor activity in 6-hydroxydopamine-lesioned rats. Neurotox Res 5:329-338.

Buddle M, Eberhardt E, Ciminello LH, Levin T, Wing R, DiPasquale K, Raley-Susman KM (2003) Microtubule-associated protein 2 (MAP2) associates with the NMDA receptor and is spatially redistributed within rat hippocampal neurons after

oxygen-glucose deprivation. Brain Res 978:38-50.

Bury SD, Jones TA (2002) Unilateral sensorimotor cortex lesions in adult rats facilitate motor skill learning with the "unaffected" forelimb and training-induced dendritic structural plasticity in the motor cortex. J Neurosci 22:8597-8606.

Cardona-Gomez GP, Mendez P, DonCarlos LL, Azcoitia I, Garcia-Segura LM (2002) Interactions of estrogen and insulin-like growth factor-I in the brain: molecular mechanisms and functional implications. J Steroid Biochem Mol Biol 83:211-217.

Castner SA, Goldman-Rakic PS (2003) Amphetamine sensitization of hallucinatory-like behaviors is dependent on prefrontal cortex in nonhuman primates. Biol Psychiatry 54:105-110.

Castner SA, Williams GV, Goldman-Rakic PS (2000) Reversal of antipsychotic-induced working memory deficits by short-term dopamine D1 receptor stimulation. Science 287:2020-2022.

Cepeda C, Radisavljevic Z, Peacock W, Levine MS, Buchwald NA (1992) Differential modulation by dopamine of responses evoked by excitatory amino acids in human cortex. Synapse 11:330-341.

Chen Y, Ghosh A (2005) Regulation of dendritic development by neuronal activity. J Neurobiol 64:4-10.

Chinen CC, Faria RR, Frussa-Filho R (2005) Characterization of the Rapid-Onset Type of Behavioral Sensitization to Amphetamine in Mice: Role of Drug-Environment Conditioning. Neuropsychopharmacology.

Choe ES, McGinty JF (2001) Cyclic AMP and mitogen-activated protein kinases are required for glutamate-dependent cyclic AMP response element binding protein and Elk-1 phosphorylation in the dorsal striatum in vivo. J Neurochem 76:401-412.

Chu CT, Levinthal DJ, Kulich SM, Chalovich EM, DeFranco DB (2004) Oxidative neuronal injury. The dark side of ERK1/2. Eur J Biochem 271:2060-2066.

Creese I, Iversen SD (1973) Blockage of amphetamine induced motor stimulation and stereotypy in the adult rat following neonatal treatment with 6-hydroxydopamine. Brain Res 55:369-382.

Criswell HE, Mueller RA, Breese GR (1990) Long-term D1-dopamine receptor sensitization in neonatal 6-OHDA-lesioned rats is blocked by an NMDA antagonist. Brain Res 512:284-290.

Criswell H, Mueller RA, Breese GR (1989) Priming of D1-dopamine receptor responses: long-lasting behavioral supersensitivity to a D1-dopamine agonist following repeated administration to neonatal 6-OHDA-lesioned rats. J Neurosci 9:125-133.

Criswell H, Mueller RA, Breese GR (1988) Assessment of purine-dopamine interactions in 6-hydroxydopamine-lesioned rats: evidence for pre- and postsynaptic influences by adenosine. J Pharmacol Exp Ther 244:493-500.

Curtis J, Finkbeiner S (1999) Sending signals from the synapse to the nucleus: possible roles for CaMK, Ras/ERK, and SAPK pathways in the regulation of synaptic plasticity and neuronal growth. J Neurosci Res 58:88-95.

Davids E, Zhang K, Tarazi FI, Baldessarini RJ (2003) Animal models of attention-deficit hyperactivity disorder. Brain Res Brain Res Rev 42:1-21.

Davies SP, Reddy H, Caivano M, Cohen P (2000) Specificity and mechanism of action of some commonly used protein kinase inhibitors. Biochem J 351:95-105.

Davis RJ (2000) Signal transduction by the JNK group of MAP kinases. Cell 103:239-252.

Davis S, Butcher SP, Morris RG (1992) The NMDA receptor antagonist D-2-amino-5-phosphonopentanoate (D-AP5) impairs spatial learning and LTP in vivo at intracerebral concentrations comparable to those that block LTP in vitro. J Neurosci 12:21-34.

Dawson TM, Ginty DD (2002) CREB family transcription factors inhibit neuronal suicide. Nat Med 8:450-451.

DeLong MR (1990) Primate models of movement disorders of basal ganglia origin. Trends Neurosci 13:281-285.

Denton RM, Tavare JM (1995) Does mitogen-activated-protein kinase have a role in insulin action? The cases for and against. Eur J Biochem 227:597-611.

Descarries L, Lemay B, Doucet G, Berger B (1987) Regional and laminar density of the dopamine innervation in adult rat cerebral cortex. Neuroscience 21:807-824.

Duncan GE, Breese GR, Criswell HE, Johnson KB, Schambra UB, Mueller RA, Caron MG, Fremeau RT, Jr. (1993) D1 dopamine receptor binding and mRNA levels are not altered after neonatal 6-hydroxydopamine treatment: evidence against dopamine-mediated induction of D1 dopamine receptors during postnatal development. J Neurochem 61:1255-1262.

Duncan GE, Criswell HE, McCown TJ, Paul IA, Mueller RA, Breese GR (1987) Behavioral and neurochemical responses to haloperidol and SCH-23390 in rats

treated neonatally or as adults with 6-hydroxydopamine. J Pharmacol Exp Ther 243:1027-1034.

el Mansari M, Radja F, Ferron A, Reader TA, Molina-Holgado E, Descarries L (1994) Hypersensitivity to serotonin and its agonists in serotonin-hyperinnervated neostriatum after neonatal dopamine denervation. Eur J Pharmacol 261:171-178.

Elzinga BM, Bremner JD (2002) Are the neural substrates of memory the final common pathway in posttraumatic stress disorder (PTSD)? J Affect Disord 70:1-17.

English JD, Sweatt JD (1997) A requirement for the mitogen-activated protein kinase cascade in hippocampal long term potentiation. J Biol Chem 272:19103-19106.

English JD, Sweatt JD (1996) Activation of p42 mitogen-activated protein kinase in hippocampal long term potentiation. J Biol Chem 271:24329-24332.

Fahlke C, Hansen S (1999) Alcohol responsiveness, hyperreactivity, and motor restlessness in an animal model for attention-deficit hyperactivity disorder. Psychopharmacology (Berl) 146:1-9.

Farooq A, Zhou MM (2004) Structure and regulation of MAPK phosphatases. Cell Signal 16:769-779.

Favata MF, Horiuchi KY, Manos EJ, Daulerio AJ, Stradley DA, Feeser WS, Van Dyk DE, Pitts WJ, Earl RA, Hobbs F, Copeland RA, Magolda RL, Scherle PA, Trzaskos JM (1998) Identification of a novel inhibitor of mitogen-activated protein kinase kinase. J Biol Chem 273:18623-18632.

Fiore RS, Bayer VE, Pelech SL, Posada J, Cooper JA, Baraban JM (1993) p42 mitogen-activated protein kinase in brain: prominent localization in neuronal cell bodies and dendrites. Neuroscience 55:463-472.

Fleischmann A, Vincent PA, Etgen AM (1991) Effects of non-competitive NMDA receptor antagonists on reproductive and motor behaviors in female rats. Brain Res 568:138-146.

Frantz K, Van Hartesveldt C (1999) Locomotion elicited by MK801 in developing and adult rats: temporal, environmental, and gender effects. Eur J Pharmacol 369:145-157.

Gabbott PL, Bacon SJ (1996) The organisation of dendritic bundles in the prelimbic cortex (area 32) of the rat. Brain Res 730:75-86.

Gerfen CR, Miyachi S, Paletzki R, Brown P (2002) D1 dopamine receptor supersensitivity in the dopamine-depleted striatum results from a switch in the regulation of ERK1/2/MAP kinase. J Neurosci 22:5042-5054.

Gerfen CR (2000) Molecular effects of dopamine on striatal-projection pathways. Trends Neurosci 23:S64-70.

Goldin M, Segal M (2003) Protein kinase C and ERK involvement in dendritic spine plasticity in cultured rodent hippocampal neurons. Eur J Neurosci 17:2529-2539.

Goldman-Rakic PS, Castner SA, Svensson TH, Siever LJ, Williams GV (2004) Targeting the dopamine D1 receptor in schizophrenia: insights for cognitive dysfunction. Psychopharmacology (Berl) 174:3-16.

Goldman-Rakic PS, Selemon LD (1997) Functional and anatomical aspects of prefrontal pathology in schizophrenia. Schizophr Bull 23:437-458.

Gong L, Kostrzewa RM, Li C (1994) Neonatal 6-hydroxydopamine and adult SKF 38393 treatments alter dopamine D1 receptor mRNA levels: absence of other neurochemical associations with the enhanced behavioral responses of lesioned rats. J Neurochem 63:1282-1290.

Gong L, Kostrzewa RM, Fuller RW, Perry KW (1992) Supersensitization of the oral response to SKF 38393 in neonatal 6-OHDA-lesioned rats is mediated through a serotonin system. J Pharmacol Exp Ther 261:1000-1007.

Gonzalez-Islas C, Hablitz JJ (2003) Dopamine enhances EPSCs in layer II-III pyramidal neurons in rat prefrontal cortex. J Neurosci 23:867-875.

Greengard P (2001) The neurobiology of dopamine signaling. Biosci Rep 21:247-269.

Greenough A, Withers GS, Wallace CS (1990) Morphological changes in the nervous system arising from behavioral experience: what is the evidence that they are involved in learning and memory? New York: F. K. Schattauder Verlag.

Gresch PJ, Walker PD (1999) Synergistic interaction between serotonin-2 receptor and dopamine D1 receptor stimulation on striatal preprotachykinin mRNA expression in the 6-hydroxydopamine lesioned rat. Brain Res Mol Brain Res 70:125-134.

Grewal SS, York RD, Stork PJ (1999) Extracellular-signal-regulated kinase signalling in neurons. Curr Opin Neurobiol 9:544-553.

Gu Z, Jiang Q, Zhang G (2001) Extracellular signal-regulated kinase 1/2 activation in hippocampus after cerebral ischemia may not interfere with postischemic cell death. Brain Res 901:79-84.

Haggerty GC, Brown G (1996) Neurobehavioral profile of subcutaneously administered MK-801 in the rat. Neurotoxicology 17:913-921.

Harada A, Teng J, Takei Y, Oguchi K, Hirokawa N (2002) MAP2 is required for dendrite elongation, PKA anchoring in dendrites, and proper PKA signal transduction. J Cell Biol 158:541-549.

Harris KM, Kater SB (1994) Dendritic spines: cellular specializations imparting both stability and flexibility to synaptic function. Annu Rev Neurosci 17:341-371.

Herdegen T, Leah JD (1998) Inducible and constitutive transcription factors in the mammalian nervous system: control of gene expression by Jun, Fos and Krox, and CREB/ATF proteins. Brain Res Brain Res Rev 28:370-490.

Hirokawa N, Hisanaga S, Shiomura Y (1988) MAP2 is a component of crossbridges between microtubules and neurofilaments in the neuronal cytoskeleton: quick-freeze, deep-etch immunoelectron microscopy and reconstitution studies. J Neurosci 8:2769-2779.

Hollister AS, Breese GR, Mueller RA (1979) Role of monoamine neural systems in L-dihydroxyphenylalanine-stimulated activity. J Pharmacol Exp Ther 208:37-43.

Hollister AS, Breese GR, Cooper BR (1974) Comparison of tyrosine hydroxylase and dopamine-beta-hydroxylase inhibition with the effects of various 6-hydroxydopamine treatments on d-amphetamine induced motor activity. Psychopharmacologia 36:1-16.

Holzer M, Rodel L, Seeger G, Gartner U, Narz F, Janke C, Heumann R, Arendt T (2001) Activation of mitogen-activated protein kinase cascade and phosphorylation of cytoskeletal proteins after neurone-specific activation of p21ras. II. Cytoskeletal proteins and dendritic morphology. Neuroscience 105:1041-1054.

Honack D, Loscher W (1993) Sex differences in NMDA receptor mediated responses in rats. Brain Res 620:167-170.

Hugues S, Deschaux O, Garcia R (2004) Postextinction infusion of a mitogen-activated protein kinase inhibitor into the medial prefrontal cortex impairs memory of the extinction of conditioned fear. Learn Mem 11:540-543.

Hummel M, Unterwald EM (2002) D1 dopamine receptor: a putative neurochemical and behavioral link to cocaine action. J Cell Physiol 191:17-27.

Impey S, Obrietan K, Wong ST, Poser S, Yano S, Wayman G, Deloulme JC, Chan G, Storm DR (1998) Cross talk between ERK and PKA is required for Ca2+ stimulation of CREB-dependent transcription and ERK nuclear translocation. Neuron 21:869-883.

Jeon SH, Kim YS, Bae CD, Park JB (2000) Activation of JNK and p38 in rat hippocampus after kainic acid induced seizure. Exp Mol Med 32:227-230.

Jin LQ, Wang HY, Friedman E (2001) Stimulated D1 dopamine receptors couple to multiple Gα proteins in different brain regions. J Neurochem 78:981-990.

Johnson GL, Lapadat R (2002) Mitogen-activated protein kinase pathways mediated by ERK, JNK, and p38 protein kinases. Science 298:1911-1912.

Johnson GV, Jope RS (1992) The role of microtubule-associated protein 2 (MAP-2) in neuronal growth, plasticity, and degeneration. J Neurosci Res 33:505-512.

Johnson KB, Criswell HE, Jensen KF, Simson PE, Mueller RA, Breese GR (1992) Comparison of the D1-dopamine agonists SKF-38393 and A-68930 in neonatal 6-hydroxydopamine-lesioned rats: behavioral effects and induction of c-fos-like immunoreactivity. J Pharmacol Exp Ther 262:855-865.

Jones LB, Stanwood GD, Reinoso BS, Washington RA, Wang HY, Friedman E, Levitt P (2000) In utero cocaine-induced dysfunction of dopamine D1 receptor signaling and abnormal differentiation of cerebral cortical neurons. J Neurosci 20:4606-4614.

Jones L, Fischer I, Levitt P (1996) Nonuniform alteration of dendritic development in the cerebral cortex following prenatal cocaine exposure. Cereb Cortex 6:431-445.

Jones TA, Kleim JA, Greenough WT (1996) Synaptogenesis and dendritic growth in the cortex opposite unilateral sensorimotor cortex damage in adult rats: a quantitative electron microscopic examination. Brain Res 733:142-148.

Kamakura S, Moriguchi T, Nishida E (1999) Activation of the protein kinase ERK5/BMK1 by receptor tyrosine kinases. Identification and characterization of a signaling pathway to the nucleus. J Biol Chem 274:26563-26571.

Kaplan DR, Miller FD (2000) Neurotrophin signal transduction in the nervous system. Curr Opin Neurobiol 10:381-391.

Karasewski L, Ferreira A (2003) MAPK signal transduction pathway mediates agrin effects on neurite elongation in cultured hippocampal neurons. J Neurobiol 55:14-24.

Karler R, Calder LD, Chaudhry IA, Turkanis SA (1989) Blockade of "reverse tolerance" to cocaine and amphetamine by MK-801. Life Sci 45:599-606.

Kebabian JW, Calne DB (1979) Multiple receptors for dopamine. Nature 277:93-96.

Kelley AE (2004) Memory and addiction: shared neural circuitry and molecular mechanisms. Neuron 44:161-179.

Kelley AE, Berridge KC (2002) The neuroscience of natural rewards: relevance to addictive drugs. J Neurosci 22:3306-3311.

Keyse SM (1998) Protein phosphatases and the regulation of MAP kinase activity. Semin Cell Dev Biol 9:143-152.

Klein RL, Hamby ME, Gong Y, Hirko AC, Wang S, Hughes JA, King MA, Meyer EM (2002) Dose and promoter effects of adeno-associated viral vector for green fluorescent protein expression in the rat brain. Exp Neurol 176:66-74.

Knapp DJ, Braun CJ, Duncan GE, Qian Y, Fernandes A, Crews FT, Breese GR (2001) Regional specificity of ethanol and NMDA action in brain revealed with FOS-like immunohistochemistry and differential routes of drug administration. Alcohol Clin Exp Res 25:1662-1672.

Knapp DJ, Duncan GE, Crews FT, Breese GR (1998) Induction of Fos-like proteins and ultrasonic vocalizations during ethanol withdrawal: further evidence for withdrawal-induced anxiety. Alcohol Clin Exp Res 22:481-493.

Kohno M, Pouyssegur J (2003) Pharmacological inhibitors of the ERK signaling pathway: application as anticancer drugs. Prog Cell Cycle Res 5:219-224.

Kolb B, Whishaw IQ (1998) Brain plasticity and behavior. Annu Rev Psychol 49:43-64.

Konradi C, Leveque JC, Hyman SE (1996) Amphetamine and dopamine-induced immediate early gene expression in striatal neurons depends on postsynaptic NMDA receptors and calcium. J Neurosci 16:4231-4239.

Kulich SM, Chu CT (2001) Sustained extracellular signal-regulated kinase activation by 6-hydroxydopamine: implications for Parkinson's disease. J Neurochem 77:1058-1066.

Kyosseva SV (2004) Mitogen-activated protein kinase signaling. Int Rev Neurobiol 59:201-220.

Lamprecht R, LeDoux J (2004) Structural plasticity and memory. Nat Rev Neurosci 5:45-54.

Lankford KL, DeMello FG, Klein WL (1988) D1-type dopamine receptors inhibit growth cone motility in cultured retina neurons: evidence that neurotransmitters act as morphogenic growth regulators in the developing central nervous system. Proc Natl Acad Sci U S A 85:2839-2843.

Laprade N, Radja F, Reader TA, Soghomonian JJ (1996) Dopamine receptor agonists regulate levels of the serotonin 5-HT2A receptor and its mRNA in a subpopulation of rat striatal neurons. J Neurosci 16:3727-3736.

Laruelle M (2000) The role of endogenous sensitization in the pathophysiology of schizophrenia: implications from recent brain imaging studies. Brain Res Brain Res Rev 31:371-384.

Lee JK, Choi SS, Lee HK, Han KJ, Han EJ, Suh HW (2002) Effects of MK-801 and CNQX on various neurotoxic responses induced by kainic acid in mice. Mol Cells 14:339-347.

Lesch M, Nyhan WL (1964) A Familial Disorder of Uric Acid Metabolism and Central Nervous System Function. Am J Med 36:561-570.

Lev S, Moreno H, Martinez R, Canoll P, Peles E, Musacchio JM, Plowman GD, Rudy B, Schlessinger J (1995) Protein tyrosine kinase PYK2 involved in Ca(2+)-induced regulation of ion channel and MAP kinase functions. Nature 376:737-745.

Liu JC, Baker RE, Sun C, Sundmark VC, Elsholtz HP (2002) Activation of Go-coupled dopamine D2 receptors inhibits ERK1/ERK2 in pituitary cells. A key step in the transcriptional suppression of the prolactin gene. J Biol Chem 277:35819-35825.

Liu L, Cavanaugh JE, Wang Y, Sakagami H, Mao Z, Xia Z (2003) ERK5 activation of MEF2-mediated gene expression plays a critical role in BDNF-promoted survival of developing but not mature cortical neurons. Proc Natl Acad Sci U S A 100:8532-8537.

Lloyd SA, Wensley B, Faherty CJ, Smeyne RJ (2003) Regional differences in cortical dendrite morphology following in utero exposure to cocaine. Brain Res Dev Brain Res 147:59-66.

Lonze BE, Ginty DD (2002) Function and regulation of CREB family transcription factors in the nervous system. Neuron 35:605-623.

Luthman J, Lindqvist E, Young D, Cowburn R (1990) Neonatal dopamine lesion in the rat results in enhanced adenylate cyclase activity without altering dopamine receptor binding or dopamine- and adenosine 3':5'-monophosphate-regulated phosphoprotein (DARPP-32) immunoreactivity. Exp Brain Res 83:85-95.

Luthman J, Bolioli B, Tsutsumi T, Verhofstad A, Jonsson G (1987) Sprouting of striatal serotonin nerve terminals following selective lesions of nigro-striatal dopamine neurons in neonatal rat. Brain Res Bull 19:269-274.

Lynch G, Larson J, Kelso S, Barrionuevo G, Schottler F (1983) Intracellular injections of EGTA block induction of hippocampal long-term potentiation. Nature 305:719-721.

Mailman RB, Lewis MH, Kilts CD (1981) Animal models related to developmental

disorders: theoretical and pharmacological analyses. Appl Res Ment Retard 2:1-12.

Mainen ZF, Sejnowski TJ (1996) Influence of dendritic structure on firing pattern in model neocortical neurons. Nature 382:363-366.

Mantych KB, Ferreira A (2001) Agrin differentially regulates the rates of axonal and dendritic elongation in cultured hippocampal neurons. J Neurosci 21:6802-6809.

Mao L, Tang Q, Samdani S, Liu Z, Wang JQ (2004) Regulation of MAPK/ERK phosphorylation via ionotropic glutamate receptors in cultured rat striatal neurons. Eur J Neurosci 19:1207-1216.

Marsden CD (1984) Motor disorders in basal ganglia disease. Hum Neurobiol 2:245-250.

Marshall CJ (1995) Specificity of receptor tyrosine kinase signaling: transient versus sustained extracellular signal-regulated kinase activation. Cell 80:179-185.

Martin KC, Michael D, Rose JC, Barad M, Casadio A, Zhu H, Kandel ER (1997) MAP kinase translocates into the nucleus of the presynaptic cell and is required for long-term facilitation in Aplysia. Neuron 18:899-912.

Matus A (1988) Microtubule-associated proteins: their potential role in determining neuronal morphology. Annu Rev Neurosci 11:29-44.

McCown TJ, Xiao X, Li J, Breese GR, Samulski RJ (1996) Differential and persistent expression patterns of CNS gene transfer by an adeno-associated virus (AAV) vector. Brain Res 713:99-107.

McQuade RD, Ford D, Duffy RA, Chipkin RE, Iorio LC, Barnett A (1988) Serotonergic component of SCH 23390: in vitro and in vivo binding analyses. Life Sci 43:1861-1869.

Miller FD, Kaplan DR (2003) Signaling mechanisms underlying dendrite formation. Curr Opin Neurobiol 13:391-398.

Morishima-Kawashima M, Kosik KS (1996) The pool of map kinase associated with microtubules is small but constitutively active. Mol Biol Cell 7:893-905.

Moy SS, Breese GR (2002) Phencyclidine supersensitivity in rats with neonatal dopamine loss. Psychopharmacology (Berl) 161:255-262.

Murphy EH, Fischer I, Friedman E, Grayson D, Jones L, Levitt P, O'Brien-Jenkins A, Wang HY, Wang XH (1997) Cocaine administration in pregnant rabbits alters cortical structure and function in their progeny in the absence of maternal seizures. Exp Brain Res 114:433-441.

Nagatsu T, Levitt M, Udenfriend S (1964) Tyrosine Hydroxylase. The Initial Step in Norepinephrine Biosynthesis. J Biol Chem 239:2910-2917.

Numan S, Lundgren KH, Wright DE, Herman JP, Seroogy KB (1995) Increased expression of 5HT2 receptor mRNA in rat striatum following 6-OHDA lesions of the adult nigrostriatal pathway. Brain Res Mol Brain Res 29:391-396.

Olanow CW (2004) The scientific basis for the current treatment of Parkinson's disease. Annu Rev Med 55:41-60.

Otani S, Daniel H, Roisin MP, Crepel F (2003) Dopaminergic modulation of long-term synaptic plasticity in rat prefrontal neurons. Cereb Cortex 13:1251-1256.

Papadeas ST, McCown TJ, Breese GR, Blake BL (in publication) Phosphorylated ERK1/2 modifies apical dendritic structure of medial prefrontal cortex pyrimidal neurons in a rat model of dopamine D1 receptor sensitization. J Neurosci.

Papadeas ST, Blake BL, Knapp DJ, Breese GR (2004) Sustained extracellular signal-regulated kinase 1/2 phosphorylation in neonate 6-hydroxydopamine-lesioned rats after repeated D1-dopamine receptor agonist administration: implications for NMDA receptor involvement. J Neurosci 24:5863-5876.

Paul A, Wilson S, Belham CM, Robinson CJ, Scott PH, Gould GW, Plevin R (1997) Stress-activated protein kinases: activation, regulation and function. Cell Signal 9:403-410.

Paxinos G, Watson C (1998) The Rat Brain in Stereotaxic Coordinates, 4 Edition. New York: Academic Press.

Pearson G, Robinson F, Beers Gibson T, Xu BE, Karandikar M, Berman K, Cobb MH (2001) Mitogen-activated protein (MAP) kinase pathways: regulation and physiological functions. Endocr Rev 22:153-183.

Pei JJ, Braak H, An WL, Winblad B, Cowburn RF, Iqbal K, Grundke-Iqbal I (2002) Up-regulation of mitogen-activated protein kinases ERK1/2 and MEK1/2 is associated with the progression of neurofibrillary degeneration in Alzheimer's disease. Brain Res Mol Brain Res 109:45-55.

Pei L, Lee FJ, Moszczynska A, Vukusic B, Liu F (2004) Regulation of dopamine D1 receptor function by physical interaction with the NMDA receptors. J Neurosci 24:1149-1158.

Perkinton MS, Ip JK, Wood GL, Crossthwaite AJ, Williams RJ (2002) Phosphatidylinositol 3-kinase is a central mediator of NMDA receptor signalling to MAP kinase (Erk1/2), Akt/PKB and CREB in striatal neurones. J Neurochem

80:239-254.

Perkinton MS, Sihra TS, Williams RJ (1999) Ca(2+)-permeable AMPA receptors induce phosphorylation of cAMP response element-binding protein through a phosphatidylinositol 3-kinase-dependent stimulation of the mitogen-activated protein kinase signaling cascade in neurons. J Neurosci 19:5861-5874.

Philpot BD, Lim JH, Halpain S, Brunjes PC (1997) Experience-dependent modifications in MAP2 phosphorylation in rat olfactory bulb. J Neurosci 17:9596-9604.

Pierce RC, Kalivas PW (1997) A circuitry model of the expression of behavioral sensitization to amphetamine-like psychostimulants. Brain Res Brain Res Rev 25:192-216.

Pierce RC, Kalivas PW (1997) Repeated cocaine modifies the mechanism by which amphetamine releases dopamine. J Neurosci 17:3254-3261.

Plech A, Brus R, Kalbfleisch JH, Kostrzewa RM (1995) Enhanced oral activity responses to intrastriatal SKF 38393 and m-CPP are attenuated by intrastriatal mianserin in neonatal 6-OHDA-lesioned rats. Psychopharmacology (Berl) 119:466-473.

Pouyssegur J, Volmat V, Lenormand P (2002) Fidelity and spatio-temporal control in MAP kinase (ERKs) signalling. Biochem Pharmacol 64:755-763.

Quinlan EM, Halpain S (1996) Emergence of activity-dependent, bidirectional control of microtubule-associated protein MAP2 phosphorylation during postnatal development. J Neurosci 16:7627-7637.

Quinlan EM, Halpain S (1996) Postsynaptic mechanisms for bidirectional control of MAP2 phosphorylation by glutamate receptors. Neuron 16:357-368.

Quinn JC, Johnson-Farley NN, Yoon J, Cowen DS (2002) Activation of extracellular-regulated kinase by 5-hydroxytryptamine(2A) receptors in PC12 cells is protein kinase C-independent and requires calmodulin and tyrosine kinases. J Pharmacol Exp Ther 303:746-752.

Racine RJ (1972) Modification of seizure activity by electrical stimulation. II. Motor seizure. Electroencephalogr Clin Neurophysiol 32:281-294.

Redmond L, Kashani AH, Ghosh A (2002) Calcium regulation of dendritic growth via CaM kinase IV and CREB-mediated transcription. Neuron 34:999-1010.

Reinoso BS, Undie AS, Levitt P (1996) Dopamine receptors mediate differential morphological effects on cerebral cortical neurons in vitro. J Neurosci Res 43:439-453.

Reszka AA, Bulinski JC, Krebs EG, Fischer EH (1997) Mitogen-activated protein kinase/extracellular signal-regulated kinase 2 regulates cytoskeletal organization and chemotaxis via catalytic and microtubule-specific interactions. Mol Biol Cell 8:1219-1232.

Reszka AA, Seger R, Diltz CD, Krebs EG, Fischer EH (1995) Association of mitogen-activated protein kinase with the microtubule cytoskeleton. Proc Natl Acad Sci U S A 92:8881-8885.

Riedel G, Platt B, Micheau J (2003) Glutamate receptor function in learning and memory. Behav Brain Res 140:1-47.

Roberson ED, English JD, Adams JP, Selcher JC, Kondratick C, Sweatt JD (1999) The mitogen-activated protein kinase cascade couples PKA and PKC to cAMP response element binding protein phosphorylation in area CA1 of hippocampus. J Neurosci 19:4337-4348.

Robinson TE, Kolb B (1999) Alterations in the morphology of dendrites and dendritic spines in the nucleus accumbens and prefrontal cortex following repeated treatment with amphetamine or cocaine. Eur J Neurosci 11:1598-1604.

Robinson TE, Kolb B (1997) Persistent structural modifications in nucleus accumbens and prefrontal cortex neurons produced by previous experience with amphetamine. J Neurosci 17:8491-8497.

Robinson TE, Becker JB (1986) Enduring changes in brain and behavior produced by chronic amphetamine administration: a review and evaluation of animal models of amphetamine psychosis. Brain Res 396:157-198.

Rodbell M (1980) The role of hormone receptors and GTP-regulatory proteins in membrane transduction. Nature 284:17-22.

Rodrigues Pdos S, Dowling JE (1990) Dopamine induces neurite retraction in retinal horizontal cells via diacylglycerol and protein kinase C. Proc Natl Acad Sci U S A 87:9693-9697.

Salter MW (2003) D1 and NMDA receptors hook up: expanding on an emerging theme. Trends Neurosci 26:235-237.

Sanchez C, Diaz-Nido J, Avila J (2000) Phosphorylation of microtubule-associated protein 2 (MAP2) and its relevance for the regulation of the neuronal cytoskeleton function. Prog Neurobiol 61:133-168.

Schaeffer HJ, Weber MJ (1999) Mitogen-activated protein kinases: specific messages from ubiquitous messengers. Mol Cell Biol 19:2435-2444.

Schmitt JM, Stork PJ (2002) PKA phosphorylation of Src mediates cAMP's inhibition of cell growth via Rap1. Mol Cell 9:85-94.

Schmued LC, Hopkins KJ (2000) Fluoro-Jade B: a high affinity fluorescent marker for the localization of neuronal degeneration. Brain Res 874:123-130.

Schwarzkopf SB, Mitra T, Bruno JP (1992) Sensory gating in rats depleted of dopamine as neonates: potential relevance to findings in schizophrenic patients. Biol Psychiatry 31:759-773.

Seamon KB, Padgett W, Daly JW (1981) Forskolin: unique diterpene activator of adenylate cyclase in membranes and in intact cells. Proc Natl Acad Sci U S A 78:3363-3367.

Seger R, Krebs EG (1995) The MAPK signaling cascade. Faseb J 9:726-735.

Selcher JC, Atkins CM, Trzaskos JM, Paylor R, Sweatt JD (1999) A necessity for MAP kinase activation in mammalian spatial learning. Learn Mem 6:478-490.

Sesack SR, Carr DB, Omelchenko N, Pinto A (2003) Anatomical substrates for glutamate-dopamine interactions: evidence for specificity of connections and extrasynaptic actions. Ann N Y Acad Sci 1003:36-52.

Sgambato V, Pages C, Rogard M, Besson MJ, Caboche J (1998) Extracellular signal-regulated kinase (ERK) controls immediate early gene induction on corticostriatal stimulation. J Neurosci 18:8814-8825.

Shen H, Tong L, Balazs R, Cotman CW (2001) Physical activity elicits sustained activation of the cyclic AMP response element-binding protein and mitogen-activated protein kinase in the rat hippocampus. Neuroscience 107:219-229.

Simson PE, Johnson KB, Jurevics HA, Criswell HE, Napier TC, Duncan GE, Mueller RA, Breese GR (1992) Augmented sensitivity of D1-dopamine receptors in lateral but not medial striatum after 6-hydroxydopamine-induced lesions in the neonatal rat. J Pharmacol Exp Ther 263:1454-1463.

Smith RD, Cooper BR, Breese GR (1973) Growth and behavioral changes in developing rats treated intracisternally with 6-hydroxydopamine: evidence for involvement of brain dopamine. J Pharmacol Exp Ther 185:609-619.

Snyder-Keller AM (1991) Development of striatal compartmentalization following pre- or postnatal dopamine depletion. J Neurosci 11:810-821.

Song J, Guan XW, Ren JQ, He W (2002) Effects of pregnancy cocaine exposure on the mother and fetus: a murine model. Sheng Li Xue Bao 54:342-348.

Spencer GE, Lukowiak K, Syed NI (1996) Dopamine regulation of neurite outgrowth from identified Lymnaea neurons in culture. Cell Mol Neurobiol 16:577-589.

Stachowiak MK, Bruno JP, Snyder AM, Stricker EM, Zigmond MJ (1984) Apparent sprouting of striatal serotonergic terminals after dopamine-depleting brain lesions in neonatal rats. Brain Res 291:164-167.

Stanciu M, Wang Y, Kentor R, Burke N, Watkins S, Kress G, Reynolds I, Klann E, Angiolieri MR, Johnson JW, DeFranco DB (2000) Persistent activation of ERK contributes to glutamate-induced oxidative toxicity in a neuronal cell line and primary cortical neuron cultures. J Biol Chem 275:12200-12206.

Stanwood GD, Parlaman JP, Levitt P (2005) Anatomical abnormalities in dopaminoceptive regions of the cerebral cortex of dopamine D1 receptor mutant mice. J Comp Neurol 487:270-282.

Stanwood GD, Washington RA, Levitt P (2001) Identification of a sensitive period of prenatal cocaine exposure that alters the development of the anterior cingulate cortex. Cereb Cortex 11:430-440.

Stanwood GD, Washington RA, Shumsky JS, Levitt P (2001) Prenatal cocaine exposure produces consistent developmental alterations in dopamine-rich regions of the cerebral cortex. Neuroscience 106:5-14.

Steketee JD (2003) Neurotransmitter systems of the medial prefrontal cortex: potential role in sensitization to psychostimulants. Brain Res Brain Res Rev 41:203-228.

Stevens KE, Luthman J, Lindqvist E, Johnson RG, Rose GM (1996) Effects of neonatal dopamine depletion on sensory inhibition in the rat. Pharmacol Biochem Behav 53:817-823.

Steward O, Halpain S (1999) Lamina-specific synaptic activation causes domain-specific alterations in dendritic immunostaining for MAP2 and CAM kinase II. J Neurosci 19:7834-7845.

Stewart J, Druhan JP (1993) Development of both conditioning and sensitization of the behavioral activating effects of amphetamine is blocked by the non-competitive NMDA receptor antagonist, MK-801. Psychopharmacology (Berl) 110:125-132.

Stoker A, Dutta R (1998) Protein tyrosine phosphatases and neural development. Bioessays 20:463-472.

Sullivan RM, Brake WG (2003) What the rodent prefrontal cortex can teach us about attention-deficit/hyperactivity disorder: the critical role of early developmental events on prefrontal function. Behav Brain Res 146:43-55.

Sweatt JD (2004) Mitogen-activated protein kinases in synaptic plasticity and memory. Curr Opin Neurobiol 14:311-317.

Sweatt JD (2001) The neuronal MAP kinase cascade: a biochemical signal integration system subserving synaptic plasticity and memory. J Neurochem 76:1-10.

Takaki M, Ujike H, Kodama M, Takehisa Y, Nakata K, Kuroda S (2001) Two kinds of mitogen-activated protein kinase phosphatases, MKP-1 and MKP-3, are differentially activated by acute and chronic methamphetamine treatment in the rat brain. J Neurochem 79:679-688.

Todd RD (1992) Neural development is regulated by classical neurotransmitters: dopamine D2 receptor stimulation enhances neurite outgrowth. Biol Psychiatry 31:794-807.

Towle AC, Criswell HE, Maynard EH, Lauder JM, Joh TH, Mueller RA, Breese GR (1989) Serotonergic innervation of the rat caudate following a neonatal 6-hydroxydopamine lesion: an anatomical, biochemical and pharmacological study. Pharmacol Biochem Behav 34:367-374.

Trentani A, Kuipers SD, Ter Horst GJ, Den Boer JA (2002) Selective chronic stress-induced in vivo ERK1/2 hyperphosphorylation in medial prefrontocortical dendrites: implications for stress-related cortical pathology? Eur J Neurosci 15:1681-1691.

Troadec JD, Marien M, Mourlevat S, Debeir T, Ruberg M, Colpaert F, Michel PP (2002) Activation of the mitogen-activated protein kinase (ERK(1/2)) signaling pathway by cyclic AMP potentiates the neuroprotective effect of the neurotransmitter noradrenaline on dopaminergic neurons. Mol Pharmacol 62:1043-1052.

Tzschentke TM (2001) Pharmacology and behavioral pharmacology of the mesocortical dopamine system. Prog Neurobiol 63:241-320.

Ujike H (2002) Stimulant-induced psychosis and schizophrenia: the role of sensitization. Curr Psychiatry Rep 4:177-184.

Ungerstedt U (1971) Adipsia and aphagia after 6-hydroxydopamine induced degeneration of the nigro-striatal dopamine system. Acta Physiol Scand Suppl 367:95-122.

Ungerstedt U (1971) Postsynaptic supersensitivity after 6-hydroxy-dopamine induced degeneration of the nigro-striatal dopamine system. Acta Physiol Scand Suppl 367:69-93.

Uretsky NJ, Schoenfeld RI (1971) Effect of L-dopa on the locomotor activity of rats pretreated with 6-hydroxydopamine. Nat New Biol 234:157-159.

Vaillant AR, Zanassi P, Walsh GS, Aumont A, Alonso A, Miller FD (2002) Signaling mechanisms underlying reversible, activity-dependent dendrite formation. Neuron 34:985-998.

Valjent E, Pages C, Herve D, Girault JA, Caboche J (2004) Addictive and non-addictive drugs induce distinct and specific patterns of ERK activation in mouse brain. Eur J Neurosci 19:1826-1836.

Valjent E, Corvol JC, Pages C, Besson MJ, Maldonado R, Caboche J (2000) Involvement of the extracellular signal-regulated kinase cascade for cocaine-rewarding properties. J Neurosci 20:8701-8709.

van Oosten RV, Verheij MM, Cools AR (2005) Bilateral nigral 6-hydroxydopamine lesions increase the amount of extracellular dopamine in the nucleus accumbens. Exp Neurol 191:24-32.

van Oosten RV, Cools AR (2002) Differential effects of a small, unilateral, 6-hydroxydopamine-induced nigral lesion on behavior in high and low responders to novelty. Exp Neurol 173:245-255.

Vanderschuren LJ, Kalivas PW (2000) Alterations in dopaminergic and glutamatergic transmission in the induction and expression of behavioral sensitization: a critical review of preclinical studies. Psychopharmacology (Berl) 151:99-120.

Vanhoutte P, Barnier JV, Guibert B, Pages C, Besson MJ, Hipskind RA, Caboche J (1999) Glutamate induces phosphorylation of Elk-1 and CREB, along with c-fos activation, via an extracellular signal-regulated kinase-dependent pathway in brain slices. Mol Cell Biol 19:136-146.

Vetter P, Roth A, Hausser M (2001) Propagation of action potentials in dendrites depends on dendritic morphology. J Neurophysiol 85:926-937.

Vossler MR, Yao H, York RD, Pan MG, Rim CS, Stork PJ (1997) cAMP activates MAP kinase and Elk-1 through a B-Raf- and Rap1-dependent pathway. Cell 89:73-82.

Vossler MR, Coco A, Strausser BT, Zaricznyj C, Macara IG (1987) Tyrosyl and phosphatidylinositol kinases of human erythrocyte membranes. J Cell Biochem 33:225-235.

Wade CB, Dorsa DM (2003) Estrogen activation of cyclic adenosine 5'-monophosphate response element-mediated transcription requires the extracellularly regulated kinase/mitogen-activated protein kinase pathway. Endocrinology 144:832-838.

Walker PD, Bishop C, Tessmer JL, Kroleweski D (2004) Evidence that serotonin 5-HT2A receptors contribute to excessive motor behaviors in dopamine-depleted rats treated with dopamine D1 receptor agonists. 2004 Abstract Viewer/Itinery

Planner Program No. 261.5.

Wang HY, Runyan S, Yadin E, Friedman E (1995) Prenatal exposure to cocaine selectively reduces D1 dopamine receptor-mediated activation of striatal Gs proteins. J Pharmacol Exp Ther 273:492-498.

Wang HY, Undie AS, Friedman E (1995) Evidence for the coupling of Gq protein to D1-like dopamine sites in rat striatum: possible role in dopamine-mediated inositol phosphate formation. Mol Pharmacol 48:988-994.

Wang XH, Levitt P, Grayson DR, Murphy EH (1995) Intrauterine cocaine exposure of rabbits: persistent elevation of GABA-immunoreactive neurons in anterior cingulate cortex but not visual cortex. Brain Res 689:32-46.

Wang J, O'Donnell P (2001) D(1) dopamine receptors potentiate nmda-mediated excitability increase in layer V prefrontal cortical pyramidal neurons. Cereb Cortex 11:452-462.

Wolf ME (2002) Addiction: making the connection between behavioral changes and neuronal plasticity in specific pathways. Mol Interv 2:146-157.

Wolf ME, Jeziorski M (1993) Coadministration of MK-801 with amphetamine, cocaine or morphine prevents rather than transiently masks the development of behavioral sensitization. Brain Res 613:291-294.

Wu GY, Deisseroth K, Tsien RW (2001) Spaced stimuli stabilize MAPK pathway activation and its effects on dendritic morphology. Nat Neurosci 4:151-158.

Xia Z, Dudek H, Miranti CK, Greenberg ME (1996) Calcium influx via the NMDA receptor induces immediate early gene transcription by a MAP kinase/ERK-dependent mechanism. J Neurosci 16:5425-5436.

Xing J, Ginty DD, Greenberg ME (1996) Coupling of the RAS-MAPK pathway to gene activation by RSK2, a growth factor-regulated CREB kinase. Science 273:959-963.

Yamagata Y, Jovanovic JN, Czernik AJ, Greengard P, Obata K (2002) Bidirectional changes in synapsin I phosphorylation at MAP kinase-dependent sites by acute neuronal excitation in vivo. J Neurochem 80:835-842.

Yao H, York RD, Misra-Press A, Carr DW, Stork PJ (1998) The cyclic adenosine monophosphate-dependent protein kinase (PKA) is required for the sustained activation of mitogen-activated kinases and gene expression by nerve growth factor. J Biol Chem 273:8240-8247.

Yin JC, Wallach JS, Del Vecchio M, Wilder EL, Zhou H, Quinn WG, Tully T (1994)

Induction of a dominant negative CREB transgene specifically blocks long-term memory in Drosophila. Cell 79:49-58.

York RD, Yao H, Dillon T, Ellig CL, Eckert SP, McCleskey EW, Stork PJ (1998) Rap1 mediates sustained MAP kinase activation induced by nerve growth factor. Nature 392:622-626.

Yuste R, Tank DW (1996) Dendritic integration in mammalian neurons, a century after Cajal. Neuron 16:701-716.

Zhen X, Du W, Romano AG, Friedman E, Harvey JA (2001) The p38 mitogen-activated protein kinase is involved in associative learning in rabbits. J Neurosci 21:5513-5519.

Zhu D, Wu X, Strauss KI, Lipsky RH, Qureshi Z, Terhakopian A, Novelli A, Banaudha K, Marini AM (2005) N-methyl-D-aspartate and TrkB receptors protect neurons against glutamate excitotoxicity through an extracellular signal-regulated kinase pathway. J Neurosci Res 80:104-113.